The seasonality of non-structural carbohydrates in mature boreal *Betula papyrifera* and potential constraints in their remobilization

by
Coral Fermaniuk

A thesis submitted in partial fulfillment of the requirements for the degree of

Master of Science

in

Forest Biology and Management

Department of Renewable Resources
University of Alberta

©Coral Fermaniuk, 2023

Abstract

Assimilated non-structural carbohydrates (NSC) can be stored as reserves in plants and remobilized during periods of asynchrony between carbon acquisition and carbon demand to fuel essential metabolic functions and growth. However, the framework of NSC allocation to reserves and their remobilization remains unclear, especially for mature trees which potentially can store large quantities of reserves. Here, I characterize the seasonal dynamics of NSC reserves in mature boreal *Betula papyrifera* and relate them to seasonal growth processes (first study), as well as determine the patterns and potential constraints of between-organ reserve remobilization. I used different patterns of stem phloem girdling to separate crown, stem and root NSC storage and their remobilization in response to induced C stress (second study). In the first study, I found that whole-tree NSC pools increased seasonally by 72% from a spring minimum to a maximum during late summer bud-set — greatly exceeding the relative change in reserves reported for more temperate conspecifics. At the organ level, the branches were the largest and most dynamic storage pool, suggesting that storage changes at the branch level largely drive whole-tree storage dynamics in these trees. In the second study, I found evidence that the crown of birch trees could store nearly double the reserves of what was observed under normal conditions, and that the stored NSC in the stem may not be universally available for remobilization to other organs (here roots) under C stress. Together, these results suggest that seasonal NSC allocation patterns appear to be highly regulated to ensure adequate distribution (allocation) of NSC to reserves throughout organs over time to support organ-level processes — however, if organs are constrained by carbon limitations, it appears that the remobilization of the organ reserve storage pools are regulated somewhat autonomously which could potentially limit the sharing of reserves within the large organism.

Preface

This thesis is an original work by Coral Fermaniuk

Chapter 2 of this thesis has been published as Fermaniuk C, Fleurial KG, Landhäusser SM (2021). Large seasonal fluctuations in whole-tree carbohydrate reserves: is storage more dynamic in boreal ecosystems? *Annals of Botany*, *128*(7), 943-957. CF, EW and SML crafted the main research questions and experimental design. CF and KGF collected data, and CF performed the data analyses. CF wrote the manuscript, KGF, EW and SML revised the manuscript.

Acknowledgements

First and foremost, the greatest thank you goes out to my supervisors, Dr. Simon Landhäusser and Dr. Erin Wiley. Simon, I am so very grateful to you for taking me on as a student and trusting me to do these projects justice. Your patience, guidance, and push for me to take ownership of this whole process these past years have instilled in me a sense of confidence that I will carry indefinitely. To Erin, thank you for sharing your invaluable wisdom and advice, and for taking the time to deal with my horrendously long emails whenever I needed clarification about something. A special thank you goes out to my colleague and friend, Killian Fleurial (Monty) — words can't express how appreciative I am of you and your unending support, humor, and for keeping me grounded when times were tough. Thank you for taking me under your wing. I would also like to thank Dr. Janusz Zwiazek for taking the time to read my thesis and for serving on my defense committee

To all members of the Landhäusser Research Group and summer students of 2018 and 2019, your friendship, support, and help in the field during those long mosquito-ridden days cannot go unrecognized — you are all incredible. Thank you to Pak Chow for the technical guidance and all lab analyses, these projects would not be what they are without your hard work. To Caren Jones and Fran Leishman, thank you for your organizational skills, guidance, and for making the lab feel like home. Thank you to Sophie Aasberg for always being there to share in the laughs/tears throughout this process — we did it! To my Silvacom crew, thank you for the support, understanding, and willingness to listen to me ramble about carbon and trees.

This research would not have been possible without the financial support from the Natural Science and Engineering Research Council (NSERC), the Faculty of Graduate Studies and Research at the University of Alberta, and the Government of Alberta.

Lastly, a heartfelt thank you to my people that pushed me to believe in and act on this ambition of mine. Mom and Dad, thank you for nurturing the little scientist in me. I would not be where I am without the unwavering support, love, and encouragement you both have provided to me. Ricky, you are the unsung hero in all of this — thank you for listening to me, for loving me, for holding down the fort, and for reminding me of what I am capable of if I put my mind to it. This has been an adventure for us both, and I would gladly do it over again with you by my side. Finally, to my sweet Jack and baby Lucy, thank you both for bringing me joy at the end of a hard day and for reminding me what this is all about.

.

Table of Contents

List of Tables

≤ 0.001. If an organ section is shaded orange, no ‘treatment’ by ‘sampling date’ interaction was detected for the given organ, and the above post-hoc tests were not conducted.

List of Figures

Figure 3-2 Average (± standard error) non-structural carbohydrate (NSC: combined sugar and starch), starch, and sugar concentrations of organ tissues over time in 30 mature *Betula papyrifera* trees subjected to different stem girdling treatments. The first date represents the initial measurements collected prior to stem girdle application. Inner bark and stemwood values depict averages across the three uppermost stem sample locations (see Figure 3-1).The inset plot in the 'Branches' panel represents the average (± standard error) moisture content (%) of the fresh branch samples. Control: n = 8, bottom girdle: n = 7, top girdle: n = 8 or 5 (31/8/18 only), and double girdle: n = 7 or 5 (31/8/18 only). To maintain the clarity of the figure, statistical comparisons and differences are provided in Table 3-1, Table A-11 and Table A-12.

Figure 3-3 Correlations between average NSC concentrations in late August of 2018 for each treatment and the proportion of trees that exhibited root pressure sap flow, root collar sprouting, canopy leaf flush, and fungal infection in the 2019 season, as well as the treatment average of branch water content in mid-May of 2019. Colours denote whether the Pearson correlation coefficient was positive (blue) or negative (red), and whether the relationship was strong (dark) or weak (light). Treatments included control (n = 8), bottom girdle (n = 7), top girdle (n = 8) and double girdle (n = 7). P-values are reported for significant tests only and were adjusted using the Behjamini-Hochberg method.

Figure 3-4 Probability of A) 2019 canopy leaf flush predicted by branch NSC concentration in mid-May of 2019, B) 2019 canopy leaf flush predicted by late August 2018 middle stem inner bark NSC concentration C) fungal disease onset (early April 2019) predicted by late August 2018 inner bark NSC concentration, E) 2019 spring root pressure sap flow predicted by late August 2018 root NSC concentration, and F) 2019 root collar sprouting predicted by late August 2018 root NSC concentration. Box D) depicts the linear relationship between branch moisture content (%) in mid-May of 2019 and late August 2018 inner bark NSC concentration.

Figure 3-5 Average (± standard error) change in inner bark carbohydrate (NSC, sugar, and starch) concentrations of upper, lower, and root collar positions from the initial measurement in mature *Betula papyrifera* trees subjected to different stem girdling treatments (control: n = 8, bottom girdle: n = 7, top girdle: n = 8, and double girdle: n = 7). (A) The change in

concentrations between 21 June 2018 (initial measurement) and 18 August 2018. (B) The change in concentrations between 21 June 2018 and 29 May 2019 after bud flush. For the lower stem region in panel (A), n = 5 for both top and double girdle treatments. For the lower stem region, hatched bars with red standard error bars present the change in concentration at the root collar position where the sample for bottom girdle and double girdle trees was taken below the bottom girdle. Different letters represent differences between treatments for the upper or lower stem samples, and numbers represent differences between treatments for root collar samples (all Tukey's HSD, $\alpha = 0.1$).

Figure 3-6 Average (± standard error) change in stemwood carbohydrate (NSC, sugar, and starch) concentrations of upper, lower, and root collar positions from the initial measurement in mature *Betula papyrifera* trees subjected to different stem girdling treatments (control: n = 8, bottom girdle: n = 7, top girdle: n = 8, and double girdle: n = 7). (A) The change in concentrations between 21 June 2018 (initial measurement) and 18 August 2018. (B) The change in concentrations between 21 June 2018 and 29 May 2019 after bud flush. For the lower stem region in panel (A), n = 5 for both top and double girdle treatments. For the lower stem region, hatched bars with red standard error bars present the change in concentration at the root collar position where the sample for bottom girdle and double girdle trees was taken below the bottom girdle. Different letters represent differences between treatments for the upper or lower stem samples, and numbers represent differences between treatments for root collar samples (all Tukey's HSD, $\alpha = 0.1$).

1. Chapter 1 – Introduction

1.1 General introduction

Approximately one-third of the global landmass is covered in forests (Bonan, 2008; FAO, 2018), however over recent decades, forested ecosystems have experienced extensive anthropogenic and climate-induced alterations in cover (FAO, 2018), composition and distribution (Beck *et al*., 2011; Martínez-Vilalta and Lloret, 2016), as well as reductions in productivity that have triggered mass dieback and mortality events across all forested continents (Allen, 2009; Allen *et al*., 2010; Anderegg *et al*., 2013; Lee *et al*., 2013; Allen *et al*., 2015; Rita *et al*., 2019). Conversely, some regions have experienced increased forest cover and productivity rates due to CO_2 fertilization combined with increased temperature and precipitation (Norby *et al*., 2005; Buma and Barret, 2015). In climates that are projected to exhibit both warming and drying trends, productivity loss and dieback may be exacerbated due to increased frequency and severity of stress events such as drought, pest, and disease outbreaks (McDowell *et al*., 2008; Allen *et al*., 2010; Anderegg and Anderegg, 2013; Paritsis and Veblen, 2011; Gaylord *et al*., 2013; Oliva *et al*., 2014).

In addition to the many ecological, economic, social, and aesthetic services forest ecosystems provide, the trees that comprise a forest are also significant drivers of ecological and climate dynamics as they provide refuge for biodiversity, stabilize soils, as well as influence biophysical and biogeochemical cycling at local, regional, and global scales (Bonan, 2008). Despite serving as large sinks for atmospheric carbon (C), forests and the trees they contain can also influence land surface temperatures and precipitation through biophysical mechanisms related to surface albedo and evapotranspiration; these biophysical effects have been shown to

lead to cooling with increased rainfall in the tropics or warming in higher latitudes of the boreal due to reduced surface albedo (Bala *et al*., 2007; Li *et al*., 2015). As such, further changes in tree cover due to disturbance or mass mortality events have the potential to exacerbate climatic shifts in the coming years, thus highlighting a need to understand how trees can withstand large changes in growing conditions over their lifespans.

As long-lived and sessile organisms, trees are highly dependent on the storage and remobilization of resources such as C, water, and mineral nutrients to maintain functionality throughout phenological transitions, as well as to withstand and recover from stochastic stress and disturbance events that limit resource acquisition (Chapin *et al*., 1990). To better anticipate forest responses to a changing climate, it is becoming increasingly more important to understand — at the individual tree level — what physiological mechanisms regulate resource storage and remobilization responses, how and when remobilization limits growth and survival, and finally, how remobilization responses may differ across species, functional types, and environmental conditions. Understanding these mechanisms of stress resistance and resilience is crucial to developing a conceptual basis for predicting tree death or survival under more variable and extreme climate conditions. In the following thesis, I aim to address aspects of this large and overarching knowledge gap, assessing the dynamics of C reserve storage and remobilization in trees, and how these dynamics relate to survival responses under induced stress

1.2 Carbon reserves

During photosynthesis, atmospheric C is fixed to produce non-structural carbohydrates (NSCs) which serve not only as building blocks for biomass production but function also as a substrate to fuel respiration, reproduction, and defense (Chapin *et al*., 1990; Hartmann and Trumbore, 2016). NSCs are known to function in a variety of other physiological processes such

as cold tolerance and cryoprotection (Sakai and Larcher, 1987; Tinus *et al*., 2000; Morin *et al*., 2007; Tarkowski and Van den Ende, 2015), cell osmotic adjustment and desiccation tolerance (Ingram and Bartels, 1996), as well as embolism repair and hydraulic maintenance (Améglio *et al*. 2001; Bucci *et al*., 2003; Améglio *et al*. 2004). In addition, plants can also store excess NSC as reserves, predominantly in the form of soluble sugars and insoluble starch, but some select species may also utilize other storage molecules such as lipids (Hoch *et al*., 2003; Hoch, 2015) or sugar alcohols (Moing, 2000). NSC reserves are stored in tissues throughout the tree and can be remobilized during periods of asynchrony in C assimilation and demand, such as during the expected phenological progression of trees in seasonal environments (Kozlowski, 1992; Martinez-Vilalta *et al.*, 2016; Furze *et al*., 2019; Fermaniuk *et al*., 2021), or during more unpredictable disturbance events such as drought (McDowell *et al*., 2008; Sala *et al*., 2010), defoliation or top kill (Lamont *et al*., 2011; Landhäusser and Lieffers, 2012; Clarke *et al*., 2013), and biotic attack (Wiley *et al*., 2016).

While the roles of reserves in tree function have been acknowledged for over a century (Hartig, 1878; Fischer, 1891; Fabricius, 1905), studies of their roles in stress tolerance and survival have gained momentum in recent years due to the marked increase in climate-related forest mortality events (Allen *et al*., 2010; Adams *et al*., 2013; Anderegg and Anderegg, 2013; Anderegg *et al*., 2013; Sevanto *et al*., 2014). And while some studies have shown that NSC concentrations are associated with stress tolerance and survival (Kobe, 1997; Canham *et al*., 1999; Gleason and Ares, 2004; Moreira *et al*., 2012; Piper and Paula, 2020), our understanding of reserve allocation and remobilization processes remain poor — particularly in large and mature trees. Despite this, single tissue NSC measures are often used as proxies for the C status of trees, as measures of C availability for physiological functions like growth and defense, and as

indicators of the susceptibility of forests to future stress and disturbance events. However, without knowledge of what governs NSC allocation and its subsequent remobilization in different organs and their redistribution throughout trees, this practice remains controversial and problematic (Hoch *et al*., 2003; Körner, 2003; Sala *et al*., 2012; Hoch, 2015).

1.3 The source-sink framework and carbon reserve phenology

The economic analogy of storage provided by Chapin *et al*. (1990) posits that carbohydrate allocation to storage pools serves as an investment to account for the temporal asynchronies in C supply (source) and demand (sink). Source tissues or organs are those that behave as net C exporters, whereas C sinks are tissues or organs which import more C than is exported (Wardlaw, 1990; Kozlowski, 1992). The strength of a sink in organ tissues is generally determined by the potential physiological activity of cells within the tissue — with higher sink strengths being associated with tissues which have a greater maximum potential for physiological activity and C import (Wardlaw, 1990; Kozlowski, 1992). However, whether an organ tissue is behaving as a C source or sink, as well as the overall strength of the sink, may fluctuate considerably over time depending on the C supply and the organ's overall demand for C.

Because C supply and sink demand both exhibit strong seasonal variation, whole-organism and organ-level reserve pool sizes are believed to be tightly linked with phenology in trees. And as tree phenological growth patterns vary widely with climate as well as among functional types and traits, NSC reserve dynamics should vary substantially as well (Martínez-Vilalta *et al*., 2016). For example, large reserve fluctuations are expected in species or populations which occupy more seasonal climates with greater source–sink asynchronies. In deciduous tree species, this would imply a build-up of reserves as growth slows towards the end

of the growing season while primary production continues, and a decline throughout the non-photosynthetic period to support maintenance respiration and early spring growth (Kozlowski, 1992; Furze *et al.*, 2019). At the organ level however, storage patterns may substantially differ in part due to differences in the timing and duration of organ growth processes (Delpierre *et al.*, 2016; Fermaniuk *et al*., 2021), differences in organ function and their roles in C dynamics, (e.g., source leaves versus root sinks), differences in the ratio of physiologically active cells (e.g., the ratio of living to dead cells), as well as the possible interplay of a 'sink hierarchy' where distance between sources and sinks and the relative position of sinks with respect to the source may affect reserve allocation and remobilization (Wright, 1989; Wardlaw, 1990; Minchin *et al.*, 1993; Landhäusser and Lieffers, 2012; Hartmann *et al.*, 2018).

Understanding NSC reserve phenology and how it may contrast across species, functional types, life history traits, and even within species with ranges that span across different climatic or disturbance regimes is an important first step toward gauging species and region-specific risk to future stress events. For example, a stressor may be more likely to induce C limitation if it occurs when NSC reserves are at their seasonal minima. Therefore, species or populations inhabiting more seasonal environments which are expected to drive larger differences between reserve minima and maxima may be more vulnerable to C limitation, at least at this time of year. Similarly, NSC reserves may more likely limit survival at a time of reserve minima in fast-growing species or populations (which rely more on a 'bet-hedging' allocation trade-off) more than 'conservative' slow-growing trees which have been shown to allocate more NSC to storage (Wright *et al*., 2004; Blumstein *et al*., 2022; Signori-Müller *et al*., 2022). Even still, responses to similar stressors may contrast intra-specifically if populations exhibit genetic differences in allocation patterns due to differing climatic and disturbance selection pressures (Blumstein *et al*.,

2020; Blumstein and Hopkins., 2021; Blumstein *et al*., 2022). Only once baseline (i.e., normal) NSC reserve phenology has been understood for a given species in a given region can we begin to develop an informed framework for NSC allocation patterns in responses to stress for that particular species.

In mature trees, NSC reserve phenology is typically inferred at the whole-tree level by observing how tissue reserve concentrations change in time over important phenological stages such as bud-flush, shoot expansion, fine root growth, and winter dormancy. Inferring whole-tree storage dynamics from these concentrations alone however is misleading since these measures do not account for the biomass of organ tissues sampled, nor do they account for differences in organ-level growth processes which makes comparisons difficult between individuals or species that have different organ biomass proportions or sizes. Though less commonly employed, a more suitable way to make these comparisons may instead be to estimate the seasonal changes of C pool sizes through allometric scaling (Hartmann *et al.*, 2018). Although some C in reserve pools may be unavailable for metabolism (Millard *et al*., 2007; Sala *et al*., 2012; Hoch, 2015; Martínez-Vilalta *et al*., 2016), scaling seasonal NSC dynamics with organ biomass could establish estimates of the total amount of reserves available to a tree in each organ and their fluctuation in time, which coupled with NSC concentrations can provide a more complete approach for comparing C dynamics across individuals and species (Barbaroux *et al.*, 2003; Furze *et al.*, 2019; Fermaniuk *et al*., 2021; Schoonmaker *et al.*, 2021).

1.4 Spatial limitations to reserve remobilization

Top-down allocation is a prominent theory that predicts C allocation priority to be greatly determined by a tissue's proximity to the canopy, with tissues closer to photosynthetic organs receiving greater access to photoassimilates under increasing C stress. This preferential

allocation is thought to be related to phloem function (Turgeon, 2006; Wiley *et al*., 2017b). Under a top-down allocation strategy, the roots would be affected first and disproportionately more than other organs when C supply is declining, as supported by the finding that root NSC pools take longer to refill following defoliation than do the branches (Landhäusser and Lieffers, 2012), as well as the finding that stemwood NSC levels, and not branch (with foliage removed) NSC levels, are reduced in Douglas Fir with Swiss Needle Cast infection (Saffell *et al*., 2014). If allocation priority is determined in this manner, C shortages may be even more exaggerated in tall, mature trees that have large stems with their own sink demands, and where canopy and root organs may be separated by great distances (Landhäusser and Lieffers, 2012).

Although tree organs are highly integrated and NSC reserves can be mobilized among them (Chapin *et al*., 1990), distance between reserve sources and sink tissues may play a role in the extent to which sinks receive remobilized NSC under C limitation. Consistent with top-down allocation theory, it is generally believed that sinks will more preferably receive remobilized NSC from local as opposed to more distant reserve sources (Ericcson *et al*., 1996). In support of this, tissue-specific declines in NSC reserves have been observed which emphasize the effect of distance on reserve accessibility and in turn suggest that C stress and starvation could theoretically be experienced disproportionately throughout a tree (Hartmann *et al*., 2013; Wiley *et al*., 2016). In tall trees, despite their lower NSC concentrations, the large biomass of wood in the stems and coarse roots of mature broadleaved can make these woody tissues the largest reserve pools in a tree (Barbaroux *et al*., 2003; Würth *et al*., 2005; Hartmann *et al*., 2018), which may lead to the assumption that these storage pools serve as a source to other, potentially more distant, sinks (such as the fine roots) during periods of C limitation. However, if a distance-dependent hierarchy exists among reserve sources and sinks, and if this hierarchy is exaggerated

in large trees, then the availability of these stem and coarse root reserves to more distant tissues during reserve remobilization is likely greatly overestimated.

1.5 *Betula papyrifera*

Paper birch (*Betula papyrifera*) is a fast growing, relatively shade-intolerant species, which extends trans-continentally across large climatic and edaphic gradients in North America from the north-west Alaskan treeline to the more temperate forests of the north-eastern USA (Safford *et al.*, 1990). Paper birch is characterized by its white outer bark and its general adaptability to a wide suite of soil, topographical, and climatic conditions. In the past century however, increased prevalence of branch dieback in birch has been observed, though presently, no notable causal agent other than rootlet injury due to freeze/thaw cycles has been attributed to these dieback events (Stroh and Miller, 2009).

Although trembling aspen (*Populus tremuloides*) is a more commonly employed boreal species to explore how C reserve allocation and remobilization patterns relates to observed deciduous dieback in North America, the clonal nature and shared root system of this species constrains our ability to assess the more specific question of how inter-organ reserve remobilization patterns relates to survival responses in natural mature stands. Unlike trembling aspen, paper birch does not share a root system and predominantly reproduces vegetatively through root collar sprouting as opposed root suckering, and as such, serves as a more suitable model species for exploring how inter-organ reserve remobilization of mature individuals in natural stands relates to survival response under C limiting conditions.

1.6 Research Objectives

The overall objective of this thesis was to investigate C reserve (NSC) phenology in mature boreal paper birch and use these findings to inform how organ NSC remobilization patterns differ

when under organ-level C limitation. More specifically, Chapter 2 aims to characterize the seasonal dynamics of tissue and organ NSC concentrations, as well as estimates of whole-tree and organ-level NSC pool sizes, in relation to defined phenological stages and growth of mature boreal *B. papyrifera*. Chapter 2 also aims to assess how the phenological patterns of NSC may differ across the range of *B. papyrifera* through contrasting reserve patterns between boreal and more temperate trees. Through a simple girdling experiment, Chapter 3 aims to explore NSC remobilization patterns at the organ-level of these same *B. papyrifera* trees functioning under reserve dependency in the roots, or in both the root and stem organs. In addition, Chapter 3 seeks to broadly partition out the storage contribution, if any, of stem NSC reserves to canopy and root tissues, and of root NSC reserves to the stem under storage dependent condition, as well as to assess any effects of distance on these processes. Lastly, Chapter 3 aims to use the effects of girdling treatments on NSC reserves and water relations to explore how these factors influence survival responses such as leaf-flush, root-collar sprouting, defense, and the re-establishment of the hydraulic system following winter.

2. Chapter 2 – Large seasonal fluctuations in whole-tree carbohydrate reserves: is storage more dynamic in boreal ecosystems?

2.1 Introduction

Non-structural carbohydrates (NSC) in trees, primarily in the form of soluble sugars and insoluble starch, act as metabolic substrates and can be stored as reserves. NSC can be remobilized from storage to support growth and other metabolic functions when a tree is in carbon deficit, such as during regular seasonal growth or during more unpredictable events like drought or defoliation. As such, NSC dynamics have been tightly linked to growth and mortality processes (Landhäusser *et al*., 2012; Adams *et al*., 2013; Sevanto *et al*., 2014), and thus have received significant attention. Nonetheless, it is still poorly understood how NSC storage dynamics, at the whole-tree and organ level, interact with both seasonal growth processes and responses to stress (Sala *et al*., 2012, Dietze *et al*., 2014).

The seasonal dynamics of NSC concentrations at the organ and whole-tree level are thought to be driven by phenological changes which vary among climates and plant functional types and traits (Martínez-Vilalta *et al*., 2016). In general, reserve fluctuations throughout the year are believed to be a function of the balance between the supply of incoming carbon (source) and the demand for growth, respiration, or other physiological processes (sinks) (Chapin *et al*., 1990) – with larger fluctuations expected to occur in more seasonal climates with greater source-sink asynchronies. Although both temperate and boreal climates are considered to be highly seasonal, the colder winter temperatures and shorter growing season characteristic of the boreal might yield a potential for larger seasonal oscillations of NSC in this region. This pattern, however, has yet to be confirmed (Martínez-Vilalta *et al*., 2016).

Regardless of climate, NSC accumulation at the whole-tree level occurs when source activity exceeds sink activity, and remobilization occurs under the opposite conditions (Mooney, 1972; Chapin *et al*. 1990); in deciduous species, this would imply a buildup of reserves as growth slows towards the end of the growing season, and a decline throughout the non-photosynthetic period to support maintenance respiration and early spring growth (Kozlowski, 1992; Furze *et al*., 2019). At the organ level however, seasonal storage patterns may contrast in part due to differences in the timing and duration of organ growth processes (Delpierre *et al*., 2016), as well as the possible interplay of a 'sink hierarchy' where a prioritized allocation of photosynthates to sinks in closer proximity to source organs may occur (Wright, 1989; Wardlaw, 1990; Minchin *et al*., 1993; Landhäusser and Lieffers, 2012; Hartmann *et al*., 2018).

In mature trees, the seasonality of carbon storage at the whole-tree level is commonly inferred by observing changes in the NSC concentrations of individual tissues or organs over time. Though these smaller scale measurements are vital when considering such functions as osmoregulation and frost tolerance, inferring whole-tree storage dynamics from these concentrations alone can be problematic. These measures provide little estimation of the storage at the whole-tree level, as organs or tissues may display contrasting seasonal NSC dynamics (Delpierre *et al*., 2016), nor do they account for the relative mass of the organs storing the NSC, making comparisons difficult between individuals or species that have different organ biomass proportions or sizes. A more suitable way to make these comparisons may be to instead estimate carbon pool sizes and their seasonal changes through the use of allometric scaling of whole-tree carbon dynamics (Hartmann *et al*., 2018). Despite the notion that some carbon in the reserve pool may be permanently sequestered and thus unavailable for metabolism (Millard *et al*., 2007; Wiley *et al*., 2016), scaling seasonal NSC dynamics with tree biomass could establish estimates

of the total amount of reserves available to a tree and their fluctuation in time, which coupled with NSC concentrations, can provide a more complete approach for comparing carbon dynamics across individuals and species (Barbaroux *et al*., 2003; Furze *et al*., 2019; Schoonmaker *et al*., 2021). However, few studies have taken this approach, as whole-tree NSC estimates are often difficult to obtain, particularly for large trees, thus there is a significant need to establish how reserve patterns at the whole-tree level relate to concentrations patterns at organ level. While such data are critical for the development and evaluation of ecosystem-level models used to predict forest responses to global change (Dietze *et al*., 2014), there are presently very few studies that use this approach with high temporal and spatial resolutions (Gough *et al*., 2009; Furze *et al*., 2019; Schoonmaker *et al*., 2021).

Paper birch (*Betula papyrifera*) is a fast growing, relatively shade-intolerant species, which extends trans-continentally across large climatic and edaphic gradients in North America from the northwest Alaskan treeline to the more temperate forests of the northeastern USA (Safford *et al*., 1990). The aim of this study was to characterize the seasonal dynamics of tissue and organ NSC concentrations, as well as estimates of whole-tree and organ level NSC pool sizes, in relation to defined phenological stages and growth of boreal *B. papyrifera* and draw parallels to data collected from *B. papyrifera* trees at a more temperate climate. Specifically, we sought to: (1) investigate seasonal shifts in carbohydrate concentrations (NSC, soluble sugar, and starch) in key tissues and organs in response to growth processes, (2) estimate, based on allometric estimates, the size of the whole-tree NSC pool and the relative contribution of different organs to that pool, and (3) explore reserve storage and remobilization at the whole-tree and organ level, by examining seasonal changes and determine the magnitude of these changes.

2.2 Materials and Methods

2.2.1 Study site description and sample collection

In late May 2018, ten healthy codominant *B. papyrifera*. Trees were selected in a large mature monospecific and even-aged birch stand located at the southern edge of the boreal dry mixedwood forest region in Alberta (54°17'13.59" N, 112°46'27.74" W). Trees in the stand showed evidence of having been cut back to their base approximately 30 years ago, thus regenerating from basal sprouts and developing a closed canopy with very little understory vegetation. The surface soil and main rooting space in this site is dominated by an 18 cm deep organic horizon that consisted of well decomposed material. Overall, the site was considered rich, with a mesic moisture regime and moderately to well-drained soils.

To allow for the repeated sampling of individual trees without severely impacting an individual stem, we selected multi-stemmed individuals (hereafter called 'trees') for this study. Selected trees had three to five stems that were all co-dominant (i.e., upper crown had access to full light conditions) and were between 9 and 13 m tall. Trees were a minimum of 20 m apart from each other. To determine the seasonal fluctuations of NSCs in *B. papyrifera*, the following seven tissues (organs) were sampled in each tree throughout the course of a year: (1) fine roots — < 2 mm diameter, (2) coarse roots — between 10 and 15 mm diameter, (3) current (1- year-old) twigs — < 3 mm diameter, (4) large diameter branch — between 4 and 7 mm diameter, (5) fully expanded leaves (when available) and springtime buds, (6) stemwood — water conducting xylem (sapwood), and (7) inner bark — including the phloem and excluding the outer bark. Xylem sap was also collected during the period between soil-thaw and bud-break by drilling a hole at breast height (0.19 mm diameter and 2.5 cm deep), connecting a spile, hose, and collection tube. Root samples were carefully collected by following roots from the base of each tree using hand pruners. Crown samples (shoot and leaf material) were collected by cutting a

branch from the outer portion of the crown fully exposed to light using a tall ladder (5 m) and a pole pruner (5 m). The two stem tissues samples (6) and (7) were collected by chiselling a 1.9 cm wide by 1.9 cm long by 1.5 cm deep sample at breast height. For the bark, the outer portion of bark tissue was separated from the inner portion (including phloem) with a razor blade. To minimize the impact of sampling on individual stems, samples were obtained from different dominant stems at each sampling date.

Sampling dates aimed to capture the main phenological stages of birch during a calendar year. Thus, samples were collected when more than half of the trees were determined to have reached a particular phenological stage. The eight sampling dates were as follows: (1) early shoot expansion —shoot expansion only with preformed leaves < 5 cm; 24 May. 2018, (2) long-shoot expansion — long-shoot growth (shoots were > 10 cm with neo-formed leaves); 19 Jun. 2018, (3) late growing season — long-shoot growth terminated (bud set), but leaves green; 7 Aug. 2018, (4) leaf abscission — leaves yellow; 3 Oct. 2018, (5) fall dormancy — soil temperatures below 3°C; 15 Nov. 2018, (6) late winter dormancy— soil still frozen but xylem sap flows; 8 Apr. 2019, (7) early spring and bud-break — bud swell and leaf tips emerging, upper 10 cm of soil thawed; 8 May. 2019, and to close the seasonal cycle (8) long-shoot expansion (2019) — long-shoot growth (shoots were < 10 cm with neo-formed leaves); 11 Jun. 2019.

To quantify the seasonal production of fine roots, root ingrowth cores were established in six areas that were spaced at a minimum of 20 to 30m apart and within 5 to 10 m of the measured *B. papyrifera* trees. Prior to establishing root ingrowth cores, the sparse herbaceous vegetation was uprooted and removed. In each area, five circular holes (15 cm diameter) were then cored to a depth of 15 cm in the late spring (24 May. 2018) and the soil discarded. The holes

were then filled with clean peat material containing no roots. One core of peat material per area was removed at each of the following five phenological stages: (3) late growing season, (4) leaf abscission, (5) fall dormancy, (7) bud-break, and (8) long-shoot expansion. *B. papyrifera* roots were identified and extracted from the cores, oven dried at 70°C, and weighed to determine total root biomass.

To determine the seasonality of radial growth in the xylem tissue, 5 cm cores were extracted at all phenological stages with an increment borer adjacent to the location of the stem NSC sample collection. The cores were then mounted onto boards, sanded to 400 grit, and scanned at a resolution of 1000 dpi. The width of the most recent xylem ring was then measured using ImageJ software (Schneider *et al*., 2012).

2.2.2 Soil moisture and climate data

To monitor soil moisture and temperature, five soil moisture/temperature sensors (5TM VWC+ Temp, Decagon Devices Incorporated, Pullman, Washington, USA) were installed at a 15 cm depth in each of the six areas previously described to examine seasonal fine root production. Sensors were set to log data at hourly intervals, and daily averages were calculated across all blocks. In general, soil moisture levels suggested that the study site had received sufficient rainfall throughout the experimental period and trees did not experience water stress. Climate data was obtained from the Abee, Alberta weather station (54.28° N,112.97° W, 12 km from study site), provided by Alberta Agriculture and Forestry, Alberta Climate Information Service (ACIS, 2019).

2.2.3 Carbohydrate analysis

Tissue samples were oven dried (at 100°C for one hour and then at 70°C for 72 hours), ground using a ball mill (TissueLyser II; QIAGEN, Hilden, Germany), and then stored in airtight

containers until analysis. Following the protocols described in Landhäusser *et al*. (2018), soluble sugar concentrations were determined after a hot ethanol (80%) extraction followed by a colorimetric quantification using phenol-sufuric acid. The phenol-sulfuric acid method was also used to determine sugar concentration of the xylem sap following a 100× dilution with deionized water. Starch was hydrolysed to glucose using α -amylase from *Bacillus licheniformis* (Sigma-Aldrich A3403) and amyloglucosidase from *Aspergillus niger* (Sigma-Aldrige A1602). Glucose concentration was quantified colorimetrically using glucose oxidase/peroxidase-O-dianisidine solution and converted to starch equivalent. All carbohydrate levels are presented as a percentage of sample dry weight.

2.2.4 Allometric scaling from NSC concentrations whole-organ and whole-tree pools

We used the NSC concentration measurements of the multi-stemmed trees described above to estimate seasonal whole-tree and organ level NSC pool sizes for *single-stemmed* birch trees, using allometric equations specific to *B. papyrifera* with a DBH > 2.5 cm (Jenkins *et al*., 2004, Chojnacky *et al*., 2013). This approach assumes that that multi- and single-stemmed birch trees have similar NSC concentrations throughout the year. To test this assumption, we compared NSC concentrations of the multi-stemmed trees with that of nine single-stemmed codominant birch trees growing in the same stand at three phenological stages during the study. These single-stemmed trees were of the same age and DBH range as our multi-stemmed trees. NSC concentrations and seasonal dynamics were similar between the two tree types (**Table A-1**). Supporting the validity of our approach.

First, to estimate the aboveground biomass (kg), bm, for each aboveground component (branches, stemwood, and inner bark) of the nine single-stemmed trees, we used the following formula based on Jenkins *et al*. (2004):

$$bm = B * f \quad (1)$$

For these aboveground components, B was estimated as a function of diameter at breast height, DBH (cm), using the equation:

$$B = \exp(\beta_0 + \beta_1 \ln \mathrm{DBH}) \quad (2)$$

where β_0 = -2.2271 and β_1= 2.4513 (table 5 in Chojnacky *et al*., 2013). Aboveground B includes foliage, branches, stemwood, and bark. The fractions (f) of foliage, stemwood, and bark were calculated based on α_0 and α_1 coefficients from table 2 in Jenkins *et al*. (2004), as:

$$f = \exp(\alpha_0 + (\alpha_1/\mathrm{DBH})) \quad (3)$$

The branch fraction was estimated by subtracting the foliage, stemwood, and bark fractions:

$$f_{Branch} = 1 - f_{Foliage} - f_{Stemwood} - f_{Bark}$$

For the belowground component (i.e., coarse roots), the same equation (2) was applied to calculate belowground B, using β_0 = -1.4485 and β_1= -0.03476 (table 6 in Chojnacky *et al*., 2013). We also included an estimate of B for the fine roots using β_0 = -1.8629 and β_1= -0.77534 (table 6 in Chojnacky *et al*., 2013). The biomass (kg) for each belowground component was then determined by multiplying the total aboveground biomass (i.e., the sum of bm_{Foliage}, bm_{Branch}, bm_{Stemwood}, and bm_{Bark}) by its respective B. For each major component (i.e., branches, stemwood, bark, and coarse roots), the average biomass of all nine single stemmed trees was then calculated and is provided in Table A-2.

Second, to obtain NSC pool size estimates of each major component for single-stemmed trees, the organ-level NSC concentrations from each of the ten multi-stemmed trees were each multiplied by the average biomass of each respective component derived for the single-stemmed trees. Since our trees were small diameter and we did not collect the whole depth of the xylem, we acknowledge that scaling up NSC concentrations based on the outer 1.5 cm could have

yielded a potential overestimation of the stemwood NSC pool size by not accounting for 1) the biomass of inactive stem tissue (i.e., heartwood), and 2) a potential decrease of NSC concentrations and seasonal fluctuation with increased sapwood depth (Hoch *et al*., 2003). However, we believe that this overestimation is minimal in our trees, as these trees had very little heartwood, and the radial decline of NSC concentrations with sapwood depth was found to be small in diffuse-porous species, such as *B. papyrifera* (Hoch *et al*., 2003; Furze *et al*., 2020). For the branches, the NSC pool was calculated using the average NSC concentrations of branch and twig samples. The pool for each component (organ) was summed together to yield a whole-tree NSC pool size. The maximum difference (greatest seasonal change) of the NSC pool size in the different organs and in the whole tree were determined by subtracting the minimum annual estimate from the maximum annual estimate of the respective pools for each individual tree and organ.

For the whole-tree NSC pool estimates, we used the estimates for coarse roots, stemwood, inner bark, and branches, but did not include fine roots and foliage, as their contribution to the overall pool size was very low. For our nine single stemmed trees, the average $bm_{\text{fine root}}$, and bm_{foliage} were 0.9 and 1.09 kg, respectively, which together represent 4.4% of the total biomass. Adding their mass produced only small differences (increases) in the whole-tree NSC pool (the maximum being a difference of 11% of the total) (Table A-3).

2.2.5 Statistical analysis

All statistical analyses were performed using R v.3.5.1 (R Core Team, 2018); linear mixed-effect models (LME) were fit by maximum likelihood using the NLME package (Pinheiro *et al*., 2020). A repeated measures approach was incorporated to account for the lack of independence among observations across sampling dates. To assess whether NSC (combined

sugar and starch), sugar, starch concentrations for each organ, whole-tree NSC pool size, fine root biomass, and xylem radial growth varied across sampling dates, we used LME models with sampling date as a fixed effect and tree or block (for fine root biomass data) as a random effect. To assess if NSC pool size and the maximum seasonal change differed between organs, we used LME models with sampling date and organ as fixed effects and tree as a random effect. In most models (stemwood sugar, stemwood starch, inner bark sugar, and fine root biomass excepted), a by stratum variance structure was incorporated to account for heteroscedasticity in model residuals. Fixed effects were tested using analyses of variance (ANOVAs), and with the exception of NSC pool size models, significant ANOVAs were further evaluated with planned contrasts using the Behjamini-Yekutieli method of P-value adjustment. Since all pairwise comparisons were of interest for NSC pool size estimates, differences among organs within a sampling date, and differences among all sampling dates within an organ and at the whole-tree level were evaluated with Tukey's honest significant difference (HSD; α=0.05). Two-tailed paired *t*-tests (α=0.05) were applied to compare concentrations of NSC, sugar, and starch of tissues between the start and end of the seasonal cycle. Normality of the paired differences and the presence of outliers were assessed through visual inspection of histograms and boxplots; when strong evidence of non-normality was present, the Wilcoxon Signed-Ranks test was used.

2.3 Results

2.3.1 Overview

NSC concentrations and NSC pools, as well as the individual fractions of soluble sugars and starch, varied seasonally at the different phenological stages for all tissues examined ($P \leq$ 0.001 for all tests; Table A-4;

Table **A-5**). However, the seasonal dynamics in concentration and pool size were dependent on the organ examined (all interactions $P \leq 0.001$; Table A-4;

Table A-5). In addition, fine root biomass and xylem radial growth differed across phenological stages (both $P \leq 0.001$). Post hoc test results are provided throughout the following subsections which are organized chronologically by phenological stage; each subsection presents the comparisons made between the title phenological stage and previous phenological stage. Pool size comparisons are detailed separately in the last subsection.

We attempted to sample the first (2018) and last (2019) collection of NSCs at a similar phenological stage (i.e., the early shoot expansion stage when only preformed leaves were present); however, we were only able to complete the last collection at a slightly later stage when some neoformed leaves were already being produced. When compared between the first and last collection, total NSC concentrations were significantly higher in the inner bark, twigs, branches, and leaves (all $P \leq 0.05$; Figure 2-1a and b) at the last collection — driven predominantly by higher starch concentrations (Table A-6; Figure 2-2a and b). Total NSC concentrations in the stemwood and coarse roots were similar between the two collections (Figure 2-1b and c), while NSC concentrations were marginally lower ($P = 0.063$) in the 2019 fine roots (Figure 2-1c). Widths of the newly produced xylem at both times did not differ between these two collections ($P = 1.00$; Figure 2-3b). Overall, these relatively slight year-to-year differences in NSC concentrations were likely not associated with differing soil or climate conditions (Figure 2-3c and d), but rather, due to samples being collected somewhat later in 2019.

2.3.2 Shoot-expansion period

Between early shoot expansion and the long shoot expansion stage where shoots produced neo-formed leaves, NSC concentrations increased significantly in the large branches

and twigs (both $P \leq 0.001$; Table 2-1; Figure 2-1a). These increases were primarily associated with increases in starch concentrations (Table 2-2; Figure 2-2a). Starch concentration also increased in the inner bark at this time ($P \leq 0.01$; Figure 2-2b), though NSC concentrations were not affected ($P = 0.12$; Figure 2-1b). At this same time, sugar and starch concentrations remained unchanged in the stemwood (both $P > 0.76$; Figure 2-2b), although radial growth of the xylem had been initiated (0.46 mm of growth, Figure 2-3b). Belowground, NSC concentrations decreased from 3.06% to 2.18% in the fine roots ($P \leq 0.001$; Figure 2-1c), which was driven by a reduction in sugar concentrations ($P \leq 0.01$; Figure 2-2c). A similar reduction in sugar concentration was also found in the coarse roots ($P \leq 0.001$; Figure 2-2c), though this reduction did not significantly affect overall NSC concentrations ($P = 0.19$; Figure 2-1c).

2.3.3 Late growing season period

Between the period of long shoot expansion and the time when shoot expansion ceased and terminal bud-set had occurred, aboveground NSC concentrations increased significantly in the twigs, branches, and stemwood (Table 2-1; Figure 2-1a and b). Much like during the shoot expansion period, this increase was largely attributed to an increase in starch concentrations (Table 2-2; Figure 2-2a and b). However, no changes in NSC concentrations were observed in the inner bark ($P = 0.96$; Figure 2-1b) and leaves ($P = 0.97$; Figure 2-1a) at this time, though sugar concentrations decreased from 5.5% to 4.4% in the inner bark ($P \leq 0.05$; Figure 2-2b). During this same time, xylem ring width had increased by an additional 0.54 mm ($P \leq 0.05$; Figure 2-3b). Belowground, NSC concentrations also increased in both the fine and coarse roots (Table 2-1; Figure 2-1c), and like aboveground tissues, this increase was driven by increased starch concentrations (Table 2-2; Figure 2-2c). Lastly, root mass in the ingrowth soil cores had accumulated to 56 g m^{-3}_{soil} ($P \leq 0.05$; Figure 2-3a).

2.3.4 Leaf abscission period

During leaf abscission, average daily air temperatures dropped below 0°C, and daily soil temperatures were near 5°C (Figure 2-3c). In comparison to the late growing season, we observed higher sugar concentrations and lower starch concentrations in all aboveground organs (Table 2-2; Figure 2-2a and b), however the increase of sugar concentrations was not significant in the twigs ($P = 0.16$). In these aboveground organs, total NSC concentrations were higher in the leaves ($P \leq 0.01$), lower in the twigs ($P \leq 0.05$), and remained unchanged in the stemwood, inner bark and large branches (all $P > 0.13$; Figure 2-1a and b). No further growth in the xylem ring was observed ($P = 1.00$; Figure 2-3b). Belowground, root NSC concentrations peaked at this time with 6.7% in the fine roots ($P \leq 0.01$; Figure 2-1c) and 5.7% in the coarse roots ($P = 0.19$; Figure 2-1c). The higher values were driven by increases in both sugar and starch concentrations (both $P \leq 0.05$) in the fine roots (Figure 2-2c), and by sugar concentrations only in the coarse roots ($P \leq 0.05$; Figure 2-2c). During this time, fine root biomass in ingrowth soil cores had increased by an additional 65.8 g to a total of 121.8 g/m^3_{soil} ($P \leq 0.01$; Figure 2-3a).

2.3.5 Fall dormancy

When average daily soil temperatures dropped to near 3°C and daytime air temperatures remained below freezing (Figure 2-3c), NSC concentrations remained unchanged in all aboveground tissues compared to the leaf abscission period in early October (Table 2-1; Figure 2-1and b). In these same tissues, significant reductions of starch were observed (Table 2-2), but only the branches experienced a significant increase in sugar concentrations ($P \leq 0.05$; Figure 2-2a and b). No further xylem growth was observed ($P = 1.00$; Figure 2-3b). Belowground, NSC concentrations were reduced from 5.7% to 4.0% in the coarse roots ($P \leq 0.01$) but remained unchanged in the fine roots ($P = 1.00$; Figure 2-1c) compared to the leaf abscission period. The

reduction of NSC in the coarse roots was solely driven by reduced starch concentrations ($P \leq 0.01$; Figure 2-2c); although starch concentrations were reduced in the fine roots ($P \leq 0.01$), this tissue also experienced a significant increase in sugar concentrations during this time ($P \leq 0.05$; Figure 2-2c). Lastly, fine root biomass had not increased since leaf abscission ($P = 1.00$; Figure 2-3a).

2.3.6 Late winter dormancy period

Soil temperatures remained near 0°C throughout the entire winter season (mid-November – early April; Figure 2-3c). Monthly average air temperatures were -7°C throughout December and January, dropped to -21°C in February, and rose to -4°C by March (Figure 2-3c). Between the early and later dormancy stage, no changes were observed in NSC concentrations in any aboveground tissue (Table 2-1; Figure 2-1a and b). However, the branch, inner bark, and stemwood tissues exhibited significant reductions in sugar concentrations towards the late dormant season that corresponded to equal increases in starch concentrations (Table 2-2; Figure 2-2and b). Starch concentration in the twigs increased from 0.27% to 0.88% ($P \leq 0.001$; Figure 2-2a) during this time, but a reduction in sugar concentrations was not detectable ($P = 1.00$; Figure 2-2a). Unlike the above-ground tissues, NSC, sugar and starch concentrations remained constant in both the fine and coarse roots during this time (Table 2-1; Table 2-2; Figure 2-1c; Figure 2-2c). Lastly, no xylem or fine root growth occurred between mid-November and early April (both $P > 0.5$; Figure 2-3a and b).

2.3.7 Early spring and budbreak period

When average daily air temperatures rose above 0°C in the early spring (Figure 2-3c) positive sap pressure began to develop in the stem and overwintering buds began to swell in preparation for flush In comparison to the late dormancy stage, we observed significantly

reduced sugar concentrations that coincided with increased starch concentrations in the twigs, branches, and inner bark (Table 2-2; Figure 2-2a and b), but total NSC remained unchanged in these tissues (all $P > 0.13$; Figure 2-1a and b). NSC concentrations did not change in the swelling buds during this time ($P = 0.27$; Figure 2-1a), however, sugar and starch concentrations were marginally reduced (both $P \leq 0.08$; Figure 2-2a). Sugar, starch and overall NSC concentrations did not change in the stemwood during this time (all $P > 0.11$; Figure 2-1b; Figure 2-2b), and no significant change in xylem ring width was detected ($P = 1.00$; Figure 2-3b). Additionally, sugar concentrations in the xylem sap collected on April 17 and April 26 did not differ ($P = 0.51$), and together averaged to 6.57± 2.09 mg/ml (±*SD*) (data not shown). By the time of bud-break, soil temperature remained near 0°C (Figure 2-3c) and NSC concentrations were reduced in the fine roots ($P \leq 0.05$) but not in the coarse roots ($P = 1.00$; Figure 2-1c), in comparison to late dormancy measurements. This change in the fine roots was solely driven by reduced sugar concentrations ($P \leq 0.01$;Figure 2-2c) and did not coincide with increased fine root biomass in the ingrowth cores ($P = 1.00$; Figure 2-3a). Only once long shoot expansion had commenced did we detect a marginal increase in root mass (46 g $m^{-3}{}_{soil}$, $P \leq 0.1$; Figure 2-3a), which was similar to the amount that had accumulated in the first part of the 2018 growing season when ingrowth soil cores were installed ($P = 0.61$).

2.3.8 Seasonal changes in whole-tree and organ-level NSC pool sizes

Throughout the growing season, the estimated whole-tree NSC pool increased from its minimum right after spring flush to its maximum at bud-set with a small decline through the leaf abscission and dormant period (Figure 2-4a). Between minimum and maximum NSC storage, the average change in the whole-tree NSC pool was 0.96 kg per tree, which represents a 72% increase of the whole-tree NSC pool over this period (Figure 2-4a).

Although the stemwood represented the largest fraction of tree biomass (Table A-2), the NSC stored in the branches made up the majority of the whole-tree NSC pool throughout the year (ca. 48-60% of the whole-tree NSC pool, Figure 2-4a and b; Table 2-3). The coarse root pool exhibited significantly greater NSC mass in comparison to the stemwood pool at all sampling dates except for late winter dormancy and bud-break (both $P = 0.41$; Figure 2-4c and d; Table 2-3). However, the mass stored in the coarse root pool was only greater than the inner bark pool during the times of early shoot expansion and leaf abscission (both $P \leq 0.024$; Figure 2-4c and d; Table 2-3). When comparing the stemwood and inner bark pools, NSC mass was significantly greater in the inner bark pool throughout all shoot expansion stages, as well as during fall dormancy (all $P \leq 0.017$; Figure 2-4c; Table 2-3).

The smallest (minimum) NSC pool size was observed during the early shoot expansion stage in the branches; however, the minimum was delayed into the long-shoot expansion stage for the stemwood and coarse roots (Figure 2-4b, c, and d). In the inner bark, this minimum NSC pool size was not reached until bud-break (Figure 2-4c). The largest (maximum) NSC pool size was observed at bud-set in the branches but was delayed into the leaf abscission period for the stemwood, inner bark, and coarse roots (Figure 2-4b, c, and d). The largest seasonal fluctuation in NSC pool size occurred in the branches, which exhibited a change in NSC (ca. 0.73 kg) nearly four times greater than that of the coarse roots (ca. 0.23 kg; $P \leq 0.001$) and stemwood (0.17 kg; $P \leq 0.001$), and nearly eight times greater than the fluctuation observed in the inner bark (ca. 0.09 kg; $P \leq 0.001$; Figure 2-4c and d). No significant difference in maximum seasonal fluctuation was observed between the coarse roots and stemwood pools ($P = 0.252$), however, both organs exhibited stronger fluctuations than the inner bark pool (both $P \leq 0.004$; Figure 2-4c and d).

2.4 Discussion

In this comprehensive seasonal NSC study, we found that the seasonal dynamics of whole-tree NSC pools of boreal *B. papyrifera* were largely in agreement with the general understanding of the dynamics of carbohydrate reserves storage in cold-temperate deciduous trees (Mooney, 1972; Chapin *et al*., 1990; Hoch *et al*., 2003). Nevertheless, the magnitude of the fluctuation in NSC pool size over the growing season was truly remarkable. From their minima, the mass of non-structural carbohydrates in the study's trees increased by over 72% throughout the growing season, greatly exceeding the seasonal NSC fluctuation observed in *B. papyrifera* from a temperate environment (ca. 28% increase; Furze *et al*., 2019). It should be noted that the seasonal fluctuation of NSCs in temperate birch did not include estimates for the inner bark NSC pool. However, if we were to exclude this component from our calculations for boreal birch, the seasonal fluctuation of the whole-tree NSC pool would be even greater (ca. 87% increase; Table A-3). Although the inner bark pool did not exhibit extensive NSC fluctuations throughout the year (Fig. 4c), the inclusion of this pool increased our estimates of whole-tree NSC storage by 14% to 23% throughout the year (Table A-3). In addition, the absolute size of the inner bark NSC pool was significantly greater than the stemwood pool at times, despite its lower biomass (Table 2-3; Table A-2). Thus, the inner bark contains a substantial proportion of the whole-tree NSC pool and should be included when estimating carbon storage in trees — an aspect which has often been overlooked in previous studies (Wiley *et al*., 2019).

In our trees, the whole-tree NSC pool built up from its minimum of 1.33 kg shortly after spring flush to its maximum of 2.29 kg late in the growing season, declining only slightly during leaf abscission and the dormant period (Figure 2-4a). In birch growing in a more temperate climate, this seasonal increase was driven solely by NSC accumulation in the branches (supporting information table S7 in Furze *et al*., 2019), whereas we observed accumulation not

only in the branches, but in the stemwood and coarse root pools as well (Figure 2-4b, c, and d). Differences in ontogenetic stage and size of the individuals between the two studies (with the temperate trees being larger and older) could at least partially explain why such a difference in the magnitude of seasonal NSC fluctuation was observed (Hartmann *et al*., 2018). For instance, the hydraulic constraints imposed with increasing tree height may require taller trees to maintain more NSC for hydraulic function, which in turn may lead to reduced fluctuations in NSC mass (Sala *et al*., 2012). In addition, we acknowledge that sampling and scaling up the most dynamic outer rings of stemwood could have resulted in a slight overestimation of NSC fluctuation in the stemwood pool and thus the whole tree, however, recent research has suggested that the degree of seasonal fluctuation may remain relatively high across sapwood depth in species with diffuse-porous wood anatomies, such as *B. papyrifera* (Furze *et al*., 2020).

Despite tree size and methodological differences between the two studies, we believe that the observed disparity in seasonal fluctuations is unlikely to be explained by these factors alone. We hypothesize that these differences might represent a response to a more northern climate, where trees experience shorter growing seasons and greater climatic (e.g., temperature) variability and may thus require a stronger drawdown of reserves in the spring to initiate new growth, as well as prioritise reserve storage across the whole tree once refilling begins (Wiley and Helliker 2012; Martínez-Vilalta *et al*., 2016). Apart from the contrasting climates that could drive these phenological differences through acclimation, one can also speculate that genetic divergences between these widely spaced populations could also play a role, with populations being exposed to differing selection pressures in their respective environments (Blumstein et al., 2020). Evidence of substantial heritable genetic variation associated with climate and significant genotype × environment interactions for the NSC concentrations in *Populus trichocarpa*

suggests that adaptive differences in storage between populations may have arisen in response to climatic differences (Blumstein and Hopkins, 2021). Alternatively, adaptive differences in storage patterns could also stem from differences in the disturbance regime between the two regions. For example, differences in constitutive defense in *B. papyrifera* was observed to be higher in more northern boreal populations of birch that are more prone to fire and browsing pressure from disturbance associated hare populations (Bryant *et al*. 2009). This could suggest a potentially greater need for reserve pools in the shoots of boreal birch populations for shoot regeneration and the production of epidermal resin glands that exude defense compounds onto the bark of the new shoots (Bryant *et al*. 2009). If true, our finding may suggest that despite the seasonal similarities between boreal and temperate environments, the differences in climate or disturbances regimes that do exist may drive selection of trees in the boreal to exhibit stronger seasonal fluctuations in NSC reserves, particularly so in the branches.

The greatest seasonal fluctuation of NSC mass we observed was in the branches of our birch trees —nearly four-fold greater than in the stemwood and coarse root pools, and eight-fold greater than the inner bark pool (Figure 2-4b, c, and d), indicating that the branch storage pools were the most dynamic and likely the main source of NSC remobilized to support processes relying on storage. Notably, the seasonal trend of NSCs in the branch pool mirrored that of the whole-tree (Figure 2-4a and b), thus suggesting that whole-tree storage dynamics were largely driven by storage changes at the branch level in these trees. Considering that the minimum branch NSC pool size occurred shortly after leaf out, we can, at least in part, attribute this fluctuation in NSC reserves to be associated with the remobilization of branch reserves to fuel the flushing and expansion of new leaves and shoots. In comparing branch carbohydrate concentrations between the pre-leaf out period at late dormancy and post-leaf period prior to

substantial shoot expansion, the difference in concentration was roughly 3.5%, which is much greater than what has been observed in temperate birch and boreal aspen (*Populus tremuloides*) during leaf flush (Landhäusser, 2011; Furze *et al*., 2019). This might also indicate that boreal birch shoots become carbon autonomous later in development compared to shoots of temperate birch or even boreal aspen (Landhäusser, 2011). The reliance of new leaf and shoot expansion on proximal NSC pools (i.e., in the twigs and branches) has been well documented in deciduous trees (e.g., Landhäusser and Lieffers, 2003; Landhäusser, 2011; Klein *et al*., 2016), however, the role of more distal pools such as those in the stem and roots is less clear during this phenological stage (Landhäusser and Lieffers, 2003; Landhäusser and Lieffers, 2012). Despite the overall cost of this process to the whole-tree carbon pool, reserves appeared to recover in the branches soon after initial shoot and leaf expansion — roughly 30 days post bud-break (Figure 2-4b), which is in line with past estimates for *Carpinus betulus*, *Fagus sylvatica,* and *P. tremuloides* (Schädel *et al*., 2009; Landhäusser, 2011).

Unlike the branches, reserve accumulation in roots was delayed into the late growing season after bud set, with the seasonal maximum being further delayed into the leaf abscission period (Figure 2-4d), likely due to competing growth sinks in the crown and stem (Landhäusser and Lieffers, 2012). Although shoot growth was mostly terminated by late June, the duration of stem radial growth extended from approximately early June to late July (Figure 2-3b). At no point throughout this period did we detect a reduction in the stemwood NSC pool (Figure 2-4c), which suggests that this growth was fueled primarily by current photoassimilates, reducing NSC available for transport belowground. The resumption of fine root growth appeared to coincide with the onset of stem radial growth by early June, but extended much later in the season, only ceasing around leaf abscission (Figure 2-3a). The significant reduction in fine root NSC

concentrations in early June (Figure 2-1c) coupled with the slight reduction in the coarse root NSC pool (Figure 2-4d) suggest that root reserves, either alone or with current photoassimilates, were remobilized to initially fuel root growth. Interestingly, the fine root mass present in August 2018 ingrowth cores (56 g m^{-3}_{soil}) was similar to the mass produced by June in the 2019 season (46 g m^{-3}_{soil}) (Figure 2-3a), seemingly indicating a burst of fine root growth early in the growing season, followed by a period of minimal growth throughout July which is well aligned with the period of stem radial growth. This apparent cessation of root growth during the period of active radial stem growth provides additional evidence supporting the concept of a sink-hierarchy in large trees (Wright, 1989; Wardlaw, 1990). Specifically, this finding supports the notion that the stem represents a higher priority sink due to its proximity to photosynthetic organs during the growing season and that the more distal root system will only start filling NSC reserves once this sink is mostly sated (Minchin *et al*., 1993; Landhäusser and Lieffers, 2012). It is also possible that this apparent shift in allocation priority from above to belowground organs may, at least in part, be regulated by changes in temperature and day length or the senescence of leaves and the breakdown of the photosynthetic system in the early fall.

Between the late growing season and leaf abscission stage, we observed a sharp increase in the NSC concentration in leaves during the abscission period, which may have consequences for nutrient availability at this site (Figure 2-1a). Despite excluding foliar NSC in our calculation of whole-tree pool size, if we were to consider the October pool size both with and without foliage, the difference equates to a loss of roughly 0.19 kg (or 8.7%) of NSC in the abscised leaves, most of which were soluble sugars. Such a buildup of soluble sugars in the foliage may be a mechanism to protect the senescing leaves from early frost damage which may otherwise prevent the complete remobilization and resorption of leaf nutrients into overwintering tissues.

This buildup could also be associated with the breakdown of phloem transport between the leaves and neighboring tissues (i.e., twigs) at the abscission zone, as has been similarly found in the senescing leaves of *Ricinus communis* (Jongebloed *et al*., 2004). Although this may be viewed as a waste of carbohydrate at the tree level, this loss of carbon to the leaf litter may benefit decomposers as an easily accessible energy source that supports rapid decomposition of leaf material and release of nutrients, facilitating greater rates of nutrient uptake for the tree (Sayer *et al*., 2006). Indeed, Zukswert and Prescott (2017) observed very rapid decomposition of *B. papyrifera* litter over a 93-day period, and interestingly, the percent of litter mass lost during this time was considerably greater than that observed for *P. tremuloides* –another fast-growing species common to the study region. Though other physical and chemical leaf/litter characteristics play a role in the decomposability of leaf material (Zukswert and Prescott, 2017), we suspect one reason for this difference is lower leaf sugar concentrations present in *P. tremuloides* at the time of abscission (ca. 14% dry weight; Landhäusser and Lieffers, 2003).

The observed reduction of fine root sugars during the early spring was likely linked to the development of root pressures in association with the characteristic period of sap exudation or "bleeding" of excised or injured *B. papyrifera* stems (Figure 2-2c). During this period of bleeding, it is thought that positive xylem pressures help refill embolisms which have accumulated in the xylem conduits over the winter (Essiamah and Eschrich, 1985; Sauter & Ambrosius, 1986; Milburn and Kallarackal, 1991; Westhoff *et al*., 2008; Hölttä *et al*., 2018). Unlike the genus *Acer* where the refilling is primarily due to a local pressurisation in the stem (Tyree, 1983), positive pressures are present throughout the whole xylem system in *Betula* — with the development of root pressure playing an important role in refilling conduits from the bottom up (Westhoff *et al*., 2008). Though the concept of root pressure has yet to be thoroughly

explained, it is generally agreed that the active uptake of mineral solutes allows for a pressure buildup as a result of an osmotic influx of soil water into the root. The expenditure of energy for this uptake would explain the loss of sugar observed in the fine roots during this time. While root reserve translocation or growth expenditure in the fine roots could also reduce root NSC concentrations, there is little evidence for fine root growth (Figure 2-3a) or changes in other organ NSC pool sizes (Figure 2-4b, c, and d) at this time.

As colder temperatures commenced in the fall, we observed a significant starch-sugar conversion in all aboveground tissues (Figure 2-2a and b) which we attribute to the development of cold hardiness (Charrier *et al*., 2013; Furze *et al*., 2019, Schoonmaker *et al*., 2021). In perennial species, this conversion into soluble sugars is a common frost protection strategy which prevents intracellular ice formation and stabilizes cell membranes and proteins during dehydration caused by extracellular ice formation (Welling and Palva, 2006; Kasuga *et al*., 2007; Morin *et al*., 2007; Tarkowski and Van den Ende, 2015). In contrast to the birch trees in our study which retained very little starch in the aboveground tissues at the onset of dormancy (ca. 2.7% of aboveground NSC; Figure 2-2a and b), starch remained a relatively important component of aboveground storage in temperate *B. papyrifera* at the height of winter (ca. 10% of aboveground NSC; Furze *et al*., 2019), which may reflect a diminished need for frost protection due to milder winters. At the time of starch conversion to soluble sugars in our trees, the branches still retained over half the whole-tree NSC, which potentially indicates a heightened need for frost protection in crown tissue where there is greater proportion of living cells in branch phloem and overwintering buds, less insulation with depth (thinner bark), and greater convective heat loss due to wind exposure. This idea is further supported by higher sugar concentrations in the branches and twigs of our trees at the beginning of dormancy (ca. 7.5% dry

weight; Figure 2-2a) compared to temperate birch at the height of winter (ca. 6.4% dry weight; estimated using pool size values (figure 5 in Furze *et al*., 2019) and organ biomass estimates (supporting information table S2) in Furze *et al*., 2019). Considering that the amount of NSC accumulated in the late fall can be positively correlated with frost tolerance (Charrier *et al*., 2013), we can speculate that any interruption of starch accumulation throughout the growing season (i.e., drought or herbivory events) could greatly reduce the extent of frost protection in these tissues at dormancy, potentially resulting in extensive tissue mortality over winter (e.g., Galvez *et al*., 2013). Frost damage to branch xylem and/or phloem due to reduced growing season starch accumulation could be a simple mechanism underlying the widespread branch dieback observed in North American birch stands. Extensive branch winter dieback was also found to be associated with reduced stemwood starch concentrations in European *Quercus spp*. following a severe drought (Bréda *et al*., 2006), and in *Quercus velutina* following complete defoliation (Wiley *et al*., 2017a).

In the roots, this starch-sugar conversion did not occur in October when soil temperatures neared 5°C, but instead was delayed into mid-November when root temperatures reached 3°C. Landhäusser *et al*. (1996) found that *B. papyrifera* seedlings collected at the arctic tree-line exhibited fine root growth when kept at a root zone temperature of 3°C; while we did not detect fine root growth at this temperature, we did however observe a large, though non-significant, decline of NSC in the coarse root pool between October and November when soil temperatures ranged between 5°C and 3°C (Figure 2-1c, Figure 2-3c). Although respiration associated with maintenance and cold acclimation likely contributed to this decline to a certain extent, we suspect that a portion of this decline also reflects a growth expenditure, potentially supporting late season root elongation and diameter growth (Desrochers *et al*., 2002; Landhäusser and

Lieffers, 2003) as *B. papyrifera* root growth appears less sensitive to low soil temperatures (i.e., 3°C) than other coexisting boreal deciduous species such as *Populus balsamifera* and *P. tremuloides* (Landhäusser *et al*., 1996; Landhäusser and Lieffers, 1998; Wan *et al*., 2001; Landhäusser, 2003), likely an appropriate adaptation for a broadleaf species that forms the northern limit of deciduous trees in North America (Landhäusser and Wein, 1994).

2.5 Tables

Table 2-1 Changes in total non-structural carbohydrates (NSC) concentrations of tissues in mature *Betula papyrifera* between subsequent sampling dates. Changes in concentrations are the differences in the estimated marginal means from the linear mixed-effects models for each specified contrast. P-values for each comparison of sampling dates were adjusted using the Behjamini-Yekutieli method and indicate significant changes in NSC concentrations accordingly: NS = not significant, (*) = $P \leq 0.1$, * = $P \leq 0.05$, ** = $P \leq 0.01$, and *** = $P \leq 0.001$.

	Change in NSC Concentration (Δ %)					
	May/18 - June/18	Jun/18 - Aug/18	Aug/18 - Oct/18	Oct/18 - Nov/18	Nov/18 - Apr/19	Apr/19 - May/19
Fine Roots	-0.88 (0.18) ***	1.08 (0.39) *	3.48 (1.02) **	-0.58 (1.08) NS	-0.41 (0.60) NS	-1.74 (0.58) *
Coarse Roots	-0.88 (0.45) NS	1.67 (0.61) (*)	1.12 (0.60) NS	-1.73 (0.47) **	-0.60 (0.30) NS	-0.03 (0.33) NS
Inner Bark	1.06 (0.39) NS	-0.48 (0.49) NS	1.01 (0.45) NS	-0.28 (0.40) NS	-0.76 (0.54) NS	-1.07 (0.47) NS
Stemwood	-0.05 (0.14) NS	0.86 (0.13) ***	0.17 (0.14) NS	-0.3 (0.12) NS	-0.08 (0.06) NS	-0.06 (0.10) NS
Branches	1.68 (0.22) ***	3.27 (0.31) ***	-1.33 (0.65) NS	0.52 (0.72) NS	-0.62 (0.48) NS	-0.09 (0.44) NS
Twigs	2.09 (0.46) ***	2.51 (0.50) ***	-2.12 (0.79) *	0.46 (0.77) NS	0.30 (0.41) NS	-0.80 (0.38) NS
Leaves & Buds	0.90 (0.79) NS	0.60 (0.82) NS	3.50 (0.93) **	NA	NA	-0.75 (0.39) NS

Table 2-2 Changes in sugar and starch concentrations of tissues in mature *Betula papyrifera* between subsequent sampling dates. Changes in concentrations are the differences in the estimated marginal means from the linear mixed-effects models for each specified contrast. P-values for each comparison of sampling dates were adjusted using the Behjamini-Yekutieli method and indicate significant changes in NSC concentrations accordingly: NS = not significant, (*) = $P \leq 0.1$, * = $P \leq 0.05$, ** = $P \leq 0.01$, and *** = $P \leq 0.001$.

	Change in Sugar and Starch Concentrations (Δ %)											
	May/18 – Jun/18		Jun/18 – Aug/18		Aug/18 – Oct/18		Oct/18 – Nov/18		Nov/18 – Apr/19		Apr/19 – May/19	
	Sugar	Starch	Sugar	Starch	Sugar	Starch	Sugar	Starch	Sugar	Starch	Sugar	Starch
Fine Roots	-0.70 (0.19) **	-0.19 (0.16) NS	-0.21 (0.13) NS	1.29 (0.34) **	1.39 (0.42) **	2.09 (0.68) *	1.85 (0.70) *	-2.42 (0.62) **	-0.13 (0.58) NS	-0.28 (0.28) NS	-1.71 (0.43) **	-0.03 (0.26) NS
Coarse Roots	-1.17 (0.17) ***	0.29 (0.30) NS	0.27 (0.24) NS	1.40 (0.47) *	0.87 (0.27) *	0.25 (0.56) NS	0.71 (0.38) NS	-2.43 (0.41) **	-0.58 (0.37) NS	-0.03 (0.13) NS	-0.36 (0.28) NS	0.33 (0.20) NS
Inner Bark	0.22 (0.37) NS	0.84 (0.25) **	-1.09 (0.37) *	0.60 (0.29) (*)	2.38 (0.37) ***	-1.37 (0.19) ***	0.01 (0.37) NS	-0.30 (0.05) ***	-1.12 (0.37) *	0.37 (0.11) **	-1.71 (0.37) ***	0.63 (0.18) **
Stemwood	-0.10 (0.09) NS	0.05 (0.08) NS	0.12 (0.09) NS	0.74 (0.08) ***	0.45 (0.09) ***	-0.28 (0.08) **	0.20 (0.09) NS	-0.50 (0.08) ***	-0.27 (0.09) *	0.19 (0.08) (*)	-0.03 (0.09) NS	-0.03 (0.08) NS
Branches	0.20 (0.22) NS	1.49 (0.27) ***	0.31 (0.13) (*)	2.96 (0.39) ***	2.25 (0.43) ***	-3.58 (0.33) ***	1.27 (0.50) *	-0.76 (0.16) ***	-1.26 (0.39) **	0.64 (0.09) ***	-1.25 (0.38) **	1.15 (0.24) ***
Twigs	0.85 (0.30) *	1.24 (0.33) **	-0.42 (0.21) NS	2.9 (0.51) ***	1.34 (0.64) NS	-3.47 (0.42) ***	1.09 (0.73) NS	-0.64 (0.16) ***	-0.31 (0.42) NS	0.61 (0.10) ***	-1.96 (0.24) ***	1.16 (0.24) ***
Leaves & Buds	-0.38 (0.64) NS	1.28 (0.47) *	0.38 (0.54) NS	0.23 (0.65) NS	4.94 (0.72) ***	-1.42 (0.48) *	NA	NA	NA	NA	-0.52 (0.36) (*)	-0.23 (0.10) (*)

Table 2-3 Estimated marginal means, standard error (SE), and Tukey's HSD (α = 0.05) comparisons for a repeated measures linear mixed-effects model testing for the effect of organ and sampling date on organ level NSC pool size (kg). Comparisons are presented as the difference in means between row organ and column organ for each sampling date, where: NS = not significant, * = $P \leq 0.05$, ** = $P \leq 0.01$, and *** = $P \leq 0.001$.

Organ	Mean NSC (kg)	SE	1. Branches	2. Stemwood
May 24, 2018				
1. Branches	0.713	0.039	–	
2. Stemwood	0.142	0.028	-0.571***	–
3. Coarse Roots	0.319	0.023	-0.394***	0.177***
June 17, 2018				
1. Branches	1.033	0.043	–	
2. Stemwood	0.133	0.026	-0.900***	–
3. Coarse Roots	0.245	0.041	-0.788***	0.112*
August 7, 2018				
1. Branches	1.524	0.042	–	
2. Stemwood	0.298	0.027	-1.226***	–
3. Coarse Roots	0.386	0.041	-1.138***	0.088 ^{NS}
October 3, 2018				
1. Branches	1.123	0.137	–	
2. Stemwood	0.331	0.028	-0.792***	–
3. Coarse Roots	0.480	0.040	-0.643***	0.149**
November 15, 2018				
1. Branches	1.313	0.053	–	
2. Stemwood	0.272	0.023	-1.041***	–
3. Coarse Roots	0.335	0.027	-0.978***	0.063^{NS}
April 8, 2019				
1. Branches	1.286	0.035	–	
2. Stemwood	0.257	0.020	-1.029***	–
3. Coarse Roots	0.284	0.026	-1.002***	0.027 ^{NS}
May 8, 2019				
1. Branches	1.210	0.049	–	
2. Stemwood	0.245	0.027	-0.965***	–
3. Coarse Roots	0.282	0.029	-0.928***	0.037 ^{NS}
June 11, 2019				
1. Branches	0.979	0.034	–	
2. Stemwood	0.170	0.025	-0.809***	–
3. Coarse Roots	0.272	0.038	-0.707***	0.102**

2.6 Figures

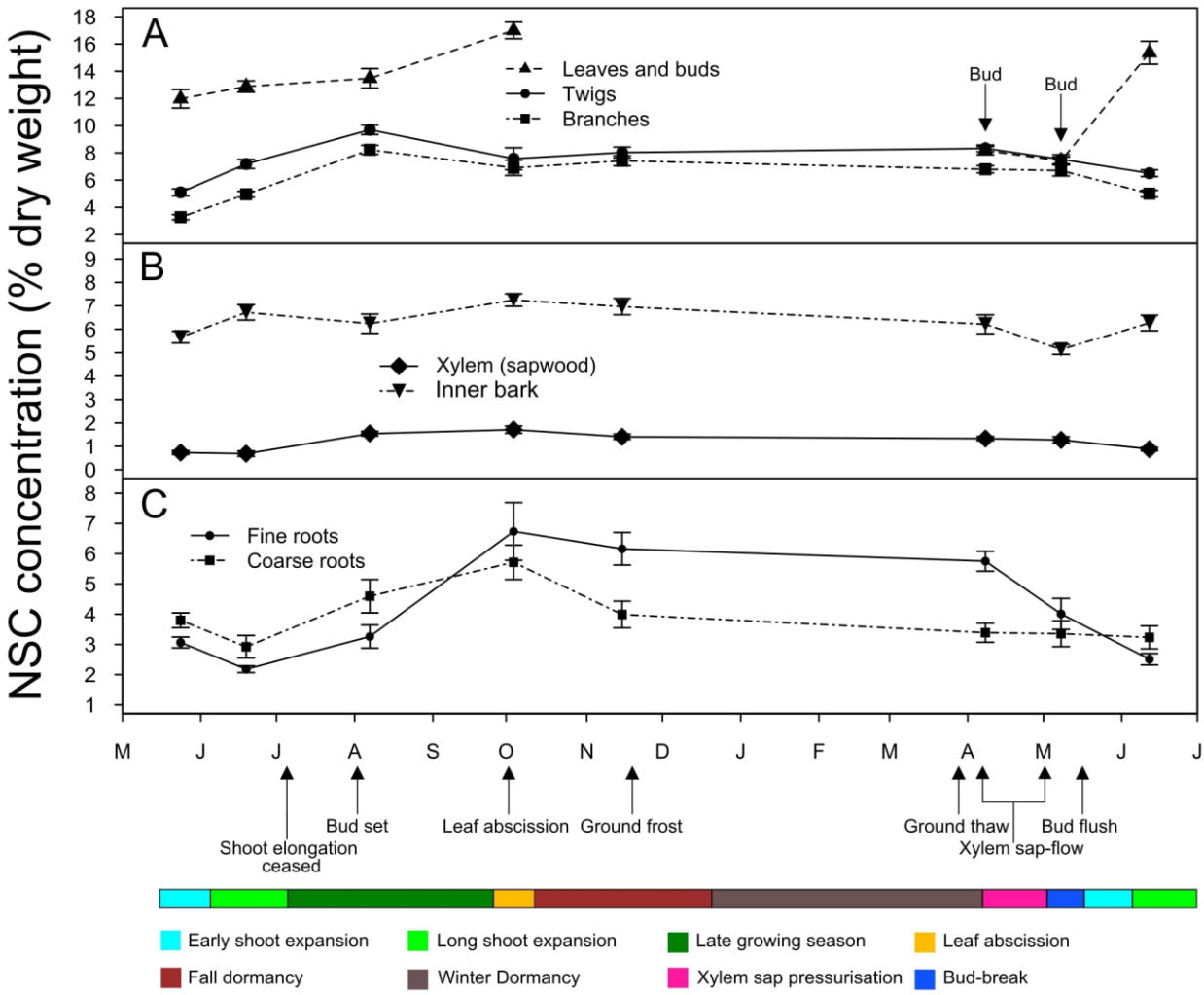

Figure 2-1. Average (± standard error) seasonal non-structural carbohydrate (NSC: combined sugar and starch) concentrations in tissues of ten *Betula papyrifera* trees. (A) Leaves and buds, current (1-year-old) twigs, and branches, (B) stem xylem and inner bark and (C) coarse and fine roots (n=10).

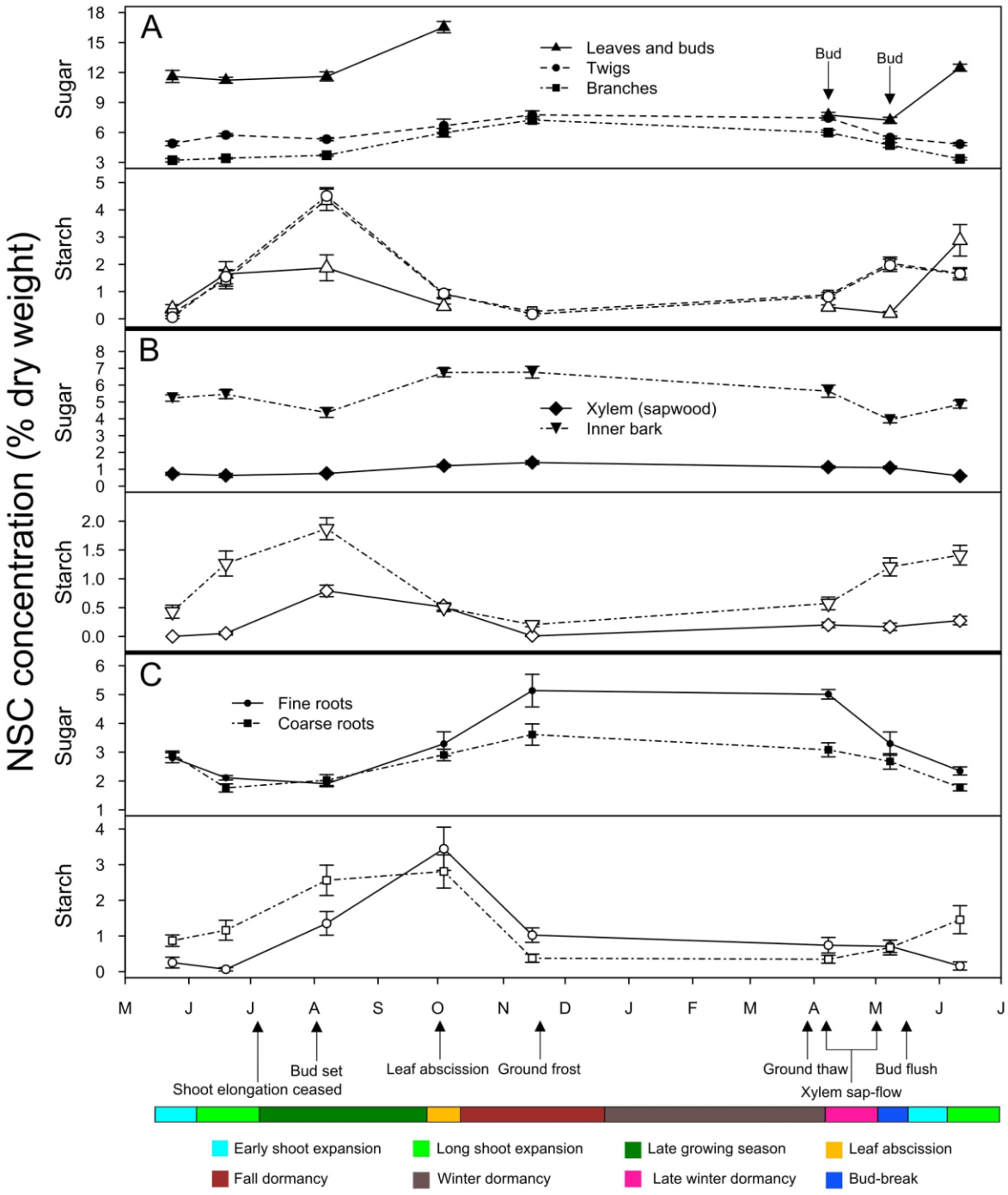

Figure 2-2 Average (± standard error) seasonal sugar and starch concentrations in tissues of ten *Betula papyrifera* trees. (A) Leaves and buds, current (1-year-old) twigs, and branches, (B) stem xylem and inner bark, and (C) coarse and fine roots (n=10).

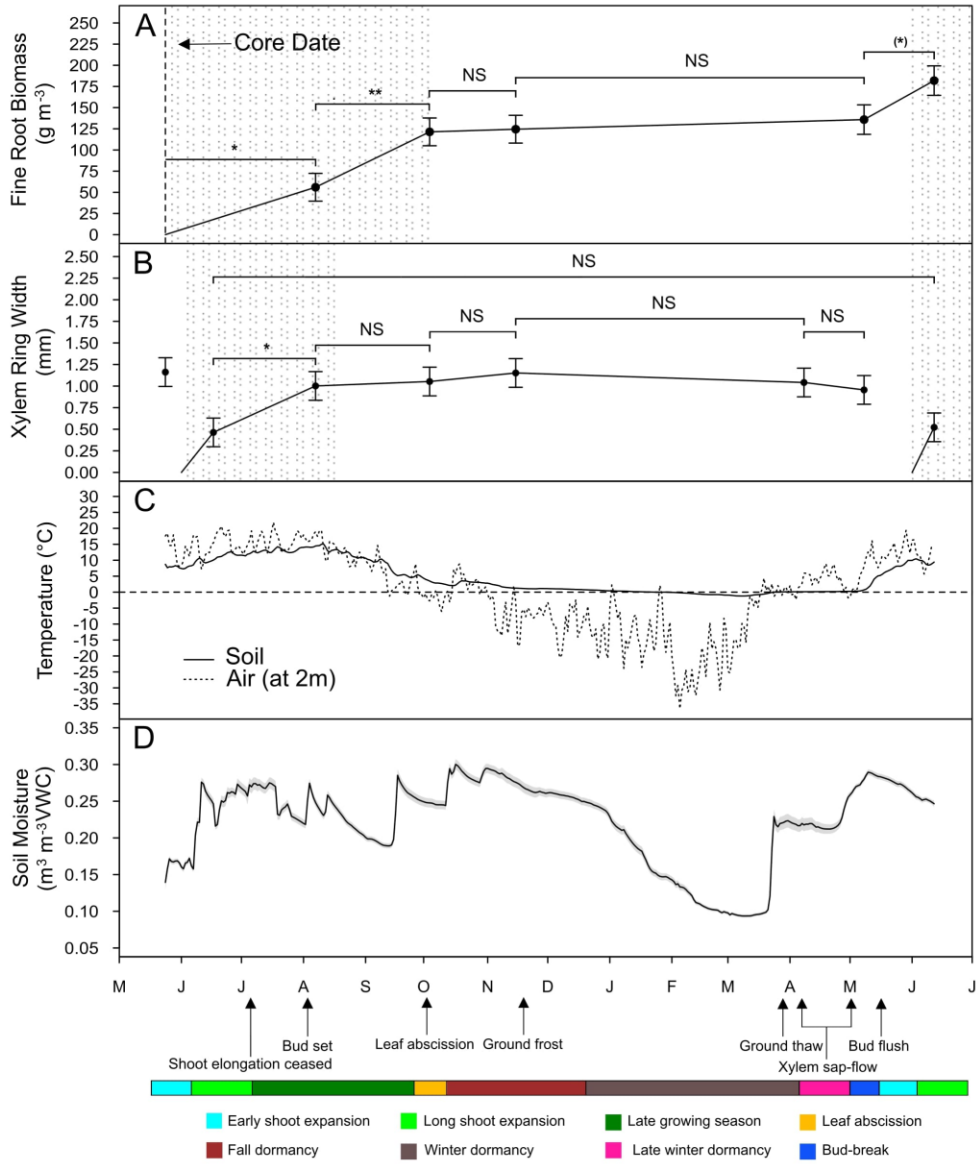

Figure 2-3 Seasonal dynamics of: (A) Fine root biomass of *Betula papyrifera*, presented as biomass (g) per m^3 of soil. (B) Secondary xylem production in *Betula papyrifera* presented as the width of the most recent xylem ring. (C) Average daily soil temperature at 15 cm depth, and daily air temperature from a nearby weather station in Abee, Alberta. (D) Average daily soil moisture at 15 cm depth. Data points in the upper two panels represent the estimated marginal means (± standard error) of repeated measures linear mixed-effects models, and brackets with asterisks denote Behjamini-Yekutieli significant differences between planned comparisons, where: NS = not significant, (*) = $P \leq 0.1$, * = $P \leq 0.05$, ** = $P \leq 0.01$, and *** = $P \leq 0.001$. The grey stippled areas represent the approximate periods of (A) fine root and (B) radial xylem growth. Shaded grey areas in the lower two panels represent the standard error.

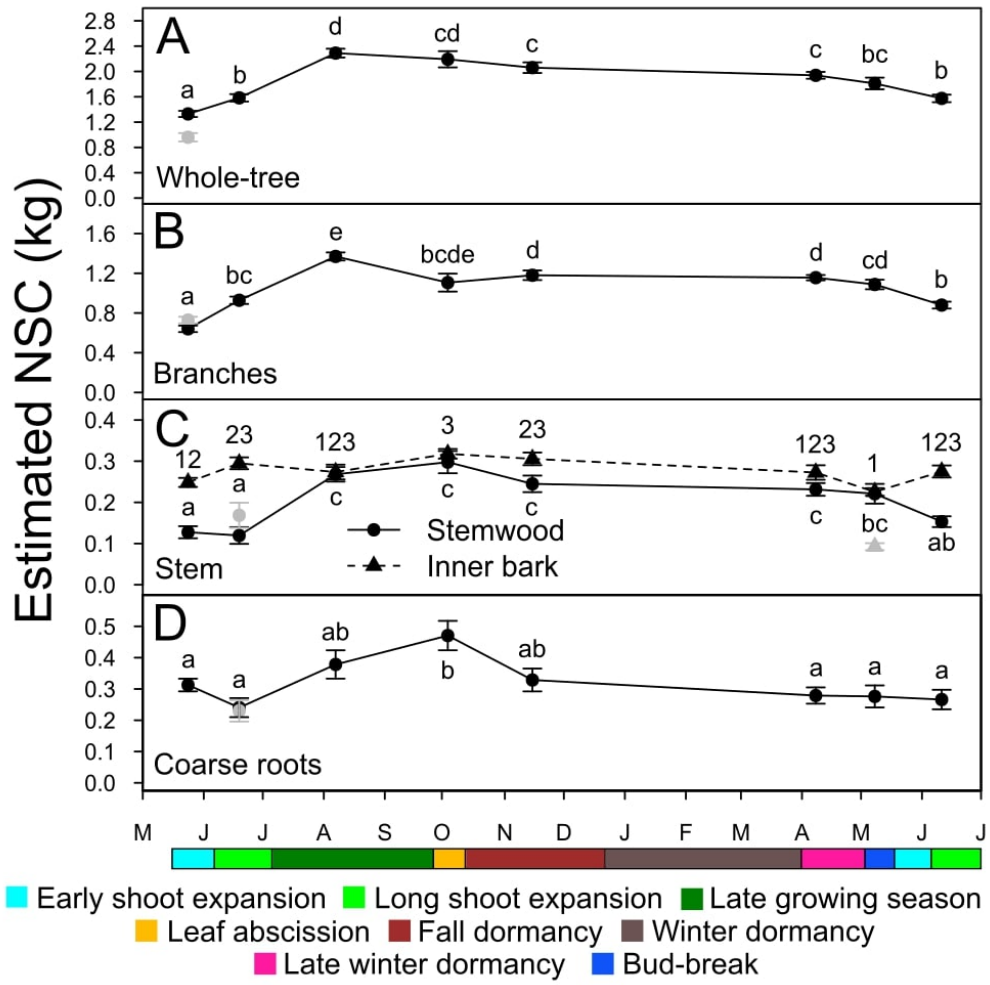

Figure 2-4 Mean pool size (black points) and maximum seasonal change (grey points) of non-structural carbohydrates (NSC, kg) in the (a) whole-tree, (b) branches, (c) stemwood, and (d) coarse roots of ten mature *Betula papyrifera* trees over a calendar year. Error bars represent standard error. The maximum seasonal change was taken as the difference between the maximum NSC (out of eight possible sampling dates) and NSC at the time of minimum pool size. Letters denote significant differences (Tukey's HSD, α=0.05) in NSC pool size among sampling dates for each organ and at the whole-tree level separately.

3. Chapter 3 – The role of the bole: constraints in the remobilization of stem reserves under experimental carbon limitation

3.1 Introduction

The storage and remobilization of resources are essential mechanisms for long-lived species such as trees to maintain functionality throughout different phenological stages as well as to withstand and recover from stochastic stress and disturbance events. In the face of future climate change, stressors such as drought, pest, and disease outbreaks which reduce carbon (C) assimilation are predicted to increase in frequency and intensity (McDowell *et al*., 2008; Allen *et al*., 2010; Paritsis and Veblen, 2011; Gaylord *et al*., 2013; Oliva *et al*., 2014; Adams et al., 2017; Seidl *et al*., 2017), thus highlighting a need to better understand how reserve remobilization and allocation patterns are linked to the physiological mechanisms associated with stress tolerance and mortality in trees.

Non-structural carbohydrates (NSC), primarily in the form of soluble sugars and starch, are widely recognized buffers against such stressors, as they can be stored, remobilized, and reallocated among tissues within an organism for respiration, growth, reproduction, or defense when C assimilation is limiting (Chapin *et al*., 1990; Dietze *et al*., 2014; Najar *et al*., 2014). In addition, NSCs are known to function in mechanisms related to cold tolerance and cryoprotection (Sakai and Larcher, 1987; Tinus *et al*., 2000; Morin *et al*., 2007; Tarkowski and Van den Ende, 2015), cell osmotic adjustment and desiccation tolerance (Ingram and Bartels, 1996), as well as embolism repair and hydraulic maintenance (Améglio *et al*. 2001; Bucci *et al*., 2003; Améglio *et al*. 2004). Nevertheless, our current understanding of NSC reserve remobilization and allocation in trees remains limited — particularly with respect to how remobilization is controlled, when, where, and how much reserves are available for

remobilization, whether these stored reserves are redistributed among organs over longer distances, and the extent to which remobilization impacts survival (Hartmann and Trumbore, 2016). Despite these uncertainties, tissue NSC measures are often utilized to estimate the C status of individual trees and to extrapolate those to larger scales to explore the susceptibility of forests to future stress and disturbance events. However, without a thorough understanding of what governs NSC allocation and remobilization, this approach remains controversial and problematic (Hoch *et al*., 2003; Körner, 2003; Sala *et al*., 2012; Hoch, 2015)**.**

Regardless of the availability of organ reserves for remobilization, perhaps the most glaring issue with respect to mature trees is that we are unsure of reserve allocation limitations imposed by organ autonomy or the distance between source and sink organs, and how it dictates whether or not available reserves are allocated to starving tissues under stress (e.g., Landhäusser and Lieffers, 2012). Tissue-specific declines of NSC have been observed under stress, thus suggesting that even if NSC *is* available for remobilization within an organ (i.e., source tissues) at a given time, these reserves may be compartmentalized, possibly due to localized dysfunctional phloem connections (Turgeon, 2006; Wiley *et al*., 2017b), and are therefore not available to fuel metabolism or survival responses in more distant sink tissues. If true, C stress and starvation could theoretically be experienced disproportionately among organs — especially so for large organisms, where organs can bridge large distances such as the branchless stem in large trees separating the canopy from the root system (Landhäusser and Lieffers, 2012).

When studying C dynamics in trees, allocation and remobilization to and from storage is most often inferred through quantifying and comparing the temporal variation in concentration or mass estimates across organ tissues (e.g., Galiano *et al*., 2011; Piper, 2011; Hartmann *et al*., 2013; Furze *et al*., 2019; Fermaniuk *et al*., 2021), however, assessing reserve dynamics can also

be achieved experimentally through isotope labelling and tracing (Epron *et al*., 2012; Hikino *et al*., 2022; Box 1 in Hartmann and Trumbore, 2016) or through artificially manipulating source and sink strength. Such manipulations can be achieved through shading (O'Brien *et al*., 2014; Wiley *et al*., 2017b; Wiley *et al*., 2019) or defoliation (Wiley *et al*., 2013) treatments, but also through direct restriction of sugar translocation, either genetically (Payyavula *et al*., 2011) or physically (i.e., phloem girdling, compression, or chilling treatments) (Johnsen *et al*., 2007; Regier *et al*., 2010; De Schepper *et al*., 2011; Henriksson *et al*., 2015; Rademacher *et al*., 2019), which prevents or severely impedes the transport of current and reserve-derived assimilates to tissues located below the restriction zone. The direct effects of phloem transport manipulation are well described and typically result in an accumulation of NSC above the restriction zone, while organ tissues below are forced to be metabolically reliant on their reserves for survival (Rademacher *et al*., 2019). Over time, this dependency will deplete storage pools in organs and induce organ mortality, however, mortality may be delayed or even prevented if an organ tissue was to receive remobilized reserves from other local or more distant tissues.

While NSCs are crucial substrates for primary metabolism, NSCs can also greatly impact tree function via secondary metabolism and their osmotic role in hydraulics. However, it remains uncertain to what extent NSC availability, and its effects on water relations limits important survival processes such as resprouting, bud flush, and defense. These processes are crucial for both short and longer-term (i.e., between season) survival, especially so under C limiting conditions, as they may help to re-establish a source of current photosynthate, provide protection against pathogen attack in weakened trees, as well as maintain the integrity of the hydraulic system which is required for photosynthesis, carbohydrate transport, and the expansion of tissues during growth. Under experimental conditions like girdling which limit phloem transport and

result in an accumulation of NSCs in some areas of the tree and a depletion of NSCs in others, these changes can be used to determine which NSC pools are important sources of C for these processes and whether the availability of NSC and/or water has the potential to limit their occurrence.

In the present study, I applied phloem girdles at the top (just below the live canopy) and/or at the bottom (base) of the stem in mature boreal *Betula papyrifera* trees. Through the strategic placement of these girdles, the stem reserve pools available for remobilization can potentially be separated, thus providing an excellent system to explore if, how, and to what extent reserves are distributed among organ tissues when functioning under storage dependency. By applying girdles at these specific locations on the stem, overall xylem transport remains intact while NSC is uninhibited between tissues which are not separated by girdles (e.g., stem and root tissues in top girdled trees), but is prevented between organs when a girdle is present (e.g., between canopy and stem in top girdled trees). By comparing organ tissue NSC concentrations across all treatment groups with high spatial resolution until mortality, we could thus explore if inter-tissue remobilization of NSC had occurred.

In more detail, the aim of this study was to firstly partition the storage contribution, if any, between stem (stemwood and inner bark) reserves (total NSC, sugar, and starch) and canopy organs (leaves, twigs, and branches), and stem and root tissues (fine and coarse roots). I hypothesize that if roots are the strongest sink for reserve derived NSC in trees where stems and roots are C limited, root NSC concentrations will be higher and stem NSC concentrations will be lower in trees with a girdle just below the canopy versus trees with a bottom girdle where stem reserves are separated from roots. Alternatively, if the stem is a stronger sink for reserve derived NSC under C limiting conditions, stem NSC concentrations will be higher and root reserves will

deplete faster in trees when girdled just below the canopy compared to trees with a girdle separating stem and roots. In contrast, if neither the stem nor the roots allocate reserves to one another under such conditions, then minimal NSC differences between girdling treatments should be observed. Secondly, I aimed to assess whether distance to sink affects reserve allocation by comparing the girdling responses of stemwood and inner bark carbohydrate concentrations in the upper and lower stem. If reserve remobilization and allocation is constrained by proximity to reserve sources, I would expect that remobilization of stem NSC to the roots or root NSC to the stem would lead to greater concentration differences between girdling treatments at the lower stem than the upper stem position. Lastly, by using the variation in NSC storage and water content among trees and girdling treatments, I aimed to explore whether NSC storage and/or water content affect functions such as spring recovery of the hydraulic system in birch, sprouting responses, bud flush, and pathogen defense.

3.2 Materials and Methods

3.2.1 Study site description

In late May 2018, 32 healthy mature codominant *B. papyrifera*. trees were selected for girdling treatments in a large mature monospecific, even aged, and closed canopy birch stand with very little understory vegetation. The stand (2 ha) is located at the southern edge of the boreal dry mixedwood forest region in Alberta (54°17’13.59” N, 112°46’27.74” W). The aboveground portion of the stand was disturbed approximately 30 years ago and had regenerated vegetatively via basal sprouting. The trees selected for treatment application all had a single dominant stem and exhibited only minor basal sprouting, were between 9 and 13 m tall, and were between 10-15 m apart from each other. The surface soil and main rooting space in this site is dominated by an 18 cm deep organic horizon that consisted of well decomposed material.

Overall, the site was considered rich, with a mesic moisture regime and moderately to well-drained soils.

3.2.2 Treatment application

Three weeks prior to treatment application, a small number of minor branches below the canopy were removed from a few trees to provide a clear 5 m stem section, and, where present, some basal sprouts were removed at the root collar (RC). Overall, the design of this study was fully randomized; however, to assure that differences among treatments were not driven by differences in tree size we ensured that all treatments had trees with a similar diameter and stem volume distribution which were as based on height and diameter at breast height (DBH at 1.3 m) measurements for each tree (Table A-7).

On 20 Jun. 2018, 5 cm wide girdles were carefully applied by removing the bark and by scraping away any cambial tissues around the circumference of the stem using a chisel and a knife. Caution was taken to not damage the underlying sapwood. The four treatments applied were: top girdle (TG, 500 cm above RC; n = 8), bottom girdle (BG, 30 cm above RC; n = 8), double girdle (DG, girdled at both 30 cm and 500 cm above RC; n = 8), and a no girdle control (no girdle; n = 8). Stem diameter was measured at 30 cm above the RC, and 500 cm above the RC. Following the girdle application, a 10 % bleach solution was applied to sterilize the wound. Girdles were maintained in regular intervals to avoid regeneration of the inner bark tissues; however, despite our efforts, the top girdles of three TG trees experienced regeneration of potentially functional phloem for a period of about 3 weeks between mid-July and early August of 2018. It appeared that during that time the upper and lower portions of these top girdles had reconnected in these trees. New buds and short basal sprouts that appeared after girdling were

removed and collected from all trees on three occasions (see sample collection below). At the end of the experiment in July of 2019, all trees were cut, and final samples were collected.

3.2.3 Sampling dates

To measure the effects of girdling on carbohydrate concentrations in organs separated by girdles, tissue samples were collected at five dates throughout the duration of the experiment. Collection dates were based on data from an earlier study that explored the seasonality of NSC reserve storage based on phenological stages in boreal birch on the same site (Fermaniuk *et al*., 2021). To obtain an initial baseline estimate of tissue carbohydrate concentrations for all sample trees, samples were collected for all 32 trees prior to girdle application on 20 Jun. 2018 during long-shoot expansion. Subsequent sampling dates were based on the following phenological stages: late growing season (termination of shoot expansion) — 31 Aug. 2018; bud flush — 13 May 2019; early shoot expansion — 29 May 2019; and mid-growing season/felling date (late shoot expansion) — 17 Jul. 2019 (Fermaniuk *et al*., 2021). At each date, samples were obtained from the following seven tissues: (1) fully expanded leaves (when available) or buds; (2) current (1- year-old) twigs — < 3 mm diameter; (3) small branch — between 4–7 mm diameter; (4) stemwood — water conducting xylem (sapwood); (5) inner bark — including the phloem and excluding the outer bark (outer bark removed using a razor blade); (6) coarse roots — between 10–15 mm diameter; and (7) fine roots — < 2 mm diameter.

The initial sample collection in 2018 prior to the girdle application established baseline organ-level carbohydrate concentration for each individual tree and confirmed that there were no significant differences initially in the phenological stages among all selected trees. Sample analyses indicated that there were no differences in NSC, sugar, or starch concentrations among the trees assigned to each treatment for the roots (average of coarse and fine), stemwood, inner

bark, and branches (average of branch and twig) prior to girdling (Table A-8). The only statistical differences in reserve concentrations that were detected among the treatments was found in the leaves, which had marginally higher NSC and sugar in DG and BG versus control trees (all $P \leq 0.1$).

3.2.4 Sample collection

Root samples were collected by carefully following roots from the base of each tree. Canopy samples (shoot and leaf material) were collected by pruning a small branch from the outer portion of the canopy that was fully exposed to light using a tall ladder (5 m) and a pole pruner (5 m). Stem samples were collected using a 1.9 cm diameter bark punch that was driven to a depth of 1.5 cm into the stem extracting a sample that included the outer and inner bark, and sapwood tissue. The outer, inner bark and sapwood (stemwood) were separated, and the outer bark discarded. For each sampling date, stem samples were collected from the following locations relative to girdle position (see Figure 3-1): control — positions 1, 3, and 5; TG — 2, 3, and 5; BG — 1, 3, 4 and 6; and DG — 2, 3, 4 and 6. The maximum distance between positions in the lower portions of the stem (double girdled trees; position 4 and 6) was 10 cm. To ensure that samples collected 10 cm apart along a stem provide NSC concentrations that were similar to each other, we selected eight additional trees at the study site, which were of the same age and DBH range as our experimental trees and collected and analysed stem samples (both stemwood and inner bark) at the same two positions along the bole that were spaced 10 cm apart and found no differences in NSC, sugar, or starch concentrations (all paired *t*-test $P > 0.22$).

During 2019, buds and basal sprouts were collected, and their number and dry mass was determined at three time points: 19 Jun., 10 Jul., and after felling on 13 Aug. Additionally we also collected and quantified the xylem sap in all trees, which can be viewed as a proxy for the

occurrence of positive root pressures, by tapping trees before bud flush (26 Apr. 2019). For that, a small hole (0.19 mm diameter and 2.5 cm deep) was drilled 10 cm above the root collar region and 20 cm below the girdle and a spile, hose, and collection tube were connected to the tree. The amount of sap collected over time was recorded and an overall flow rate of xylem sap was calculated from these measurements for each individual tree.

3.2.5 Soil moisture and climate data

To monitor site soil moisture and temperature, five soil moisture/temperature sensors (5TM VWC+ Temp, Decagon Devices Incorporated, Pullman, Washington, USA) were installed at a 15 cm depth at six points within the site (spaced 20–30m apart). Each measurement point was within 5–10 m of subject trees. Sensors were set to log data at hourly intervals, and daily averages were calculated across all points. In general, soil moisture levels suggested that the study site had received sufficient rainfall throughout the experimental period and trees did not experience water stress (Figure A-1). General climate data was obtained from the Abee, Alberta weather station (54.28° N,112.97° W, 12 km from study site), provided by Alberta Agriculture and Forestry, Alberta Climate Information Service (ACIS, 2019).

3.2.6 Sample preparation and carbohydrate analyses

Tissue samples were oven dried (at 100°C for one hour and then at 70°C for 72 hours), finely ground using a ball mill (TissueLyser II; QIAGEN, Hilden, Germany), and then stored in airtight containers until laboratory analysis. For all sampling dates after the initial measurement, moisture content (%) of sampled branches was determined by weighing branch samples before and after drying. Sprout biomass (g) was determined for each tree at the three collection times and the cumulative sprout biomass was calculated.

Following the protocols described in Landhäusser *et al.* (2018), soluble sugar concentrations were determined after hot ethanol (80%) extraction followed by a colorimetric quantification using phenol-sulfuric acid. The phenol-sulfuric acid method was also used to determine sugar concentration of the xylem sap following a 100× dilution with deionized water. Starch was hydrolysed to glucose using α -amylase from *Bacillus licheniformis* (Sigma-Aldrich A3403) and amyloglucosidase from *Aspergillus niger* (Sigma-Aldrige A1602). Glucose concentration was quantified colorimetrically using glucose oxidase/peroxidase-O-dianisidine solution and converted to starch equivalent. All analyses included a lab standard for *Populus tremuloides* root tissue (n = 70) of 10.04 ± 0.46 % dry weight sugar, and 7.86 ± 0.34 dry weight starch. We report all carbohydrate concentrations as a percentage of sample dry weight.

3.2.7 Calculations and statistical analyses

From both field and laboratory observations, there were two trees, one BG and one DG tree, that did not follow the typical trajectory of decline we saw in all the other girdled trees. Throughout the entire experiment, these two trees were largely indistinguishable from the controls in terms of tissue sample characteristics (physical appearance and carbohydrate levels), as well as in the amounts of sap and sprouts produced in the 2019 season. As intraspecific root connections are possible in birch (Kozlowski and Cooley, 1961), we suspect that these trees could have been connected through functional root grafts with neighboring non-experimental trees. Based on these observations, we considered these two trees natural outliers, and thus removed them from the dataset prior to statistical analyses. Additionally, preliminary analyses showed that the root carbohydrate concentrations unexpectedly increased between the first and second measurement in three TG trees which, as previously mentioned, had experienced phloem regeneration (over less than three weeks) at the girdle site. Two other DG trees showed a similar

trend, but we did not observe any obvious phloem regeneration so we suspect that they might have had some initial root connections. These preliminary analyses highlighted that these five trees exhibited roughly double the root NSC concentration ($P < 0.001$) in comparison to all other girdled trees by the second sampling date in late August. In addition, these five trees also exhibited higher late August NSC concentrations at the lowermost (positions 5 or 6) stemwood and inner bark samples in comparison to other girdled trees (both $P < 0.05$). However, root and lowermost stem reserve patterns in these five trees did not markedly differ from their counterpart trees for the remainder of the study period. Therefore, samples from these five trees were removed from the root and lower stem analyses for the second sampling date only.

For organ-level analyses, tissue concentrations were first condensed into one measure for each organ (leaves/buds, branches, inner bark, stemwood, and roots) per tree per sampling date (see Methods A-1). We also assessed the effects of stem girdling at finer spatial resolutions in the stemwood and inner bark tissues by calculating changes in concentrations in the upper and lower stem of all trees and the root collar sample (position 6) for BG and DG trees. For each individual tree, change in concentrations were calculated by subtracting the initial concentrations from concentrations observed at the same location during the late growing season (31 Aug.), early shoot expansion (29 May), and at the felling date (17 Jul.). At the late growing season measurement, NSC concentrations of stemwood and inner bark samples collected at the mid-stem (position 3; Figure 3-1) were also compared among groups.

All statistical analyses were performed using R v.3.5.1 (R Core Team, 2018); linear mixed-effect (LME) models were fit by maximum likelihood using the NLME package (Pinheiro *et al.*, 2021). To assess whether organ-level carbohydrate (NSC, sugar, and starch) concentrations, branch moisture content, and leaf size varied across treatments over time, we

used LME models with sampling date, girdling treatment, and their interaction as fixed effects and tree as a random effect. A repeated measures approach was used to account for the repeated sampling of individual trees across sampling dates. Because our main goal was to test for differences between the different girdling treatments as opposed to differences between girdled and control trees, we did not include the control group in the organ-level reserve models. However, the seasonal concentration dynamics in the control trees were still presented to demonstrate how girdled trees deviated from the controls. In addition, linear models with treatment as a fixed effect were used to assess differences among all treatments (including controls) in changes in NSC concentrations in August, late May, and July, as well as in xylem sap flow rate, xylem sap sugar concentration, and the accumulated biomass of sprouts produced in 2019.

In most of the above-described models, a by stratum variance structure was incorporated to account for heteroscedasticity in model residuals. Fixed effects were tested using analyses of variance (ANOVAs) with a sequential sum of squares (SS), though in the case of xylem sap flow, xylem sap sugar concentrations, and sprout biomass models, type III SS were incorporated to account for highly unbalanced observations. For all models, significant ANOVAs were further evaluated using 1) planned contrasts to assess the changes within a treatment group between consecutive sampling dates (Behjamini-Yekutieli method of P-value adjustment at $\alpha = 0.1$), and/or using 2) all pairwise contrasts within a sampling date to assess the differences among treatment groups at a given time. In models where controls were excluded and only three groups were compared, the P-values for all pairwise comparisons were adjusted using Fishers least significant difference (Fishers LSD; $\alpha = 0.1$); when controls were included, P-values were adjusted using Tukey's honest significant difference (Tukey's HSD; $\alpha = 0.1$).

Finally, using either variation among treatments or among trees in all treatments, we also tested whether NSC storage and/or water content impacted important physiological/phenological events such as xylem sap flow, root collar sprouting, leaf flushing, and defense against pathogen infection. We first used Pearson correlation tests with Benjamini-Hochberg adjusted p-values ($\alpha = 0.1$) to test for correlations between the average late growing season NSC concentrations (root, middle stemwood, middle inner bark, and branch) for each treatment and (1) the proportion of trees within each treatment (controls included) that exhibited xylem sap flow (root pressure), root collar sprouting, leaf flushing, and pathogen infection in the second season, and (2) the average branch moisture content for each treatment in early spring. Similarly, the relationship between average branch moisture content in early spring and the proportion of trees within each treatment that flushed was also evaluated using a Pearson correlation test ($\alpha = 0.1$). Secondly, using variation among trees across treatments, we tested whether the probabilities of producing root pressure, sprouting, leaf flushing, and pathogen infection were related to NSC concentrations and water content with logistic regression, which also allowed for the identification of potential physiological thresholds. Finally, the relationship between late growing season stem NSC concentration and branch moisture content in early spring of the following season was evaluated using linear regression. For all regression models, model fit was assessed by examining the standardized residuals.

3.3 Results

3.3.1 Organ level girdling responses

As anticipated, the control trees exhibited a seasonal swing of NSC reserve concentrations between a maximum in late summer and a minimum in spring and early summer

(Figure 3-2). For a detailed description of NSC phenology in these *B. papyrifera* trees, see Fermaniuk *et al*. (2021).

While root reserves (NSC, sugar, and starch concentrations) in the girdled trees deviated from the seasonal pattern observed in control trees, they did not differ substantially among the girdling treatments (all girdling × date interactions $P > 0.2$; Figure 3-2; Table A-9). By late August of the first growing season, the NSC concentrations in roots of control trees nearly doubled, however, all girdled treatments declined on average by 0.3, 0.8 and 1% for starch, sugar and NSC, respectively and after that did not change significantly for the remainder of the experiment (Figure 3-2; Table 3-1; Table A-10; Table A-11). As such, by the termination of the study, the roots of girdled trees appeared dead and NSC concentrations were ~ 1.5%, mostly in the form of soluble sugars, compared to 2.4% sugars and 1.7% starch in the controls.

Reserve concentrations in the stemwood and inner bark varied seasonally by sampling date, but the seasonal dynamics differed among the girdle treatments for both tissue types (all interactions $P \leq 0.001$). For the stemwood, NSC and sugar concentrations when averaged across the stem in TG and DG trees decreased continuously with little difference between the two treatments for all but the second sampling date in late August 2018 (Figure 3-2; Table 3-1). At that time, the stemwood of DG trees exhibited a reduction in NSC concentration which was not observed in TG trees which might suggest a translocation of NSC from the roots to the stem (Figure 3-2; Table 3-1). In stark contrast, stemwood NSC in BG trees increased over the first growing season to a concentration that was 36% higher than the controls but declined over the dormant period to a concentration similar to the controls (Figure 3-2). At the termination of the study, however, stemwood NSC concentration of BG trees had declined substantially to 0.67% which was similar to the DG trees and not different from the TG trees (Figure 3-2; Table 3-1).

Reserve concentrations in the inner bark of girdled trees followed similar patterns, however unlike in the stemwood, the inner bark of both TG and DG trees exhibited strong initial sugar-driven reductions of NSC concentrations which were 69% (DG) and 53% (TG) lower than controls in late August. Like the stemwood however, these initial reductions of sugar in the inner bark were stronger in DG versus TG trees (Figure 3-2; Table 3-1), again, potentially suggesting a translocation of NSC from the roots to the stem.

While branch NSC concentrations were generally higher in all girdling treatments compared to controls, these treatments did have significantly different branch NSC, sugar, and water content dynamics. Sugar and NSC reductions in BG trees during the second growing season were much greater compared to TG and DG trees (both interactions $P \leq 0.01$; Figure 3-2; Table 3-1; Table A-10), producing much lower final branch NSC concentration in BG trees (2.5%) than in TG and DG trees (~4.7%, both $P \leq 0.05$). The seasonal fluctuations of NSC reserves in the branches of girdled trees were largely driven by starch concentrations, which did not differ among the girdling treatments (interaction $P = 0.45$). Moisture content of branches was similar between girdled and control trees over the first season (~26%) (inset Figure 3-2). However, by early spring of the second growing season, moisture content in the branches of TG and DG trees declined to 21% and the branches appeared brown and desiccated, while BG trees maintained a moisture content of 41% which was similar to the control. Branch moisture levels at this time in spring were also positively related to the previous late-season inner bark NSC concentrations (Adjusted $R^2 = 0.59$, $P \leq 0.001$; Figure 3-3; Figure 3-4d) and only at the end of the study did BG trees exhibit reduced branch moisture content similar to the other two girdling treatments (inset Figure 3-2).

After the first growing season, NSC concentrations in leaves of girdled trees were ~67% higher than the controls, driven by increases in both sugars and starch concentrations — however, the increase in starch was greater in leaves of TG and DG than BG trees (interaction $P \leq 0.001$; Figure 3-2). During the early flush period in May, NSC and sugar concentrations in the buds of girdled trees continued to be 25%-42% higher than the controls, but starch concentrations were similar (Figure 3-2). At that time, all overwintered buds in the control trees were swelling and first leaf tips were emerging; in contrast, bud swell only occurred in four BG, one DG tree, and one TG tree. At full leaf flush (late May), NSC concentrations increased in the controls, but only the four BG trees expanded leaves and thus accumulated sugars and NSC relative to unflushed buds (both interaction $P \leq 0.001$; Figure 3-2). These new leaves were however much smaller (1.0 ± 0.7 cm^2), and internodal growth was absent compared to the controls where leaves were 12.6 ± 0.6 cm^2 in area and shoots had elongated 2-5 cm by that time. The buds of all remaining girdled trees failed to flush and, by late May, were brown and dry, indicating they had died-off. Between treatments and across all trees, we found that the ability to flush was positively associated with higher inner bark NSC concentrations during the previous August (> ~ 5% dry weight; $P \leq 0.01$;Figure 3-3b; Figure 3-4b) as well as higher branch moisture levels in early spring (> ~ 25%; $P \leq 0.05$; Figure 3-4a).

3.3.2 Spatial effects of girdling on stem NSC reserves

Overall, the control trees had similar inner bark and stemwood reserve concentrations (NSC) between the upper and lower stem position (500 and 30 cm above root collar, respectively). The maximum difference in concentrations between both stem positions was 0.7% and 0.5% for the inner bark and stemwood, respectively, yielding mostly no or sometimes a

slight negative NSC concentration gradient from the lower to the upper stem position over the experimental period (Table A-12).

Since the stemwood and inner bark reserve concentrations were initially the same among the girdling treatments and the control trees, we used the change from the initial reserve concentrations in the inner bark and stemwood for each individual tree to explore differences among the girdling treatments (Table A-13). Depending on the treatments, girdled trees exhibited contrasting inner bark carbohydrate dynamics at all stem positions between the initial and August measurement of the first growing season (Table A-13). In BG trees, inner bark starch and NSC concentrations increased at both upper and lower stem positions (above girdle) similar to control trees (Figure 3-5a). In contrast, and driven primarily by sugar concentrations, inner bark NSC concentrations in the TG and DG trees were reduced similarly by ~4.3% at the upper stem position (below girdle) by August, while a significantly larger reduction in NSCs occurred at the lower stem position in DG trees than in TG trees (-3.6% vs -0.7%) (Figure 3-5a) which might suggest a remobilization of root reserves upward to this position in TG trees. This minimal change in inner bark NSC concentration at the lower stem of TG trees thus created a negative sugar concentration gradient (Δ-2.5%) from the lower to the upper stem position, with higher reserve concentrations at the lower stem position. At this time in late August, starch and NSC concentrations in the inner bark at the mid stem position in BG and control trees were similar to each other but higher in comparison to TG and DG trees (all $P \leq 0.001$), however, sugar concentrations were only significantly higher in the controls compared to DG trees ($P \leq 0.05$; Figure A-2a). Stem tissues collected below the bottom girdle in BG and DG trees, exhibited sugar-driven NSC declines in BG (-1.8%) and DG trees (-3.2%) in the inner bark by the end of

the first growing season, and the decline in DG trees was significantly greater than the decline observed at the lower stem of TG trees (Figure 3-5a).

With the exception of root collar starch, stemwood carbohydrate dynamics at the upper, lower, and root collar positions over the first growing season (Table A-13) were different among the treatments. Similar to the control, BG trees increased stemwood NSC concentrations (particularly starch) at both stem positions by late August; however, at the upper stem position, the increase was significantly larger (more than double) than seen in the control (Figure 3-6a). Thus, this large increase created a positive NSC gradient (Δ0.9%) from the lower to upper stem position in BG trees. In contrast, stemwood NSC concentrations declined equally (~0.3%) at the upper stem position of TG and DG, but at the lower stem, NSC concentrations (driven by starch) increased slightly (+0.3%) in TG trees which significantly differed from the slight decline (-0.2%) observed in DG trees (Figure 3-6). At that same time, stemwood NSC concentrations at the mid stem position were highest in BG trees, intermediate in controls, and lowest in TG and DG trees (all $P \leq 0.05$; Figure A-2b). At the root collar position of BG and DG trees, the change from initial stemwood concentration did not differ from the change observed in TG trees (Figure 3-6a).

By late May of the following season, changes in NSC concentrations from initial concentrations showed mostly the same patterns of differences among the inner bark and stemwood of girdled trees (Figure 3-5 and Figure 3-6). However, at this point in the study, there was no longer a significant difference between TG and DG trees in terms of inner bark NSC concentration changes at the lower stem position, with both groups exhibiting ~ 4.5% lower NSC than the initial concentrations (Figure 3-5b). For both stem tissues, the decline in reserves at the upper and lower stem positions was only observed in BG trees when the latter part of the second

growing season was included, and at that time, reserve concentrations at both stem positions were similar to the two other girdling treatments (Figure A-3).

3.3.3 Xylem sap flow, sprouting responses, and disease resistance

Early during the second growing season (2019) all control trees showed flow of xylem sap (as an indication of positive root pressures), while also producing some minor sprouting from the root collar; but these processes were greatly impacted by girdling treatments. Only three TG and two DG trees exhibited xylem sap flow, and no flow was evident in any of the BG trees. The soluble sugar concentration of the xylem sap did not differ among the controls and the five girdled trees (~4.8%); however, the rate of xylem sap flow was marginally higher in control trees (0.8 ± 0.2 mL/s) compared to the TG trees (0.3 ± 0.1 mL/s; $P = 0.06$), though flow rates did not differ from the two DG trees (0.6 ± 0.6 mL/s). Unlike controls, very few girdled trees exhibited root collar sprouting (three TG, three DG, and one BG tree) during the second growing season, however, among the trees that did sprout, there were no treatment differences in the amount of sprout mass produced (< 2.2 g dry mass for all treatments).

The reduced prevalence of xylem sap flow and sprouting in girdling treatments appeared to be associated with lower root reserve concentrations. First, of the girdled trees that produced sap, all but one TG tree had shown an unexpected increase in root carbohydrate concentrations late in the previous season. Similarly, all five girdled trees which sprouted —apart from one DG tree and the BG tree — also had exhibited increased root carbohydrate concentrations late in the previous season. Second, the occurrence of xylem sap flow and sprouting were both significantly correlated with the prior August root NSC concentration both between treatments ($P \leq 0.05$; Figure 3-3) and among all trees (Figure 3-4e and f). Specifically, these processes became more

likely to occur when late August root NSC concentrations were above ~ 2.5% (Figure 3-4e and f).

Lastly, in all girdle treatments we observed the development of canker-like formations and discoloured wood in stems by the latter half of the study period in 2019. We believe this was due to wound colonization by an opportunistic fungal pathogen *Botryosphaeria,* which was not detected in the controls though they that had similar wounds from sample collection. The proportion of infected trees varied substantially between treatments: TG and DG trees had a higher infection frequency earlier in the season, in comparison to the BG trees (Figure A-4). And between treatments, the prevalence of fungal infection by mid-May was significantly and negatively correlated with the average inner bark NSC concentrations late in the previous growing season ($P \leq 0.05$; Figure 3-3). The probability of fungal infection was also negatively correlated with late season inner bark NSC across all trees, with the likelihood of early fungal infection increasing once inner bark NSC concentrations fell below 6% ($P \leq 0.05$; Figure 3-4c).

3.4 Discussion

3.4.1 NSC allocation and remobilization between organs

While I hypothesized that the root system would be a strong sink and import NSC from the stem reserves when faced with C-limitation from girdling, the results instead suggest NSC reserves were allocated from the root system upward toward the stem/root collar in these *B. papyrifera* trees. In comparison to the stems of DG trees which were isolated from the canopy and roots, the stems of TG trees which were only disconnected from the canopy exhibited smaller late season reductions in stemwood and inner bark NSC concentrations (Figure 3-2; Table 3-1), specifically at the lower stem (Figure 3-5a; Figure 3-6a), presumably because the stems of TG trees could import remobilized C from the root system. In contrast, all girdled

treatments had similar stemwood NSC dynamics at the root collar (position below the location of the bottom girdle), where tissues maintained connectivity with the roots. This in turn could explain why I failed to observe differences in root carbohydrate responses across girdled trees. The similar declines in root NSC by the end of the first growing season further support the idea that stem reserves were not a source of stored C to the roots. A greater priority in the stems when NSC supply from the canopy is limited (i.e., TG trees), might result in the remobilization of root reserves towards the stem, further reducing the NSC availability for the root system and affecting processes such as late season fine root growth and frost protection (Fermaniuk *et al*., 2021), which ultimately may result in trees being more vulnerable to hydraulic limitation in the following season.

The lack of evidence of C import from the stem to the roots may cast doubt on either the exceptional sink strength of the root systems (and associated microorganisms) or the importance of the stem as a source of reserves, particularly when the stem is faced with C-limitation. Due to the large proportion of biomass found in the stemwood of mature trees, stems are typically considered one of the largest reserve pools (Barbaroux *et al*., 2003; Würth *et al*., 2005; Hartmann *et al*., 2018), however these results suggest that size alone may not determine whether a reserve pool will act as a source to other, potentially more distant, sinks (such as the fine roots) during periods of C limitation. If true, the proposed constraint on storage pools in stems underlines the problematic nature of using the C reserve status in the stem of mature trees as an indicator of overall resiliency, as the use of such proxies may grossly over-predict survival under future stress and disturbances — at least in the case of species like *B. papyrifera*. Instead, my findings support the suggestion that C reserve dynamics in mature trees do not follow a “one-pool fits all” framework but rather that organ storage pools are regulated independently as somewhat

autonomous units, and that reserve remobilization under stress may potentially differ greatly between organs within a tree (Landhäusser and Lieffers, 2012; Richardson *et al*., 2013; Richardson *et al*., 2015; Hartmann *et al*., 2018).

While I found evidence that roots supplied some NSC to the stem following girdling in TG trees, it appears that distance from the roots (reserve source) affected distribution of these reserves to the wood and inner bark within the stem of TG trees. At the lower stem position, TG trees had higher reserve concentrations in comparison to the DG trees where the stem was isolated; however, differences did not exist at the mid and upper stem positions, suggesting that the re-allocation of root reserves did not extend past the lower stem region (Figure 3-5a; Figure 3-6a). This response could represent an effect of reserve source proximity, with the lower stem tissues being closer to the reserve source in the roots compared to tissues higher up on the stem. Whatever the mechanism, considering that *B. papyrifera* sprouts prolifically from the base of its stem when disturbed (Safford *et al*., 1990), this allocation pattern may be an adaptation that preserves the lower stem via root reserve remobilization and support future sprouting from this portion of the stem. Sprouting is considered an adaptive recovery strategy of species occupying areas prone to aboveground disturbance (Bond and Midgely, 2003), and as such, I suspect this reserve remobilization pattern is suitable for a root collar-sprouting species, like *B. papyrifera*, when the supply of current assimilates is lacking. Remobilization of NSC to the root collar were also observed in girdled *Populus deltoides* × *nigra tree* sapling (Regier *et al*., 2010), and coppiced *Betula pubescens* (Luostarinen and Kuappi, 2005), with many studies highlighting a link between increased root storage and sprouting in species occupying disturbance prone environments (Pate *et al*., 1990; Bowen and Pate, 1993; Iwasa and Kubo, 1997; Sakai *et al*., 1997; Bollmark *et al*., 1999; Landhäusser and Lieffers, 2002).

Although TG and DG trees were functioning under reserve dependency in the stem and roots and appeared to import reserves from the roots to the lower stem/root collar stemwood over the first season, DG trees showed a particularly large-sugar driven decline of inner bark NSC at the root collar which was not evident in the TG trees (Figure 3-5a); this finding could suggest that additional reserves were allocated to this region in TG trees — potentially from the inner bark higher up on the stem. Unlike the stemwood, which at the time of girdling was at its seasonal minimum concentration, the inner bark reserve pools had already begun recovering prior to girdling (Fermaniuk *et al.*, 2021), thus potentially providing some available NSCs for remobilization. The inner bark is often overlooked as an important storage organ due to its small mass and role in C transport (Rosell, 2016), however, it may act as a considerable source of NSC under C limiting conditions (Wiley *et al.*, 2019) such as those observed here in TG trees. Further, despite BG stems having access to current assimilates, I observed no differences in inner bark sugar concentrations at the mid-stem position across girdled trees in late August (Figure A-3a), which could suggest that inner bark sugar concentrations were actively maintained in C limited stems possibly to preserve phloem functionality and facilitate top-down transport of reserves to the lower stem/root collar region. Although the bulk bark sugar concentrations may not be a good indicator for sieve tube sugar concentrations, we can speculate that low sugar concentrations would reduce the osmotic influx of xylem water into the phloem, which in turn would diminish the turgor required for carbohydrate transport (Hölttä *et al.*, 2006; Sevanto, 2014); if true, maintaining higher inner bark sugar concentrations at the middle stem position could be interpreted as mechanism of tall stems to preserve transport under C limiting conditions.

3.4.2 NSC and water availability impacts on physiology

The ability of trees to accumulate even small amounts of NSC in the roots by late in the 2018 growing season appeared to dictate whether girdled trees generated positive root pressures (as indicated by the flow of sap in the spring) and produced basal sprouts in the 2019 season. We found significant positive correlations between root NSC concentrations in late August of the first season and the occurrence of root pressures and collar sprouting in the following season (Figure 3-3), with both events being predicted to occur if NSC concentrations were > 2.5% (Figure 3-4e and f). This finding is consistent with the suggestion that the generation of root pressure in *B. papyrifera* is related to energy expenditure in the fine roots (Fermaniuk *et al.*, 2021). Moreover, five out of the six girdled trees that exhibited at least some positive root pressures were those that had either restored phloem connections in top girdles or had potentially received limited support through root grafts with neighboring trees (see methods), allowing some starch build-up to occur in the roots. These five trees also produced between 2 to 180 times more sprout mass in 2019 than two other girdled trees that sprouted but did not exhibit the increase in starch in the root system by August of the previous season. These findings highlight the link between longer-term (i.e., between season) resiliency and even minor reserve accumulation in the root tissues of *B. papyrifera*, as root reserves serve not only as substrate for sprout regeneration at the root collar, but also provide fuel for the development of root pressures which is important for rehydrating tissues where sprouts emerge.

Although NSC reserves in the stem and canopy may directly support leaf flush through remobilizations to the expanding buds, the results observed here suggest that NSCs, particularly those in the inner bark of BG trees, played a more indirect role in the flushing process through osmotic mechanisms that promoted the rehydration of the upper stem and canopy tissues

following winter. Embolised xylem conduits are common in boreal trees following winter, and embolism refilling processes are required for trees such as birch to ensure adequate water supply to new growth in the spring. In birch, the development of positive root pressures in the spring may aid in vessel refilling from the bottom-up, however, additional osmotic mechanisms may be required for embolism refilling in vessels higher up on the stem (Westhoff *et al*., 2008; Westhoff *et al*., 2009). My findings corroborate this idea. First, I found that late August inner bark NSC concentrations were significantly and positively correlated with branch moisture levels prior to bud burst in the next season (Figure 3-3). Second, while I found that both bark NSC and branch moisture were positively related to the occurrence of leaf flush in the second season, there were no significant relationships between flushing and branch or root NSC concentration which suggests that these organs did not serve as significant sources of NSC for this process (Figure 3-3). Moreso, the only girdled trees which underwent leaf flush were those in the BG treatment. The strong accumulation of NSC (to nearly double the control level) in the stemwood of BG trees (Figure 3-2) likely provided enough lateral osmotic potential early in the second season to potentially draw out stored water from the heartwood and provide turgor for bud and leaf tissue expansion — even despite the absence of root pressures. In contrast, the few TG and DG trees that *did* produce root pressure but could not accumulate NSC in the stem did not show evidence of hydraulic maintenance; instead, branch moisture levels were low and branch sugar concentrations were high throughout the remainder of the second season (Figure 3-2), suggesting a sink-limitation to new growth and early onset of drought-induced mortality in the branches. It is possible that high sugar concentrations in the branches of these trees were maintained because desiccation occurred before these sugars could be metabolized (Hartmann *et al*., 2013; Wiley *et*

al., 2016), or perhaps because these sugars were maintained as osmotica and were unavailable for metabolism (Ingram and Bartels, 1996; McDowell, 2011; Sala *et al*., 2012).

On a similar note, I also observed a significant inverse relationship between inner bark NSC concentrations in late August and pathogenic fungal infection in the following season (Figure 3-3), highlighting the important role of NSCs in disease resiliency. Trees with stems that were restricted access from canopy NSCs were found to be infected at a higher frequency and earlier in the second season in comparison to trees that could allocate canopy NSCs to the stem (Figure A-4). Moreover, I found that inner bark NSC concentrations of < 6% by the end of the first growing season were positive indicators of fungal infection in the stem by the following May (Figure 3-4c) — likely due to insufficient reserve availability for the production of defense compounds like phenolics. Similar results were discussed in relation to the natural durability against *Antrodia* spp which induce heartwood decay in *Tectona grandis* (Niamké *et al*., 2011).

3.5 Tables

Table 3-1 Organ-level total non-structural carbohydrate (NSC) concentrations of girdled (BG= bottom girdled, TG = top girdled, DG = double girdled) *Betula papyrifera* trees over time. Diagonal cells shaded dark grey provide the estimated marginal mean and standard error of NSC concentration for each treatment group at each sampling date, and Δ denotes the standard error and significance (Behjamini-Yekutieli, α =0.1) of the paired difference (change) in estimated marginal means between the column date and previous date. Light grey cells denote the difference in estimated marginal means between column group and row group within each sampling date, and each corresponding white cell indicates whether this difference is significant (Fishers LSD, α =0.1). NS= not significant, $^{(*)}$ = $P \leq 0.1$, * = $P \leq 0.05$, ** = $P \leq 0.01$, or *** = $P \leq 0.001$. If an organ section is shaded orange, no 'treatment' by 'sampling date' interaction was detected for the given organ, and the above post-hoc tests were not conducted.

Total NSC (% dry weight)
Leaves & buds

	June/18			Aug/18			13 May/19			29 May/19			Jul/19		
	BG	TG	DG	BG	TG	DG	BG	TG	DG	BG	TG	DG	BG	TG	DG
BG	14.20 (1.00)	-2.01 (1.34)	0.04 (1.40)	18.48 (2.05) Δ:(2.15) NS	4.20 (2.96)	4.00 (2.65)	9.35 (0.54) Δ:(1.98) ***	0.46 (0.78)	-0.36 (0.84)	12.40 (0.72) Δ:(0.48) ***	-2.77 (0.89)	-3.75 (0.97)	3.79 (1.04) Δ:(1.00) ***	1.55 (1.35)	2.01 (1.32)
TG	NS	12.19 (0.89)	2.05 (1.32)	NS	22.68 (2.13) Δ:(2.19) ***	-0.20 (2.71)	NS	9.81 (0.55) Δ:(2.08) ***	-0.82 (0.84)	**	9.63 (0.51) Δ:(0.21) NS	-0.98 (0.83)	NS	5.34 (0.87) Δ:(0.70) ***	0.46 (1.19)
DG	NS	NS	14.24 (0.98)	NS	NS	22.48 (1.68) Δ:(1.78) ***	NS	NS	8.99 (0.64) Δ:(1.62) ***	**	NS	8.65 (0.65) Δ:(0.49) NS	NS	NS	5.80 (0.82) Δ:(0.71) ***

Total NSC (% dry weight)

Branches

	June/18			Aug/18			13 May/19			29 May/19			Jul/19		
	BG	TG	DG	BG	TG	DG	BG	TG	DG	BG	TG	DG	BG	TG	DG
BG	6.15 (0.42)	-0.08 (0.52)	0.19 (0.60)	10.07 (0.44) Δ:(0.51) ***	0.14 (0.62)	-0.61 (0.75)	7.32 (0.44) Δ:(0.53) ***	0.28 (0.71)	0.14 (0.74)	5.37 (0.38) Δ:(0.48) ***	1.33 (0.64)	1.19 (0.73)	2.46 (0.40) Δ:(0.44) ***	2.46 (0.56)	2.03 (0.84)
TG	NS	6.07 (0.30)	0.27 (0.51)	NS	10.21 (0.43) Δ:(0.42) ***	-0.75 (0.74)	NS	7.60 (0.55) Δ:(0.63) ***	-0.14 (0.82)	(*)	6.70 (0.51) Δ:(0.69) NS	-0.14 (0.81)	***	4.92 (0.39) Δ:(0.56) *	-0.43 (0.84)
DG	NS	NS	6.34 (0.41)	NS	NS	9.46 (0.60) Δ:(0.65) ***	NS	NS	7.46 (0.60) Δ:(0.78) *	NS	NS	6.56 (0.63) Δ:(0.80) NS	*	NS	4.49 (0.74) Δ:(0.92) (*)

Inner bark

	June/18			Aug/18			13 May/19			29 May/19			Jul/19		
	BG	TG	DG	BG	TG	DG	BG	TG	DG	BG	TG	DG	BG	TG	DG
BG	5.80 (0.34)	0.15 (0.49)	0.56 (0.51)	8.70 (0.60) Δ:(0.59) ***	-4.59 (0.67)	-6.03 (0.68)	5.29 (0.42) Δ:(0.65) ***	-3.79 (0.53)	-4.63 (0.53)	5.34 (0.30) Δ:(0.39) NS	-3.46 (0.46)	-4.53 (0.38)	1.42 (0.54) Δ:(0.51) ***	-0.66 (0.60)	-1.01 (0.60)
TG	NS	5.95 (0.35)	0.41 (0.52)	***	4.11 (0.30) Δ:(0.33) ***	-1.44 (0.44)	***	1.50 (0.32) Δ:(0.30) ***	-0.84 (0.46)	***	1.88 (0.35) Δ (0.35) NS	-1.07 (0.43)	NS	0.76 (0.27) Δ:(0.30) ***	-0.35 (0.36)
DG	NS	NS	6.36 (0.39)	***	**	2.67 (0.33) Δ:(0.38) ***	***	(*)	0.66 (0.32) Δ:(0.31) ***	***	*	0.81 (0.24) Δ:(0.21) NS	(*)	NS	0.41 (0.25) Δ:(0.05) ***

Total NSC (% dry weight)

Stemwood

	June/18			Aug/18			13 May/19			29 May/19			Jul/19		
	BG	TG	DG	BG	TG	DG	BG	TG	DG	BG	TG	DG	BG	TG	DG
BG	0.84 (0.06)	0.04 (0.09)	0.16 (0.10)	2.57 (0.11) Δ:(0.11) ***	-1.61 (0.17)	-1.93 (0.12)	1.61 (0.11) Δ:(0.14) ***	-0.88 (0.12)	-0.73 (0.14)	1.46 (0.09) Δ:(0.13) NS	-0.52 (0.11)	-0.67 (0.12)	0.67 (0.06) Δ:(0.10) ***	-0.17 (0.07)	-0.02 (0.12)
TG	NS	0.88 (0.07)	0.12 (0.11)	***	0.96 (0.14) Δ:(0.14) NS	-0.32 (0.15)	***	0.73 (0.05) Δ:(0.14) NS	0.15 (0.10)	***	0.94 (0.06) Δ:(0.06) *	-0.15 (0.09)	*	0.50 (0.04) Δ:(0.05) ***	0.15 (0.11)
DG	NS	NS	1.00 (0.08)	***	*	0.64 (0.06) Δ:(0.09) ***	***	NS	0.88 (0.09) Δ:(0.09) ***	***	NS	0.79 (0.07) Δ:(0.10) NS	NS	NS	0.65 (0.10) Δ:(0.11) NS

Roots

	June/18			Aug/18			13 May/19			29 May/19			Jul/19		
	BG	TG	DG	BG	TG	DG	BG	TG	DG	BG	TG	DG	BG	TG	DG
BG	2.58 (0.28)			1.39 (0.20)			2.18 (0.79)			1.54 (0.36)			1.21 (0.31)		
		2.79 (0.28)			1.73 (0.29)			1.57 (0.19)			1.38 (0.16)			1.32 (0.45)	
DG			2.60 (0.27)			1.76 (0.19)			2.24 (0.38)			1.69 (0.35)			1.89 (0.40)

3.6 Figures

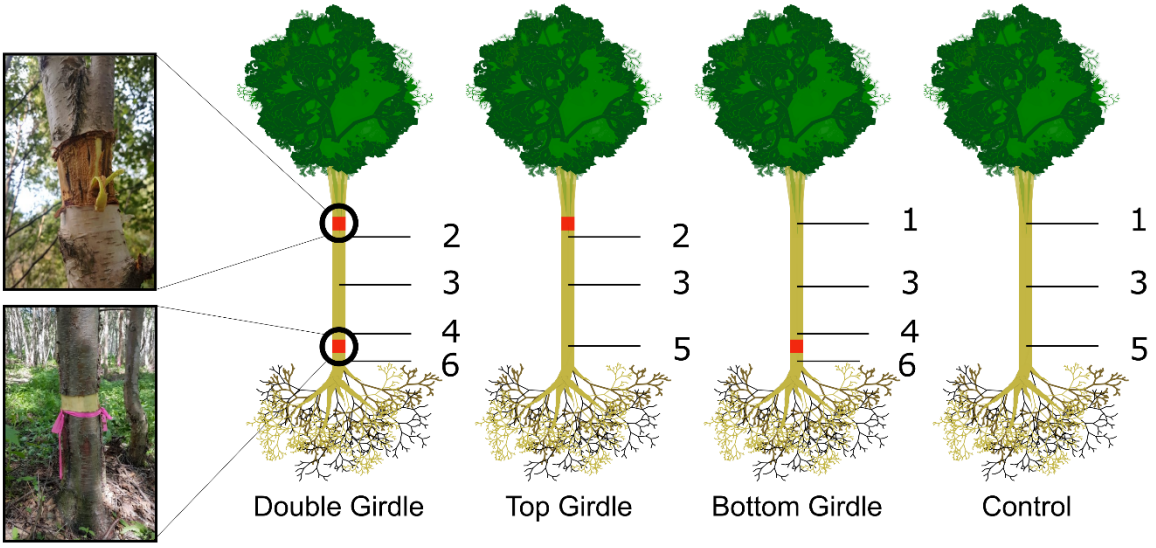

Figure 3-1 Illustration of the girdle treatments and the position of stem sample collection for each treatment group.

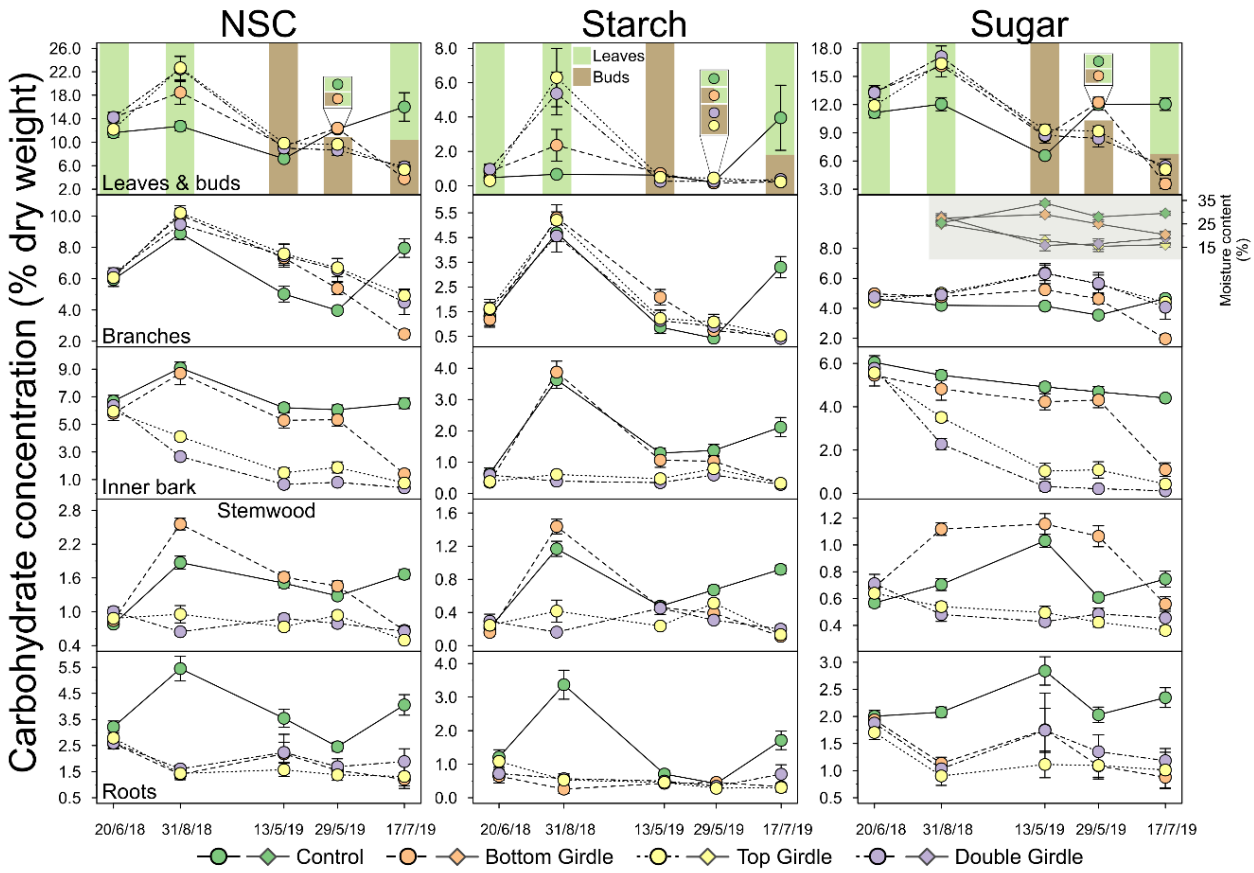

Figure 3-2 Average (± standard error) non-structural carbohydrate (NSC: combined sugar and starch), starch, and sugar concentrations of organ tissues over time in 30 mature *Betula papyrifera* trees subjected to different stem girdling treatments. The first date represents the initial measurements collected prior to stem girdle application. Inner bark and stemwood values depict averages across the three uppermost stem sample locations (see Figure 3-1 Illustration of the girdle treatments and the position of stem sample collection for each treatment group.The inset plot in the 'Branches' panel represents the average (± standard error) moisture content (%) of the fresh branch samples. Control: n = 8, bottom girdle: n = 7, top girdle: n = 8 or 5 (31/8/18 only), and double girdle: n = 7 or 5 (31/8/18 only). To maintain the clarity of the figure, statistical comparisons and differences are provided in Table 3-1, Table A-10 and Table A-11.

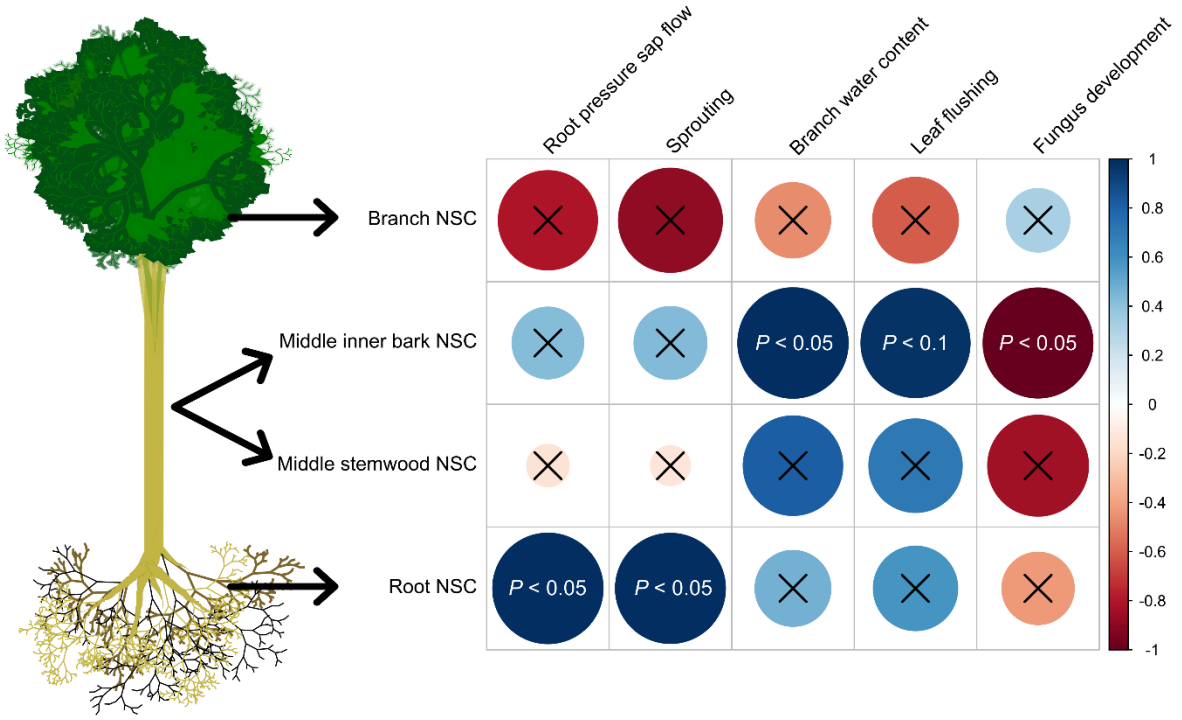

Figure 3-3 Correlations between average NSC concentrations in late August of 2018 for each treatment and the proportion of trees that exhibited root pressure sap flow, root collar sprouting, canopy leaf flush, and fungal infection in the 2019 season, as well as the treatment average of branch water content in mid-May of 2019. Colours denote whether the Pearson correlation coefficient was positive (blue) or negative (red), and whether the relationship was strong (dark) or weak (light). Treatments included control (n = 8), bottom girdle (n = 7), top girdle (n = 8) and double girdle (n = 7). P-values are reported for significant tests only and were adjusted using the Behjamini-Hochberg method.

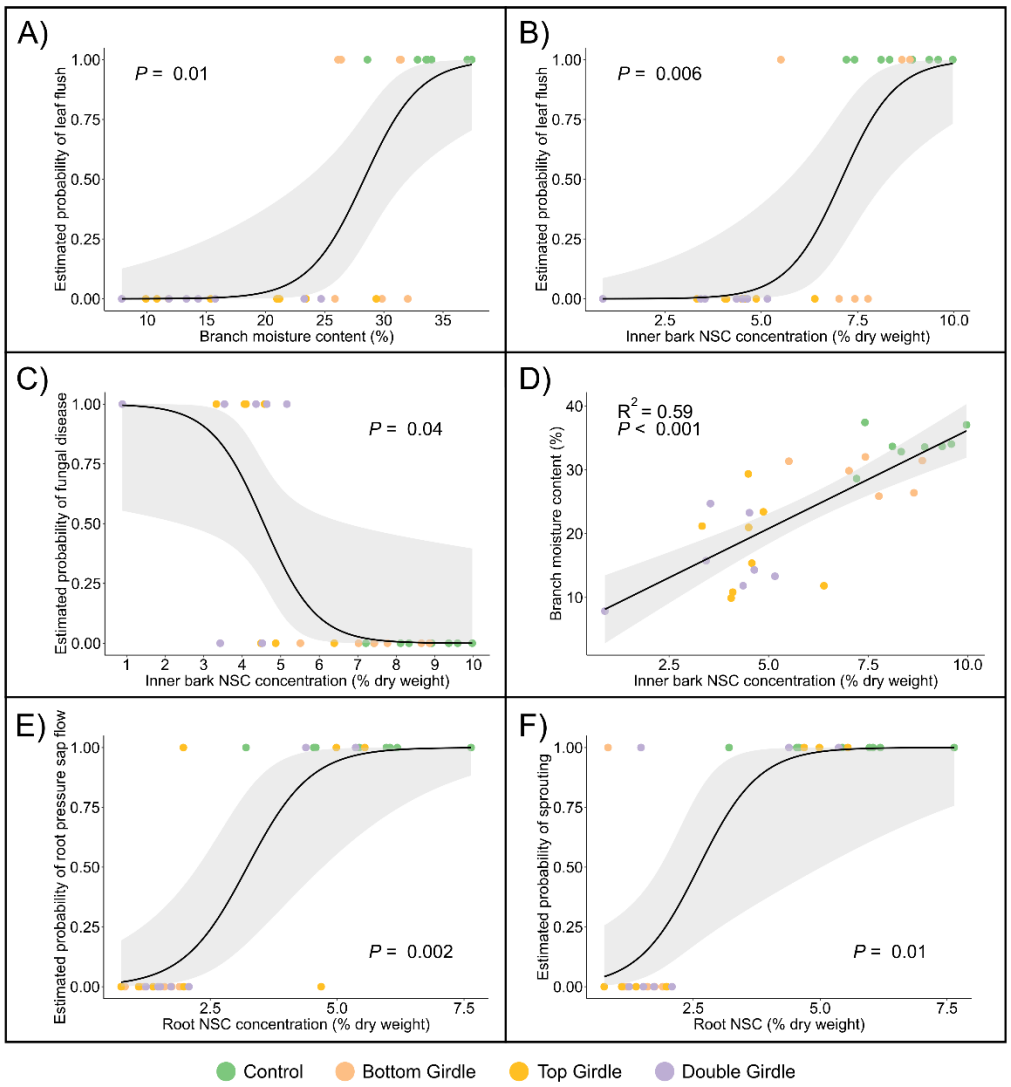

Figure 3-4 Probability of A) 2019 canopy leaf flush predicted by branch NSC concentration in mid-May of 2019, B) 2019 canopy leaf flush predicted by late August 2018 middle stem inner bark NSC concentration C) fungal disease onset (early April 2019) predicted by late August 2018 inner bark NSC concentration, E) 2019 spring root pressure sap flow predicted by late August 2018 root NSC concentration, and F) 2019 root collar sprouting predicted by late August 2018 root NSC concentration. Box D) depicts the linear relationship (with adjusted R^2) between branch moisture content (%) in mid-May of 2019 and late August 2018 inner bark NSC concentration.

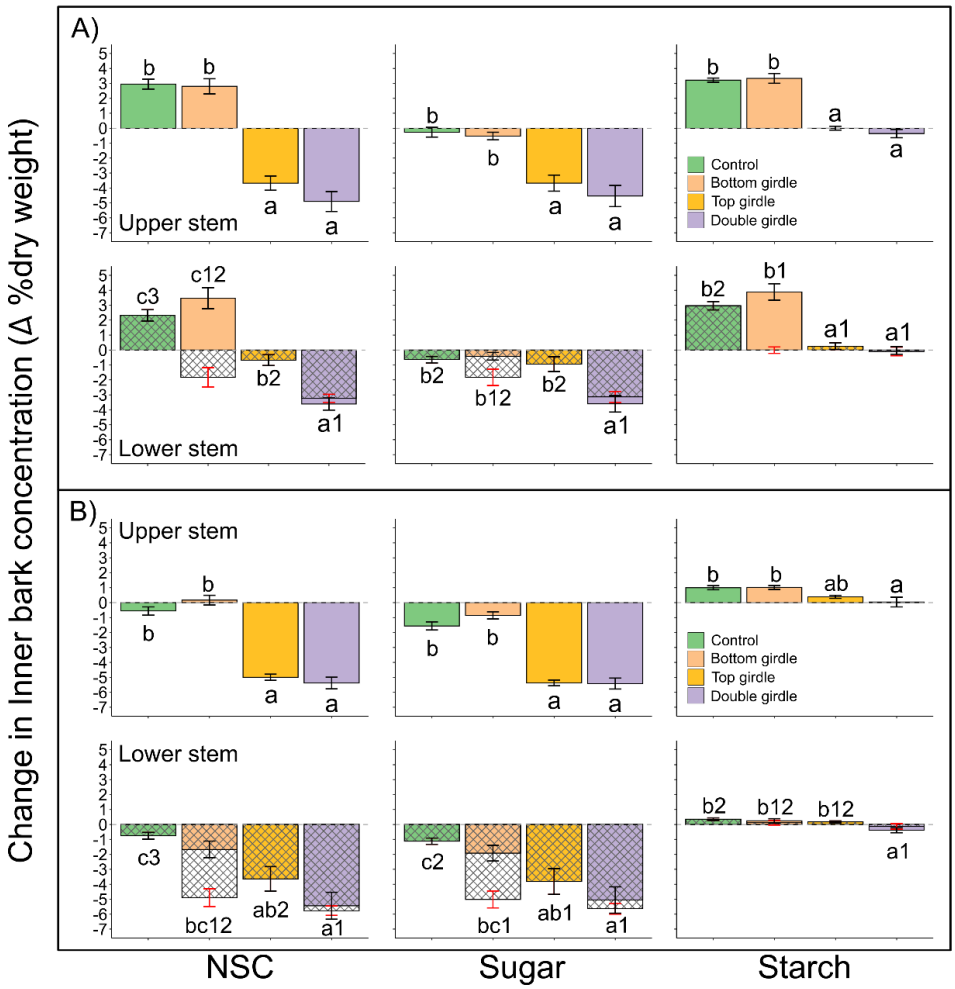

Figure 3-5 Average (± standard error) change in inner bark carbohydrate (NSC, sugar, and starch) concentrations of upper, lower, and root collar positions from the initial measurement in mature *Betula papyrifera* trees subjected to different stem girdling treatments (control: n = 8, bottom girdle: n = 7, top girdle: n = 8, and double girdle: n = 7). (A) The change in concentrations between 21 June 2018 (initial measurement) and 18 August 2018. (B) The change in concentrations between 21 June 2018 and 29 May 2019 after bud flush. For the lower stem region in panel (A), n = 5 for both top and double girdle treatments. For the lower stem region, hatched bars with red standard error bars present the change in concentration at the root collar position where the sample for bottom girdle and double girdle trees was taken below the bottom girdle. Different letters represent differences between treatments for the upper or lower stem samples, and numbers represent differences between treatments for root collar samples (all Tukey's HSD, $\alpha = 0.1$).

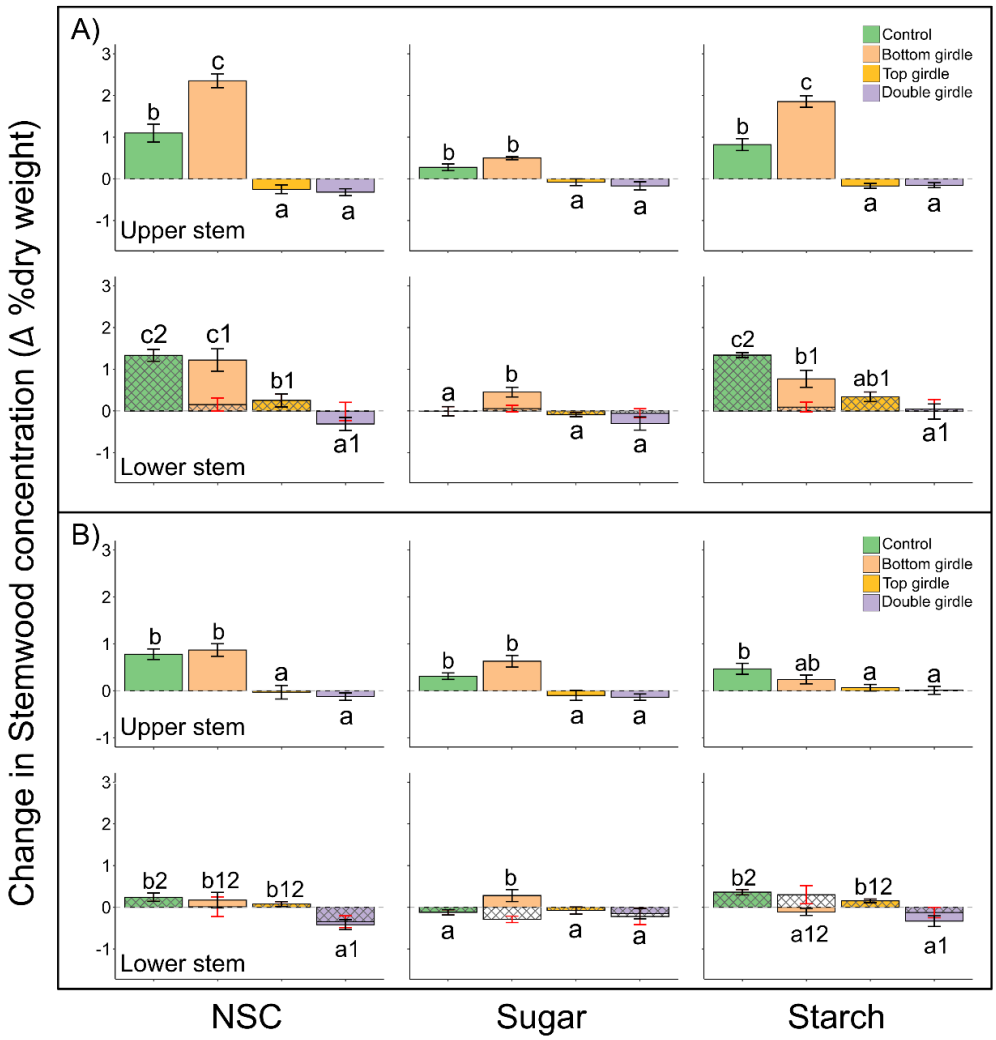

Figure 3-6 Average (± standard error) change in stemwood carbohydrate (NSC, sugar, and starch) concentrations of upper, lower, and root collar positions from the initial measurement in mature *Betula papyrifera* trees subjected to different stem girdling treatments (control: n = 8, bottom girdle: n = 7, top girdle: n = 8, and double girdle: n = 7). (A) The change in concentrations between 21 June 2018 (initial measurement) and 18 August 2018. (B) The change in concentrations between 21 June 2018 and 29 May 2019 after bud flush. For the lower stem region in panel (A), n = 5 for both top and double girdle treatments. For the lower stem region, hatched bars with red standard error bars present the change in concentration at the root collar position where the sample for bottom girdle and double girdle trees was taken below the bottom girdle. Different letters represent differences between treatments for the upper or lower stem samples, and numbers represent differences between treatments for root collar samples (all Tukey's HSD, $\alpha = 0.1$).

4. Chapter 4 – Research synthesis, limitations, and future directions

4.1 Research synthesis

The primary objective of this thesis was to explore non-structural carbohydrate (NSC) partitioning, allocation, and remobilization patterns in mature boreal *Betula papyrifera.* More specifically, the goals were to (1) characterize the seasonal shifts (phenology) of NSC reserves, both in concentration and mass estimates, of organ tissues in mature *B. papyrifera*, and relate them to seasonal growth processes (Chapter 2), and (2) determine the patterns and potential constraints of between organ (branch, stem, roots) and within-stem reserve remobilization when functioning under girdling-induced carbon (C) stress, and relate these stress allocation dynamics to important survival responses. Both studies required assessing the dynamism of tissue/organ NSC reserve concentrations which gives insight into when, where, and how much reserves are being mobilized and reallocated throughout the tree over time — a process that is particularly difficult to achieve in mature trees simply due to size-related methodological challenges. For Chapter 2, these objectives were achieved through describing the changes in organ reserve concentrations and mass estimates over 7 important phenological stages in mature boreal *B. papyrifera*. For Chapter 3 however, the objectives were achieved experimentally in these same trees though use of girdling treatments at different locations on the stem. Through different stem girdling treatments, I was able to explore if, how, and to what extent reserves are distributed among organ tissues when functioning under storage dependency, and how these dynamics differ from those expected under normal seasonal conditions. Both of these research chapters are crucial for improving our understanding of C allocation patterns of mature trees, largely because

these processes are more commonly, and perhaps less accurately, inferred from seedlings or sapling studies due to increased experimental feasibility (see Hartmann *et al*., 2018).

The first study (Chapter 2) characterized the seasonal patterns of NSC reserve concentrations and mass estimates in organ tissues as well as at the whole-tree level of mature boreal *Betula papyrifera* throughout a calendar year. Though it is known that carbohydrate concentrations in tree organs can fluctuate in time as a response to varying strengths of C supply (source) and demand (sink) such as during the changing of seasons (Chapin *et al*., 1990), these fluctuations can vary substantially across different organs, species, functional types, life history traits, as well as across biomes (Martínez-Vilalta *et al*., 2016). Understanding C reserve phenology and how it may contrast across these parameters is an important first step toward gauging species and region-specific risk to stochastic stress events that may rely on C reserves to fuel survival responses. This study contributed to a knowledge gap in the literature, as to the best of my knowledge, it was the first to comprehensively estimate whole-tree and organ-level NSC pool size dynamics in relation to the phenology of mature boreal *B. papyrifera*, in addition to also contrasting these dynamics to mature B. papyrifera in a more temperate climate. The species and region-specific estimates of organ and whole-tree NSC pool estimates provided here can furthermore serve as crucial data to evaluate and improve vegetation models used to forecast forest responses to future environmental conditions.

Chapter 2 revealed that at the whole-tree level, NSC mass in boreal B. papyrifera increased by over 72% from their minima in spring to their maxima late in the growing season — an estimate which greatly exceeded the 28% annual fluctuation of reserves observed in more temperate B. papyrifera trees. Unlike temperate B. papyrifera which exhibited seasonal accumulations of NSC only in the branches (Furze *et al*., 2019), boreal *B. papyrifera* exhibited

accumulations in the branches, stemwood, and coarse root NSC pools. Although differences in ontogenetic stage and size of the individuals between the two studies (with the temperate trees being larger and older) could at least partially explain why such a difference in the magnitude of seasonal NSC fluctuation was observed, this result could also represent an acclimatory response to the increased temperature variability and shorter growing seasons of boreal climates. The more extreme climatic conditions in the boreal could necessitate a stronger drawdown of reserves in the spring to initiate new growth, and perhaps induce a prioritization of reserve formation across the whole tree once pool refilling begins (Wiley and Helliker, 2012; Martínez-Vilalta *et al.*, 2016). It can be speculated that similar differences in annual reserve fluctuations may be observed in species with ranges that span across contrasting moisture regimes, with less extreme fluctuations predicted to occur in drier environments due to a stronger reliance on NSC for hydraulic function (Sala *et al*., 2012). It is also possible that the larger fluctuations of NSC reserves observed in boreal *B. papyrifera* represents a genetic divergence between temperate and boreal populations, either due to climatic differences or possibly to differences in disturbance regimes — with boreal populations being prone to stronger fire and browsing pressures. Such pressures may require larger reserve pools in the branches for shoot regeneration and the production of epidermal resin glands that exude defense compounds onto the bark of the new shoots (Bryant *et al.*, 2009). The extent in which differences in NSC reserve fluctuations between populations is genetically regulated and/or represents an acclimatory/plastic response to ambient conditions could be further explored through use of common garden experiments such as in Blumstein *et al*. (2020), Blumstein and Hopkins (2021), and Blumstein *et al*. (2022).

Although the stemwood represented the largest biomass fraction in these mature trees, Chapter 2 revealed that the branch reserve pool i) made up the majority of whole-tree NSC

throughout the year and ii) was much more dynamic than reserve pools in the coarse roots, stemwood, and inner bark; together, these results suggest that the branches were probably the main source of remobilized NSC to support processes relying on storage. I anticipate the larger absolute size and greater fluctuation of the branch NSC pool in these boreal trees represents a combined effect of increased reliance on branch reserves for shoot defence processes or regeneration (as mentioned previously; Bryant *et al*., 2009), for remobilization in early spring to fuel the flushing and expansion of new leaves and shoots (Landhäusser and Lieffers, 2003; Landhäusser, 2011; Klein *et al.*, 2016), but also for canopy frost tolerance (i.e., soluble sugar accumulation) which is important for trees occupying cold northern environments (Charrier *et al*., 2013). Such as in the roots of *Populus* species under drought (see Galvez *et al*., 2013), reduced NSC accumulation in the branches due to events which limit C acquisition (i.e., drought or herbivory) could greatly increase susceptibility to branch xylem and/or phloem damage in trees exposed to freezing temperatures. I suspect this simple mechanism may be a contributing factor to the widespread branch dieback observed in North American birch stands.

The timing of organ reserve pool refilling and the onset/duration of growth in the canopy, stem, and roots observed in Chapter 2 also highlighted the existence of a top-down sink-hierarchy in these *B. papyrifera* trees. Due to the close proximity of branches to photosynthetic organs, I found that the branch reserve pools began refilling before the stemwood and coarse roots, which supports the idea that the allocation of newly acquired photoassimilates to growth sinks is largely determined by sink distance from C source (Wright, 1989; Wardlaw, 1990). Although shoot, stem diameter, and fine root growth were all observed early in the growing season, the only organ which exhibited reductions in NSC concentration at this time was the roots — likely reflecting this organ's distance from source C and its subsequent reliance on

reserves to fuel early growth. Interestingly, and in further support of the proposed top-down sink hierarchy, fine root growth appeared to be interrupted midway through the growing season, presumably due to the competing diameter growth sink in the stem; only by late autumn once growth sinks in aboveground organs had ceased did fine root growth resume. The top-down allocation strategy observed here may have large implications for how these trees experience periods of C limitation, because as C supply declines, the roots should be affected first and disproportionately more than other organs in closer proximity to the canopy.

The second study (Chapter 3) built upon this discussion of source-sink distance effects as well as the role of the stem in the distribution and usage of NSC reserves through evaluating if and how reserves are redistributed among tree storage compartments (branch, stem, roots) when C transport from the canopy is restricted at the upper and/or lower stem via phloem girdling. The strategic placement of girdles at these locations on the stem allowed for us to partition out the potential reserve contribution and remobilization patterns of connected organs through comparisons of tissue NSC concentrations over time to treatments where the same organ reserve pools were separated by girdles. The placement of girdles at the upper and/or lower stem also allowed for the detection of any spatial constraints on inter-organ and intra-stem reserve remobilization patterns in these tall trees. Studies such as this that consider mature tree C reserve dynamics across multiple organs and tissues under C stress are rare — especially so when remobilization patterns are assessed at high temporal and spatial resolutions. As such, this study serves as an excellent contribution towards furthering the mechanistic understanding of NSC allocation patterns in large and mature trees functioning under prolonged periods of C stress.

Despite the common perception that stored C in organs of mature trees may be available for redistribution throughout the organism during periods of C limitation, Chapter 3 revealed that

stem NSC reserves in mature *B. papyrifera* trees may not be easily remobilized to other, perhaps more distant, organ sinks like the roots under such conditions. The lack of observed C import from the stem to the roots may cast doubt on either the exceptional sink strength of the root systems (and associated microorganisms) or the importance of the stem (despite its large biomass) as a source of reserves, particularly when the stem is faced with C limitation. This finding is in alignment with Chapter 2 in that stem reserves did not appear to be remobilized to the canopy in spring to fuel bud flush and early shoot expansion. Together, these results may reveal the problematic nature of using the stem C reserve status as an indicator of overall tree resiliency, as the use of such proxies could be irrelevant when predicting survival under future stress and disturbance events. A more realistic approach may be to instead consider organ storage pools as being regulated independently as somewhat autonomous units — further reason for C stress and starvation to be organ-specific and complex.

Although Chapter 3 provided evidence that reserve allocation from the stem to other organs like the roots was negligible, NSC did appear to be imported into the lower stem/root collar region, potentially from both the roots and the inner bark higher up on the stem. When considering the export of root reserves, reserve allocation did not appear to extend beyond the lower stem region; this could suggest that i) reserve allocation to stem sinks was largely limited by distance from source roots, and/or ii) the amount of exported root reserves was also fairly minimal in these trees. If a greater sink priority existed in stems when NSC supply was limited, and if the roots contributed even minor amounts of reserves to these sinks, then the pool of NSC available in the roots to fuel local processes such as fine root growth and frost protection would be reduced (Fermaniuk *et al*., 2021) — potentially resulting in greater vulnerability to hydraulic limitation in the following season. Whatever the mechanism, the allocation patterns observed

here could represent an adaptive recovery strategy that preserves the lower stem reserve pool to support future sprouting responses.

Chapter 3 also highlighted how, and to what extent, the reduced supply of NSC in the stem and roots of girdled *B. papyrifera* affected functions such as sprouting, the spring recovery of the hydraulic system, bud flush, and pathogen defence in the second season. Low root carbohydrate concentrations by the end of the first growing negatively impacted the occurrence of xylem sap flow and sprouting in the second growing season, with potential root NSC thresholds of > 2.5% dry weight for the occurrence of these events. Similarly, trees with C limited stems were generally unable to recover their hydraulic system and expand new buds and shoots in the second season, presumably due to the lack of lateral osmotic gradients which would allow for the access of stem water reserves and potential refilling of embolized vessels to the buds. The thresholds for bud flush were >5% inner bark NSC in the first growing season and >25% branch moisture content early in the second growing season. An inner bark NSC threshold of ~6% NSC at the end of the first growing season also appeared to determine whether trees were able to defend against pathogenic fungal infection in the stem tissues by May of the second growing season, highlighting the importance of NSC reserves in the production of defense compounds and disease resiliency.

The combined interpretation of both studies suggests that C allocation under normal seasonal conditions and reserve remobilization under induced C stress may not follow the same framework and could potentially be regulated by different mechanisms. Throughout the growing season, Chapter 2 revealed that NSCs were able to accumulate throughout all tree organs, however, under C limitation (Chapter 3), the remobilization of NSC reserves between organs appeared to be more constrained. Although primary production slows towards the end of the

season, trees in Chapter 2 were not subject to drastic C limitation and thus were able to maintain a somewhat even-flow allocation of current assimilates from the canopy to the stem and finally to the roots as storage pools filled top-down. In contrast, the apparent constraint on the remobilization of reserves from storage in trees with a girdle below the canopy emphasizes that remobilization under C limitation might be more complex, with distance and organ C supply potentially becoming increasingly more important drivers of remobilization as C supply from the canopy declines.

Lastly, although results in Chapter 2 suggested that the branches were likely the most important storage pool in these boreal trees under normal seasonal conditions, Chapter 3 revealed that the crown has the capacity to store nearly double the amount of NSCs – thus leading to the question of why additional storage in the crown did not occur. This finding might suggest that the allocation of newly assimilated C to storage might not follow the simplified framework that storage sinks in tissues of closest proximity to the leaves receive C and fill up first, and only once these sinks are sated, does excess C flow down to more distant storage sinks in the stem and roots. The allocation of C to storage in trees is likely a genetically regulated mechanism (Blumstein *et al*., 2022) which could ensure that C supply is not overly disproportionate among organs when conditions are not C limiting. Such a mechanism could warrant the availability of at least some reserves in organs below the canopy if C stress were to occur — a process that could be particularly important if inter-organ reserve remobilization is constrained and/or organs storage pools are regulated somewhat autonomously.

4.2 Experimental limitations

This research was able to characterize the seasonal shifts of NSC reserve pools in terms of mass and concentrations, as well as identify the patterns and constraints of reserve allocation

and remobilization both within and between organs of mature boreal *B. papyrifera* functioning under C limiting conditions. The study of mature trees to assess C reserve allocation and remobilization patterns in natural environments is a less common but required step towards accurately gauging how forests will respond to a changing climate. However, in natural environments, mature tree reserve allocation patterns are difficult to assess both observationally and experimentally due to i) tree size/access constraints on organs, ii) the possibility for confounding and complex interactions with many environmental variables, as well as iii) the potential for whole-organism stress responses to span over long temporal horizons.

In the first study (Chapter 2), one issue of studying larger trees was that allometric equations had to be used to estimate organ and whole-tree NSC pools over time. Though accurate quantification of NSC pools can be achieved at the whole-organism level in seedlings or saplings through destructive sampling and processing of all tissue mass over time, it is not feasible to apply such techniques to numerous mature trees at many timepoints throughout a calendar year. Allometric equations specific to birch in North America were incorporated to account for this inherent size constraint (Jenkins *et al*., 2004; Chojnacky *et al*., 2014), however, the application of such generalized equations rests on the broad assumption that allometric relationships remain consistent with tree dimensions (i.e., dbh or height) within families and across environmental or geographical ranges — a caveat that may not entirely be true. Research has highlighted how generalized allometric equations may yield inaccurate estimates of both above and belowground tree biomass (Xing *et al*., 2019), and as such, the absolute mass of NSC pool in organs pools estimated in Chapter 2 should be interpreted with some level of caution.

Due to the potential for mature trees to withstand long periods under stress, trees in Chapter 3 were girdled at a point when stemwood and root reserve pools were at a seasonal

minimum (early summer) as a means to lessen the time until organ death, however, this methodology could have influenced the pattern and degree (or lack thereof) of remobilizations observed between these two organs over time. Although Chapter 3 revealed that the stemwood did not serve as a significant source of stored C to the roots when both stem and roots were functioning under C limiting conditions, it is possible that the lack of reserve remobilization reflects stemwood C supply being below a threshold for remobilization at the time of girdling. Similarly, the somewhat minor mobilization of root reserves to the lower stem/root collar could have potentially been stronger and detected in tissues higher up on the stem if more root reserves were available at the time of girdling.

Though stem girdling in is an excellent means to experimentally manipulate carbohydrate allocation in mature trees, the degree to which girdling treatments in Chapter 3 were actually representative of common environmental conditions which limit C supply, as well as the responses these conditions elicit, should be carefully considered when generalizing the results observed here. Stem girdling, manual defoliation, and herbivory may all limit C allocation to the stem and roots through reductions of C supply from the canopy, however, natural herbivory may illicit defense responses which otherwise would not occur under experimental manipulations of C supply to organs (Piper & Fajardo, 2014; Piper *et al*., 2015). In addition, trees in natural environments may respond or acclimate to C limitation with processes and mechanisms which mitigate C stress; these processes and mechanisms, such as sprouting (following the onset of C limitation), regrowth of damaged tissues (e.g., phloem at girdle sites), as well as the potential receipt of supplementary carbohydrates from belowground (e.g., mycorrhizal networks and/or root grafts), were suppressed and/or not considered in detail within this study. These are

important future considerations, as they constitute more realistic responses of trees under C limiting conditions.

4.3 Future research

Together, these two studies contributed to the current understanding of NSC reserve phenology in boreal trees, as well as provided valuable insight into how reserve are allocated and remobilized under conditions of C limitation in mature trees. In addition, it also highlighted several new research opportunities:

1. **Explore, in greater detail, how geographical range influences intraspecific differences in seasonal reserve pool fluctuations in species other than *B. papyrifera* with ranges that span large climatic and edaphic gradients.** Chapter 2 highlighted the potential for geographical location and disturbance regime to drive strong differences in reserve storage and usage on an intraspecific level. Though there is a continued need for detailed studies of seasonal C storage dynamics in trees, assessing how these fluctuations may diverge even within a species according to climate and disturbance will help with the development of more robust and region-specific vegetation models as well as determine when, and in what organs, different populations may be most at risk of C limitation.

2. **Assess if the observed source-sink dynamics remain consistent when mature *B. papyrifera* trees are girdled later in the growing season once reserve pools in the stemwood and roots have begun to refill.** Though C allocation can be regulated by both sink strength and priority, the capacity for an organ to act as a source of reserves to sinks is also inherently limited by the supply of C within the source organ itself. Chapter 3 provided insight into how mature *B. papyrifera* may respond to C limitation at the start of

the growing season when reserves in the stemwood and roots were at a seasonal minimum, however, further assessment into how NSC allocation patterns may vary temporally or spatially under different reserve pool sizes in a species, and the extent to which these patterns may drive differences in survival outcomes, could provide a more complete understanding of how these trees will respond to stress and disturbance at different times of year.

3. **Explore the osmotic roles of stem NSCs in early spring, and how these mechanisms dictate whether trees refill embolized xylem conduits and re-establish hydraulic conductivity under situations where positive pressures are not evident and/or root water uptake is compromised.** Chapter 3 suggests a strong role of NSC accumulation in the inner bark as a means of at least temporarily restoring the hydraulic system after winter when root water uptake was potentially compromised, however, the exact mechanism and source of water remains somewhat unclear. Though I suspect this water was drawn out from storage in the heartwood via radial osmotic gradients, it is also possible that refilling processes were related water uptake through the lenticels (Westhoff *et al*., 2009). Future studies should incorporate stronger molecular analyses and the monitoring of organ water storage to elucidate the role of NSCs in embolism reversal following winter, as well as highlight the likely source of water for these processes when root mortality is high and insufficient root water uptake is observed.

4. **Investigate, in greater detail, how reserve allocation priorities under C limitation relate to secondary metabolism such as constitutive and inducible defence against**

herbivory and pathogen attack. C reserves are crucial for defence against biotic attack; however, the extent reserves are delegated to secondary metabolite production for defence versus other competing sinks under C limiting conditions is still a relatively unknown component of the C allocation framework. Here I found a positive relationship between stem NSC content in girdled trees and susceptibility to fungal infection in the following growing season, however, this was not explored in great detail. Future studies should investigate the trade-offs between reserve allocation to defence and other physiological demands important for survival under C stress.

.

Literature Cited

Adams, H. D., Germino, M. J., Breshears, D. D., Barron-Gafford, G. A., Guardiola-Claramonte, M., Zou, C. B., & Huxman, T. E. (2013). Nonstructural leaf carbohydrate dynamics of Pinus edulis during drought-induced tree mortality reveal role for carbon metabolism in mortality mechanism. *New Phytologist*, *197*(4), 1142-1151

Adams, H. D., Zeppel, M. J. B., Anderegg, W. R. L., Hartmann, H., Landhäusser, S. M., Tissue, D. T., Huxman, T. E., Hudson, P. J., Franz, T. E., Allen, C. D., Anderegg, L. D. L., Barron-Gafford, G. A., Beerling, D. J., Breshears, D. D., Brodribb, T. J., Bugmann, H., Cobb, R. C., Collins, A. D., Dickman, L. T., Duan, H., Ewers, B. E., Galiano, L., Galvez, D. A, Garcia-Forner, N., Gaylord, M. L., Germino, M. J., Gessler, A., Hacke, U. G., Hakamada, R., Hector, A., Jenkins, M. W., Kane, J. M., Kolb, T. E., Law, D. J., Lewis, J. D., Limousin, J., Love, D. M., Macalady, A. K., Martínez-Vilalta, J., Mencuccini, M., Mitchell, P. J., Muss, J. D., O'Brien, M. J., O'Grady, A. P., Pangle, R. E., Pinkard, E. A., Piper, F. I., Plaut, J. A., Pockman, W. T., Quirk, J., Reinhardt, K., Ripullone, F., Ryan, M. G., Sala, A., Sevanto, S., Sperry, J. S., Vargas, R., Vennetier, M., Way, D. A., Xu, C., Yepez, E. A., & McDowell, N. G. (2017). A multi-species synthesis of physiological mechanisms in drought-induced tree mortality. *Nature Ecology & Evolution*, *1*(9),1285-1291.

Alberta Climate Information Services (ACIS). (2019). *Current and Historical Alberta Weather Station Data*. Retrieved from https://agriculture.alberta.ca/acis.

Allen, C. D. (2009) Climate-induced forest dieback: as escalating global phenomenon. *Unasylva 231*(232), 60.

Allen, C. D., Macalady, A. K., Chenchouni, H., Bachelet, D., McDowell, N., Vennetier, M., Kitzberger, T., Rigling, A., Breshears, D. D., Hogg, E. T., Gonzalez, P., Fensham, R., Zhang, Z., Castro, J., Demidova, N., Lim, J., Allard, G., Running, S. W., Semerci, A., & Cobb, N. (2010). A global overview of drought and heat-induced tree mortality reveals emerging climate change risks for forests. *Forest Ecology and Management*, *259*(4), 660-684.

Allen, C. D., Breshears, D. D., & McDowell, N. G. (2015). On underestimation of global vulnerability to tree mortality and forest die-off from hotter drought in the Anthropocene. *Ecosphere*, *6*(8), 1-55.

Améglio, T., Ewers, F. W., Cochard, H., Martignac, M., Vandame, M., Bodet, C., & Cruiziat, P. (2001). Winter stem xylem pressure in walnut trees: effects of carbohydrates, cooling and freezing. *Tree Physiology*, *21*(6), 387-394.

Améglio, T., Decourteix, M., Alves, G., Valentin, V., Sakr, S., Julien, J. L., Petel, G., Guilliot, A., & Lacointe, A. (2004). Temperature effects on xylem sap osmolarity in walnut trees: evidence for a vitalistic model of winter embolism repair. *Tree Physiology*, *24*(7), 785-793.

Anderegg, W. R., & Anderegg, L. D. (2013). Hydraulic and carbohydrate changes in experimental drought-induced mortality of saplings in two conifer species. *Tree Physiology*, *33*(3), 252-260.

Anderegg, W. R., Kane, J. M., & Anderegg, L. D. (2013). Consequences of widespread tree mortality triggered by drought and temperature stress. *Nature Climate Change*, *3*(1), 30-36.

Bala, G., Caldeira, K., Wickett, M., Phillips, T. J., Lobell, D. B., Delire, C., & Mirin, A. (2007). Combined climate and carbon-cycle effects of large-scale deforestation. *Proceedings of the National Academy of Sciences* 104: 6550–6555.

Barbaroux, C., Bréda, N., & Dufrêne, E. (2003). Distribution of above-ground and below-ground carbohydrate reserves in adult trees of two contrasting broad-leaved species (Quercus petraea and Fagus sylvatica). *New Phytologist*, *157*(3), 605-615.

Beck, P. S., Juday, G. P., Alix, C., Barber, V. A., Winslow, S. E., Sousa, E. E., Heiser, P., Herriges, J. D., & Goetz, S. J. (2011). Changes in forest productivity across Alaska consistent with biome shift. *Ecology letters*, *14*(4), 373-379.

Blumstein, M., Richardson, A., Weston, D., Zhang, J., Muchero, W., & Hopkins, R. (2020). A new perspective on ecological prediction reveals limits to climate adaptation in a temperate tree species. *Current Biology*, *30*(8), 1447-1453.

Blumstein, M., & Hopkins, R. (2021). Adaptive variation and plasticity in non-structural carbohydrate storage in a temperate tree species. *Plant, Cell & Environment*, *44*(8), 2494-2505.

Blumstein, M., Sala, A., Weston, D. J., Holbrook, N. M., & Hopkins, R. (2022). Plant carbohydrate storage: intra-and inter-specific trade-offs reveal a major life history trait. *New Phytologist*, *235*(6), 2211-2222.

Bréda, N., Huc, R., Granier, A., & Dreyer, E. (2006). Temperate forest trees and stands under severe drought: a review of ecophysiological responses, adaptation processes and long-term consequences. *Annals of Forest Science*, *63*(6), 625-644.

Bollmark, L., Sennerby-Forsse, L., & Ericsson, T. (1999). Seasonal dynamics and effects of nitrogen supply rate on nitrogen and carbohydrate reserves in cutting-derived Salix viminalis plants. *Canadian Journal of Forest Research*, *29*(1), 85-94.

Bonan, G. B. (2008). Forests and climate change: forcings, feedbacks, and the climate change benefits of forests. *Science* 320, 1444–1449. doi: 10.1126/science.1155121.

Bond, W. J., & Midgley, J. J. (2003). The evolutionary ecology of sprouting in woody plants. *International Journal of Plant Sciences*, *164*(S3), S103-S114.

Bowen, B. J., & Pate, J. S. (1993). The significance of root starch in post-fire shoot recovery of the resprouter Stirlingia latifolia R. Br.(Proteaceae). *Annals of Botany*, *72*(1), 7-16.

Bryant, J. P., Clausen, T. P., Swihart, R. K., Landhäusser, S. M., Stevens, M. T., Hawkins, C. D., Carrière, S., Kirilenko, A. P, Veitch, A. M., Popko, R. A., Cleland, D. T., Williams, J. H., Jakubas, W. J., Carlson, M. R., Lehmkuhl Bodony, K., Cebrian, M., Paragi, T. F., Picone, P. M., Moore, J. E., Packee, E. C., & Malone, T. (2009). Fire drives transcontinental variation in tree birch defense against browsing by snowshoe hares. *The American Naturalist*, *174*(1), 13-23.

Bucci, S. J., Scholz, F. G., Goldstein, G., Meinzer, F., & Sternberg, L. D. S. (2003). Dynamic changes in hydraulic conductivity in petioles of two savanna tree species: factors and mechanisms contributing to the refilling of embolized vessels. *Plant, Cell & Environment*, *26*(10), 1633-1645.

Buma, B., & Barrett, T. M. (2015). Spatial and topographic trends in forest expansion and biomass change, from regional to local scales. *Global Change Biology*, *21*(9), 3445-3454.

Canham, C. D., Kobe, R. K., Latty, E. F., & Chazdon, R. L. (1999). Interspecific and intraspecific variation in tree seedling survival: effects of allocation to roots versus carbohydrate reserves. *Oecologia*, *121*(1), 1-11.

Chapin III, F. S., Schulze, E. D., & Mooney, H. A. (1990). The ecology and economics of storage in plants. *Annual Review of Ecology and Systematics*, *21*(1), 423-447.

Charrier, G., Cochard, H., & Améglio, T. (2013). Evaluation of the impact of frost resistances on potential altitudinal limit of trees. *Tree Physiology*, *33*(9), 891-902.

Chojnacky, D. C., Heath, L. S., & Jenkins, J. C. (2014). Updated generalized biomass equations for North American tree species. *Forestry*, *87*(1), 129-151.

Clarke, P. J., Lawes, M. J., Midgley, J. J., Lamont, B. B., Ojeda, F., Burrows, G. E., Enright, N. J., & Knox, K. J. E. (2013). Resprouting as a key functional trait: how buds, protection and resources drive persistence after fire. *New Phytologist*, *197*(1), 19-35.

Delpierre, N., Vitasse, Y., Chuine, I., Guillemot, J., Bazot, S., & Rathgeber, C. B. (2016). Temperate and boreal forest tree phenology: from organ-scale processes to terrestrial ecosystem models. *Annals of Forest Science*, *73*(1), 5-25.

Desrochers, A., Landhäusser, S. M., & Lieffers, V. J. (2002). Coarse and fine root respiration in aspen (Populus tremuloides). *Tree Physiology*, *22*(10), 725-732.

De Schepper, V., Vanhaecke, L., & Steppe, K. (2011). Localized stem chilling alters carbon processes in the adjacent stem and in source leaves. *Tree Physiology*, *31*(11), 1194-1203.Deslippe, J. R., & Simard, S. W. (2011). Below-ground carbon transfer among Betula nana may increase with warming in Arctic tundra. *New Phytologist*, *192*(3), 689-698.

Dietze, M. C., Sala, A., Carbone, M. S., Czimczik, C. I., Mantooth, J. A., Richardson, A. D., & Vargas, R. (2014). Nonstructural carbon in woody plants. *Annual Review of Plant Biology*, *65*, 667-687.

Epron, D., Bahn, M., Derrien, D., Lattanzi, F. A., Pumpanen, J., Gessler, A., Högberg, P., Maillard, P., Dannoura, M., Gérant, D., & Buchmann, N. (2012). Pulse-labelling trees to study carbon allocation dynamics: a review of methods, current knowledge and future prospects. *Tree Physiology*, *32*(6), 776-798.

Ericsson, T., Rytter, L., & Vapaavuori, E. (1996). Physiology of carbon allocation in trees. *Biomass and Bioenergy*, *11*(2-3), 115-127.

Essiamah, S., & Eschrich, W. (1985). Changes of starch content in the storage tissues of deciduous trees during winter and spring. *IAWA Journal*, *6*(2), 97-106.

Fabricius L. (1905). Untersuchungen über den St*ä*rke-und Fettgehalt der Fichte aufder oberbayerischen Hochebene. *Naturwissenschaftliche Zeitung für Land-u. Forstwirtschaft, 3*, 137.

FAO, 2018. The State of the World's Forests 2018 - Forest pathways to sustainable development. Rome.

Fermaniuk, C., Fleurial, K. G., Wiley, E., & Landhäusser, S. M. (2021). Large seasonal fluctuations in whole-tree carbohydrate reserves: is storage more dynamic in boreal ecosystems?. *Annals of Botany*, *128*(7), 943-957.

Fischer A. 1891. Beitrage zur Physiologie der Holzgew*ä*chse. *Jahrbücher für wissenschaftliche Botanik, 22*, 73–160.

Furze, M. E., Huggett, B. A., Aubrecht, D. M., Stolz, C. D., Carbone, M. S., & Richardson, A. D. (2019). Whole-tree nonstructural carbohydrate storage and seasonal dynamics in five temperate species. *New Phytologist*, *221*(3), 1466-1477.

Furze, M. E., Huggett, B. A., Aubrecht, D. M., Stolz, C. D., Carbone, M. S., & Richardson, A. D. (2019). Whole-tree nonstructural carbohydrate storage and seasonal dynamics in five temperate species. *New Phytologist*, *221*(3), 1466-1477.

Galiano, L., Martínez-Vilalta, J., & Lloret, F. (2011). Carbon reserves and canopy defoliation determine the recovery of Scots pine 4 yr after a drought episode. *New Phytologist*, *190*(3), 750-759.

Galvez, D. A., Landhäusser, S. M., & Tyree, M.T. (2013). Low root reserve accumulation during drought may lead to winter mortality in poplar seedlings. *New Phytologist, 198*, 139-148.

Gaylord, M. L., Kolb, T. E., Pockman, W. T., Plaut, J. A., Yepez, E. A., Macalady, A. K., Pangle, R. E., & McDowell, N. G. (2013). Drought predisposes piñon–juniper woodlands to insect attacks and mortality. *New Phytologist*, *198*(2), 567-578.

Gleason, S. M., & Ares, A. (2004). Photosynthesis, carbohydrate storage and survival of a native and an introduced tree species in relation to light and defoliation. *Tree Physiology*, *24*(10), 1087-1097.

Gough, C. M., Flower, C. E., Vogel, C. S., Dragoni, D., & Curtis, P. S. (2009). Whole-ecosystem labile carbon production in a north temperate deciduous forest. *Agricultural and Forest Meteorology*, *149*(9), 1531-1540.

Hartig T. (1878). *Anatomie und Physiologie der Holzpflanzen Dargestellt in der Entstehungsweise und im Entwickelungsverlaufe der Einzelzelle, der Zellsysteme, der Pflanzenglieder und der Gesammtpflanze*. Berlin, Heidelberg, Germany: Springer.

Hartmann, H., Ziegler, W., Kolle, O., & Trumbore, S. (2013). Thirst beats hunger–declining hydration during drought prevents carbon starvation in Norway spruce saplings. *New Phytologist*, *200*(2), 340-349.

Hartmann, H., & Trumbore, S. (2016). Understanding the roles of nonstructural carbohydrates in forest trees–from what we can measure to what we want to know. *New Phytologist*, *211*(2), 386-403.

Hartmann, H., Adams, H. D., Hammond, W. M., Hoch, G., Landhäusser, S. M., Wiley, E., & Zaehle, S. (2018). Identifying differences in carbohydrate dynamics of seedlings and mature trees to improve carbon allocation in models for trees and forests. *Environmental and Experimental Botany*, *152*, 7-18.

Hikino, K., Danzberger, J., Riedel, V. P., Hesse, B. D., Hafner, B. D., Gebhardt, T., Rehschuh, R., Ruehr, N. K., Brunn, M., Bauerle, T. L., Landhäusser, S. M., Lehmann, M. M., Rötzer, T., Pretzsch, H., Buegger, F., Weikl, F., Pritsch, K., & Grams, T. E. (2022). Dynamics of initial carbon allocation after drought release in mature Norway spruce—Increased belowground allocation of current photoassimilates covers only half of the carbon used for fine-root growth. *Global Change Biology*, *28*(23), 6889-6905.

Henriksson, N., Tarvainen, L., Lim, H., Tor-Ngern, P., Palmroth, S., Oren, R., Marshall, J., & Näsholm, T. (2015). Stem compression reversibly reduces phloem transport in Pinus sylvestris trees. *Tree Physiology*, *35*(10), 1075-1085.

Hoch, G., Richter, A., & Körner, C. (2003). Non-structural carbon compounds in temperate forest trees. *Plant, Cell & Environment*, *26*(7), 1067-1081.

Hoch G. (2015). Carbon reserves as indicators for carbon limitation in trees. In: U. Luttge, W. Beyschlag (Eds.), *Progress in Botany* (pp.321-346). Springer International Publishing.

Hölttä, T., Vesala, T., Sevanto, S., Perämäki, M., & Nikinmaa, E. (2006). Modeling xylem and phloem water flows in trees according to cohesion theory and Münch hypothesis. *Trees*, *20*(1), 67-78.

Hölttä, T., Dominguez Carrasco, M. D. R., Salmon, Y., Aalto, J., Vanhatalo, A., Bäck, J., & Lintunen, A. (2018). Water relations in silver birch during springtime: How is sap pressurised?. *Plant Biology*, *20*(5), 834-847.

Ingram, J., & Bartels, D. (1996). The molecular basis of dehydration tolerance in plants. *Annual Review of Plant Physiology and Plant Molecular Biology*, *47*, 377–403.

Iwasa, Y. O. H., & Kubo, T. (1997). Optimal size of storage for recovery after unpredictable disturbances. *Evolutionary Ecology*, *11*(1), 41-65

Jenkins, J. C., Chojnacky, D. C., Heath, L. S., & Birdsey, R. A. (2004). *Comprehensive database of diameter-based biomass regressions for North American tree species.* Northeastern Research Station, Newtown Square, PA, USA: USDA Forest Service.

Johnsen, K., Maier, C., Sanchez, F., Anderson, P., Butnor, J., Waring, R., & Linder, S. (2007). Physiological girdling of pine trees via phloem chilling: proof of concept. *Plant, Cell & Environment*, *30*(1), 128-134.

Jongebloed, U., Szederkényi, J., Hartig, K., Schobert, C., & Komor, E. (2004). Sequence of morphological and physiological events during natural ageing and senescence of a castor bean leaf: Sieve tube occlusion and carbohydrate back-up precede chlorophyll degradation. *Physiologia Plantarum*, *120*(2), 338-346.

Kasuga, J., Arakawa, K., & Fujikawa, S. (2007). High accumulation of soluble sugars in deep supercooling Japanese white birch xylem parenchyma cells. *New Phytologist*, *174*(3), 569-579.

Klein, T., Vitasse, Y., & Hoch, G. (2016). Coordination between growth, phenology and carbon storage in three coexisting deciduous tree species in a temperate forest. *Tree Physiology*, *36*(7), 847-855.

Kobe, R. K. (1997). Carbohydrate allocation to storage as a basis of interspecific variation in sapling survivorship and growth. *Oikos*, 226-233

Körner, C. (2003). Carbon limitation in trees. *Journal of Ecology*, *91*(1), 4-17.

Kozlowski, T. T. (1992). Carbohydrate sources and sinks in woody plants. *The Botanical Review*, *58*(2), 107-222.

Kozlowski, T. T., & Cooley, J. H. (1961). Natural root grafting in northern Wisconsin. *Journal of Forestry*, *59*(2), 105-107.

Lamont, B. B., Enright, N. J., & He, T. (2011). Fitness and evolution of resprouters in relation to fire. *Plant Ecology*, *212*(12), 1945-1957.

Landhäusser, S. M., & Wein, R. W. (1993). Postfire vegetation recovery and tree establishment at the Arctic treeline: climate-change-vegetation-response hypotheses. *Journal of Ecology*, 665-672.

Landhäusser, S. M., Wein, R. W., & Lange, P. (1996). Gas exchange and growth of three arctic tree-line tree species under different soil temperature and drought preconditioning regimes. *Canadian Journal of Botany*, *74*(5), 686-693.

Landhäusser, S. M., & Lieffers, V. J. (1998). Growth of Populus tremuloides in association with Calamagrostis canadensis. *Canadian Journal of Forest Research*, *28*(3), 396-401.

Landhäusser, S. M., & Lieffers, V. J. (2002). Leaf area renewal, root retention and carbohydrate reserves in a clonal tree species following above-ground disturbance. *Journal of Ecology*, *90*(4), 658-665.

Landhäusser, S. M. (2003). Effect of soil temperature on rooting and early establishment of balsam poplar cuttings. *Tree Planters Notes*, *50*(1), 34-37.

Landhäusser, S. M., & Lieffers, V. J. (2003). Seasonal changes in carbohydrate reserves in mature northern Populus tremuloides clones. *Trees*, *17*(6), 471-476.

Landhäusser, S. M. (2011). Aspen shoots are carbon autonomous during bud break. *Trees*, *25*(3), 531-536.

Landhäusser, S. M., & Lieffers, V. J. (2012). Defoliation increases risk of carbon starvation in root systems of mature aspen. *Trees*, *26*(2), 653-661.

Landhäusser, S. M., Pinno, B. D., Lieffers, V. J., & Chow, P. S. (2012). Partitioning of carbon allocation to reserves or growth determines future performance of aspen seedlings. *Forest Ecology and Management*, *275*, 43-51.

Landhäusser, S. M., Chow, P. S., Dickman, L. T., Furze, M. E., Kuhlman, I., Schmid, S., Wiesenbauer, J., Wild, B., Gleixner, G., Hartmann, H. & Hoch, G (2018). Standardized protocols and procedures can precisely and accurately quantify non-structural carbohydrates. *Tree Physiology*, *38*(12), 1764-1778.

Lee, J. E., Frankenberg, C., van der Tol, C., Berry, J. A., Guanter, L., Boyce, C. K., Fisher, J. B., Morrow, E., Worden, J. R., Asefi, S., Badgley, G., & Saatchi, S. (2013). Forest productivity and water stress in Amazonia: observations from GOSAT chlorophyll fluorescence. *Proceedings of the Royal Society B: Biological Sciences*, 280, 20130171. doi:10.1098/rspb.2013.0171.

Li, Y., Zhao, M., Motesharrei, S., Mu, Q., Kalnay, E., & Li, S. (2015). Local cooling and warming effects of forests based on satellite observations. *Nature Communications*, *6*(1), 1-8.

Luostarinen, K., & Kauppi, A. (2005). Effects of coppicing on the root and stump carbohydrate dynamics in birches. *New Forests*, *29*(3), 289-303.

Marshall, J. D., & Waring, R. H. (1985). Predicting fine root production and turnover by monitoring root starch and soil temperature. *Canadian Journal of Forest Research*, *15*(5), 791-800.

Martínez-Vilalta, J., & Lloret, F. (2016). Drought-induced vegetation shifts in terrestrial ecosystems: The key role of regeneration dynamics. *Global and Planetary Change*, *144*, 94-108.

Martínez-Vilalta, J., Sala, A., Asensio, D., Galiano, L., Hoch, G., Palacio, S., Piper, F.I., & Lloret, F. (2016). Dynamics of non-structural carbohydrates in terrestrial plants: a global synthesis. *Ecological Monographs*, *86*(4), 495-516.

Mayr, S., Schmid, P., Laur, J., Rosner, S., Charra-Vaskou, K., Dämon, B., & Hacke, U. G. (2014). Uptake of water via branches helps timberline conifers refill embolized xylem in late winter. *Plant Physiology*, *164*(4), 1731-1740.

McDowell, N., Pockman, W. T., Allen, C. D., Breshears, D. D., Cobb, N., Kolb, T., Plaut, J., Sperry, J., West, A., Williams, D.G., & Yepez, E. A. (2008). Mechanisms of plant survival and mortality during drought: why do some plants survive while others succumb to drought?. *New Phytologist*, *178*(4), 719-739.

McDowell, N. G. (2011). Mechanisms linking drought, hydraulics, carbon metabolism, and vegetation mortality. *Plant Physiology*, *155*(3), 1051-1059.

Milburn, J.A., & Kallarackal, J. (1991). Sap exudation. *In* Physiology of Trees. Ed. A.S. Raghavendra. Wiley, New York, pp 385–402.

Millard, P., Sommerkorn, M., & Grelet, G. A. (2007). Environmental change and carbon limitation in trees: a biochemical, ecophysiological and ecosystem appraisal. *New Phytologist*, *175*(1), 11-28.

Minchin, P. E. H., Thorpe, M. R., & Farrar, J. F. (1993). A simple mechanistic model of phloem transport which explains sink priority. *Journal of Experimental Botany*, *44*(5), 947-955.

Moing, A. (2000) Sugar alcohols as carbohydrate reserves in some higher plants. In: A. K. Gupta, N. Kaur (Eds.) *Developments in Crop Science* (pp.337–358). Elsevier, Amsterdam.

Mooney, H. A. (1972). The carbon balance of plants. *Annual Review of Ecology and Systematics*, *3*(1), 315-346.

Moreira, B., Tormo, J., & Pausas, J. G. (2012). To resprout or not to resprout: factors driving intraspecific variability in resprouting. *Oikos*, *121*(10), 1577-1584.

Morin, X., Améglio, T., Ahas, R., Kurz-Besson, C., Lanta, V., Lebourgeois, F., Miglietta, F., & Chuine, I. (2007). Variation in cold hardiness and carbohydrate concentration from dormancy induction to bud burst among provenances of three European oak species. *Tree Physiology*, *27*(6), 817-825.

Najar, A., Landhäusser, S. M., Whitehill, J. G., Bonello, P., & Erbilgin, N. (2014). Reserves accumulated in non-photosynthetic organs during the previous growing season drive plant defenses and growth in aspen in the subsequent growing season. *Journal of Chemical Ecology*, *40*(1), 21-30.

Niamké, F. B., Amusant, N., Charpentier, J. P., Chaix, G., Baissac, Y., Boutahar, N., Adima, A. A., Kati-Coulibaly, S., & Jay-Allemand, C. (2011). Relationships between biochemical

attributes (non-structural carbohydrates and phenolics) and natural durability against fungi in dry teak wood (Tectona grandis L. f.). *Annals of Forest Science*, *68*(1), 201-211.

Norby, R. J., DeLucia, E. H., Gielen, B., Calfapietra, C., Giardina, C. P., King, J. S., Ledford, J., McCarthy, H. R., Moore, D. J. P., Ceulemans, R., De Angelis, P., Finzi, A. C., Karnosky, D. F., Kubiske, M. E., Lukac, M., Pregitzer, K. S., Scarascia-Mugnozza, G., Schlesinger, W. H., & Oren, R. (2005). Forest response to elevated CO2 is conserved across a broad range of productivity. *Proceedings of the National Academy of Sciences*, *102*(50), 18052-18056.

O'Brien, M. J., Leuzinger, S., Philipson, C. D., Tay, J., & Hector, A. (2014). Drought survival of tropical tree seedlings enhanced by non-structural carbohydrate levels. *Nature Climate Change*, *4*(8), 710-714.

Oliva, J., Stenlid, J., & Martínez-Vilalta, J. (2014). The effect of fungal pathogens on the water and carbon economy of trees: implications for drought-induced mortality. *New Phytologist*, *203*(4), 1028-1035.

Paritsis, J., & Veblen, T. T. (2011). Dendroecological analysis of defoliator outbreaks on Nothofagus pumilio and their relation to climate variability in the Patagonian Andes. *Global Change Biology*, *17*(1), 239-253.

Pate, J. S., Froend, R. H., Bowen, B. J., Hansen, A., and Kuo, J. (1990). Seedling growth and storage characteristics of seeder and resprouter species of Mediterranean-type ecosystems of SW Australia. *Annals of Botany*, *65*(6), 585-601

Payyavula, R. S., Tay, K. H., Tsai, C. J., & Harding, S. A. (2011). The sucrose transporter family in Populus: the importance of a tonoplast PtaSUT4 to biomass and carbon partitioning. *The Plant Journal*, *65*(5), 757-770.

Pinheiro, J., Bates, D., DebRoy, S., Sarkar, D., & R Core Team (2021). *nlme: Linear and Nonlinear Mixed Effects Models*. R package version 3.1-144, https://CRAN.R-project.org/package=nlme.

Piper, F. I. (2011). Drought induces opposite changes in the concentration of non-structural carbohydrates of two evergreen Nothofagus species of differential drought resistance. *Annals of Forest Science*, *68*(2), 415-424.

Piper, F. I., & Fajardo, A. (2014). Foliar habit, tolerance to defoliation and their link to carbon and nitrogen storage. *Journal of Ecology*, *102*(5), 1101-1111.

Piper, F. I., Gundale, M. J., & Fajardo, A. (2015). Extreme defoliation reduces tree growth but not C and N storage in a winter-deciduous species. *Annals of Botany*, *115*(7), 1093-1103.

Piper, F. I., & Fajardo, A. (2016). Carbon dynamics of Acer pseudoplatanus seedlings under drought and complete darkness. *Tree Physiology*, *36*(11), 1400-1408.

Piper, F. I., & Paula, S. (2020). The role of nonstructural carbohydrates storage in forest resilience under climate change. *Current Forestry Reports*, *6*(1), 1-13

Pruyn, M. L., Gartner, B. L., & Harmon, M. E. (2002). Respiratory potential in sapwood of old versus young ponderosa pine trees in the Pacific Northwest. *Tree Physiology*, *22*(2-3), 105-116.

R Core Team (2018). R: A language and environment for statistical computing. R Foundation for Statistical Computing, Vienna, Austria. URL https://www.R-project.org.

Rademacher, T. T., Basler, D., Eckes-Shephard, A. H., Fonti, P., Friend, A. D., Le Moine, J., & Richardson, A. D. (2019). Using direct phloem transport manipulation to advance understanding of carbon dynamics in forest trees. *Frontiers in Forests and Global Change*, *2*, 11. doi: 10.3389/ffgc.2019.00011.

Regier, N., Streb, S., Zeeman, S. C., & Frey, B. (2010). Seasonal changes in starch and sugar content of poplar (Populus deltoides× nigra cv. Dorskamp) and the impact of stem girdling on carbohydrate allocation to roots. *Tree Physiology*, *30*(8), 979-987.

Richardson, A. D., Carbone, M. S., Keenan, T. F., Czimczik, C. I., Hollinger, D. Y., Murakami, P., Schaberg, P. G., & Xu, X. (2013). Seasonal dynamics and age of stemwood nonstructural carbohydrates in temperate forest trees. *New Phytologist*, *197*(3), 850-861.

Richardson, A. D., Carbone, M. S., Huggett, B. A., Furze, M. E., Czimczik, C. I., Walker, J. C., Xu, X., Schaberg, P. G., & Murakami, P. (2015). Distribution and mixing of old and new nonstructural carbon in two temperate trees. *New Phytologist*, *206*(2), 590-597.

Rosell, J. A. (2016). Bark thickness across the angiosperms: more than just fire. *New Phytologist*, *211*(1), 90-102.

Saffell, B. J., Meinzer, F. C., Woodruff, D. R., Shaw, D. C., Voelker, S. L., Lachenbruch, B., & Falk, K. (2014). Seasonal carbohydrate dynamics and growth in Douglas-fir trees experiencing chronic, fungal-mediated reduction in functional leaf area. *Tree Physiology*, *34*(3), 218-228.

Safford, L. O., Bjorkbom, J. C., & Zasada, J. C. (1990). Betula papyrifera Marsh, paper birch. In: R. M. Burns, B. H. Honkala (Eds.), *Silvics of North America: Volume 2. Hardwoods* (pp. 604-611), Agricultural Handbook 654. Washington, DC: USDA Forest Service.

Sakai, A., & Larcher, W. (1987). *Frost survival of plants: responses and adaptation to freezing stress*. Berlin-Heidelburg: Springer-Verlag.

Sakai, A., Sakai, S., & Akiyama, F. (1997). Do sprouting tree species on erosion-prone sites carry large reserves of resources?. *Annals of Botany*, *79*(6), 625-630.

Sala, A., Piper, F., and Hoch, G. (2010). Physiological mechanisms of drought-induced tree mortality are far from being resolved. *New Phytologist 186*, 274–281.

Sala, A., Woodruff, D. R., & Meinzer, F. C. (2012). Carbon dynamics in trees: feast or famine?. *Tree Physiology*, *32*(6), 764-775.

Sauter, J. J., & Ambrosius, T. (1986). Changes in the partitioning of carbohydrates in the wood during bud break in Betula pendula Roth. *Journal of Plant Physiology*, *124*(1-2), 31-43.

Sayer, E. J. (2006). Using experimental manipulation to assess the roles of leaf litter in the functioning of forest ecosystems. *Biological Reviews*, *81*(1), 1-31.

Sellin, A., Niglas, A., Õunapuu, E., & Karusion, A. (2013). Impact of phloem girdling on leaf gas exchange and hydraulic conductance in hybrid aspen. *Biologia Plantarum*, *57*(3), 531-539.

Sevanto, S. (2014). Phloem transport and drought. *Journal of Experimental Botany*, *65*(7), 1751-1759.

Sevanto, S., Mcdowell, N. G., Dickman, L. T., Pangle, R., & Pockman, W. T. (2014b). How do trees die? A test of the hydraulic failure and carbon starvation hypotheses. *Plant, Cell & Environment*, *37*(1), 153-161.

Schädel, C., Blöchl, A., Richter, A., & Hoch, G. (2009). Short-term dynamics of nonstructural carbohydrates and hemicelluloses in young branches of temperate forest trees during bud break. *Tree Physiology*, *29*(7), 901-911.

Schneider, C. A., Rasband, W. S., & Eliceiri, K. W. (2012). NIH Image to ImageJ: 25 years of image analysis. *Nature Methods*, *9*(7), 671-675.

Schoonmaker, A. S., Hillabrand, R., Lieffers, V. J., Chow, P. S., & Landhäusser, S. M (2021). Seasonal dynamics of non-structural carbon pools and their relationship to growth in two boreal conifer tree species. *Tree Physiology.* doi:10.1093/treephys/tpab013.

Signori-Müller, C., Oliveira, R. S., Valentim Tavares, J., Carvalho Diniz, F., Gilpin, M., de V. Barros, F., ... & Galbraith, D. (2022). Variation of non-structural carbohydrates across the fast–slow continuum in Amazon Forest canopy trees. *Functional Ecology*, *36*(2), 341-355.

Stroh, E. D., & Miller, J. P. (2009). Paper birch decline in the Niobrara River Valley, Nebraska: Weather, microclimate, and birch stand conditions. U. S. Geological Survey Open-file Report 2009–1221, 19 p.

Tarkowski, Ł. P., & Van den Ende, W. (2015). Cold tolerance triggered by soluble sugars: a multifaceted countermeasure. *Frontiers in Plant Science*, *6*, 203.

Tinus, R. W., Burr, K. E., Atzmon, N., & Riov, J. (2000). Relationship between carbohydrate concentration and root growth potential in coniferous seedlings from three climates during cold hardening and dehardening. *Tree Physiology*, *20*(16), 1097-1104.

Turgeon, R. (2006). Phloem loading: how leaves gain their independence. *BioScience, 56*, 15–24.

Tyree, M. T. (1983). Maple sap uptake, exudation, and pressure changes correlated with freezing exotherms and thawing endotherms. *Plant Physiology*, *73*(2), 277-285.

Wan, X., Zwiazek, J. J., Lieffers, V. J., & Landhäusser, S. M. (2001). Hydraulic conductance in aspen (Populus tremuloides) seedlings exposed to low root temperatures. *Tree Physiology*, *21*(10), 691-696.

Wardlaw, I. F. (1990) The control of carbon partitioning in plants. *New Phytologist, 116*, 341–381.

Weber, R., Schwendener, A., Schmid, S., Lambert, S., Wiley, E., Landhäusser, S. M., Hartmann, H., & Hoch, G. (2018). Living on next to nothing: tree seedlings can survive weeks with very low carbohydrate concentrations. *New Phytologist*, *218*(1), 107-118.

Welling, A., & Palva, E. T. (2006). Molecular control of cold acclimation in trees. *Physiologia Plantarum*, *127*(2), 167-181.

Westhoff, M., Schneider, H., Zimmermann, D., Mimietz, S., Stinzing, A., Wegner, L.H., Kaiser, W., Krohne, G., Shirley, S., Jakob, P. & Bamberg, E. (2008). The mechanisms of refilling of xylem conduits and bleeding of tall birch during spring. *Plant Biology*, *10*(5), 604-623.

Westhoff, M., Zimmermann, D., Schneider, H., Wegner, L. H., Geßner, P., Jakob, P., Bamberg, E., Shirley, St., Bentrup, F. W., & Zimmermann, U. (2009). Evidence for discontinuous water columns in the xylem conduit of tall birch trees. *Plant Biology*, *11*(3), 307-327.

Wiley, E., & Helliker, B. (2012). A re-evaluation of carbon storage in trees lends greater support for carbon limitation to growth. *New Phytologist*, *195*(2), 285-289.

Wiley, E., Huepenbecker, S., Casper, B. B., & Helliker, B. R. (2013). The effects of defoliation on carbon allocation: can carbon limitation reduce growth in favour of storage?. *Tree Physiology*, *33*(11), 1216-1228.

Wiley, E., Rogers, B. J., Hodgkinson, R., & Landhäusser, S. M. (2016). Nonstructural carbohydrate dynamics of lodgepole pine dying from mountain pine beetle attack. *New Phytologist*, *209*(2), 550-562.

Wiley, E., Casper, B. B., & Helliker, B. R. (2017a). Recovery following defoliation involves shifts in allocation that favour storage and reproduction over radial growth in black oak. *Journal of Ecology*, *105*(2), 412-424

Wiley, E., Hoch, G., & Landhäusser, S. M. (2017b). Dying piece by piece: carbohydrate dynamics in aspen (Populus tremuloides) seedlings under severe carbon stress. *Journal of Experimental Botany*, *68*(18), 5221-5232.

Wiley, E., King, C. M., & Landhäusser, S. M. (2019). Identifying the relevant carbohydrate storage pools available for remobilization in aspen roots. *Tree Physiology*, *39*(7), 1109-1120.

Wright, C.J. (1989) Interactions between vegetative and reproductive growth. *In* Manipulation of Fruiting. Ed. C. J. Wright. Butterworths, London.

Wright, I. J., Reich, P. B., Westoby, M., Ackerly, D. D., Baruch, Z., Bongers, F., Cavender-Bares, J., Chapin, T., Cornelissen, J. H., Diemer, M., Flexas J., Garnier, E., Groom, P. K., Gulias, J., Hikosaka, K., Lamont, B. B., Lee, T., Lee, W., Lusk, C., Midgley, J. J., Navas, M.L., Niinemets, Ü., Oleksyn, J., Osada, N., Poorter, H., Poot, P., Prior, L., Pyankov, V. I., Roumet, C., Thomas, S. C., Tjoelker, M. G., Veneklaas, E. J., & Villar, R. (2004). The worldwide leaf economics spectrum. *Nature*, *428*(6985), 821-827.

Würth, M. K., Pelaez-Riedl, S., Wright, S. J., & Körner, C. (2005). Non-structural carbohydrate pools in a tropical forest. *Oecologia*, *143*(1), 11-24.

Xing, D., Bergeron, J. C., Solarik, K. A., Tomm, B., Macdonald, S. E., Spence, J. R., & He, F. (2019). Challenges in estimating forest biomass: use of allometric equations for three boreal tree species. *Canadian Journal of Forest Research*, *49*(12), 1613-1622.

Zukswert, J. M., & Prescott, C. E. (2017). Relationships among leaf functional traits, litter traits, and mass loss during early phases of leaf litter decomposition in 12 woody plant species. *Oecologia*, *185*(2), 305-316

Zwieniecki, M. A., Melcher, P. J., Feild, T. S., & Holbrook, N. M. (2004). A potential role for xylem–phloem interactions in the hydraulic architecture of trees: effects of phloem girdling on xylem hydraulic conductance. *Tree Physiology*, *24*(8), 911-917.

Appendix

Methods

Methods A-1 Whole-organ concentration calculations.

For the stemwood and inner bark, I averaged the NSC, sugar, and starch concentrations of the uppermost three stem samples (see Fig. 1) for each tree at each sampling date to produce an average whole-stemwood and whole-inner bark concentration. Likewise, concentrations at each sampling date for each individual tree were averaged across the branch and twig tissues, as well as across the coarse and fine root tissues. In situations where trees within a treatment group exhibited differential bud break patterns (i.e., some flushed, but some did not), leaves were collected when present on a tree, but otherwise, only bud samples were collected. When this occurred, concentrations were not presented separately for leaves and buds within a treatment group but were averaged together to yield one measure of NSC, sugar, and starch for the leaves and buds as a whole. Prior to modelling the differences in leaf size across treatment groups over time, leaf size was first subset to include sampling dates where at least one girdle treatment group had leaves present (e.g., 21 Jun. 2018, 31 Aug. 2018, and 29 May. 2019).

Tables

Table A-1 Comparison of mean NSC (% dry weight) and standard error (SE) of organs over time for multi-stemmed and single stemmed *Betula papyrifera* trees from a monospecific birch stand located at the southern edge of the boreal dry mixedwood forest region in Alberta (54 °17'13.59" N, 112 °46'27.74" W). All trees were of the same age and DBH range.

Multi-stem			Single stem		
19 June 2018	Mean NSC (% dry weight)	SE	20 June 2018	Mean NSC (% dry weight)	SE
Coarse Roots	2.92	0.245	Coarse Roots	3.21	0.420
Stemwood	0.69	0.117	Stemwood	0.66	0.029
Branches	4.85	0.496	Branches	4.96	0.217
Twigs	7.05	0.463	Twigs	7.19	0.333
7 August 2018			29 August 2018		
Coarse Roots	4.60	0.550	Coarse Roots	5.56	0.554
Stemwood	1.54	0.101	Stemwood	1.62	0.107
Branches	8.23	0.335	Branches	7.92	0.376
Twigs	9.70	0.349	Twigs	9.86	0.526
8 May 2019			13 May 2019		
Coarse Roots	3.35	0.427	Coarse Roots	3.00	0.451
Stemwood	1.27	0.138	Stemwood	1.50	0.124
Branches	6.71	0.403	Branches	4.73	0.480
Twigs	7.53	0.338	Twigs	5.31	0.552

Table A-2 Diameter at breast height (cm) of the nine single-stemmed trees used to calculate the average biomass (± s.e.) of the coarse root, stemwood, inner bark, and branch fractions of *Betula papyrifera* trees at the study site. Biomass fractions were calculated using allometric scaling theory with standard coefficients and equations specific to *Betula papyrifera* provided by Jenkins *et al*. (2004) and Chojnacky *et al*. (2013).

		Estimated Biomass (kg)				
Tree	DBH (cm)	Coarse root	Stemwood	Inner bark	Branch	Total
1	8.1	4.0	6.9	2.0	8.8	21.6
2	8.6	4.6	8.2	2.3	9.8	24.9
3	8.8	4.8	8.7	2.4	10.1	26.1
4	9.7	6.1	11.9	3.2	12.3	33.6
5	10.5	7.4	15.1	3.9	14.4	40.8
6	11.5	9.2	19.5	4.9	16.9	50.5
7	12.1	10.5	22.8	5.6	18.8	57.7
8	13.2	12.9	29.4	7.1	22.2	71.7
9	13.8	14.5	33.7	8.0	24.3	80.5
Average Biomass (kg)		8.2 ± 1.27	17.4 ± 3.22	4.39 ± 0.72	15.3 ± 1.87	45.3 ± 7.09

Table A-3 Average (± s.e.) whole-tree NSC pools of *Betula papyrifera* throughout a calendar year when: A) all organ pools considered, B) coarse root, stemwood, inner bark and branch pools considered, and C) only the coarse root, stemwood, and branch pools considered. The difference (kg) represents the relative storage contribution of non-woody organs to the whole-tree NSC pool, where: A-B represents the contribution of the fine roots and foliage, B-C represents the contribution of the inner bark, and A-C represents the total contribution of fine roots, foliage, and inner bark to the whole-tree NSC pool.

	Whole-tree NSC pool (kg)			Difference (kg)		
	A. Fine & Coarse root, Inner bark, Stemwood, Branch, Foliage	B. Coarse root, Inner bark, Stemwood, Branch	C. Coarse root, Stemwood, Branch	A-B	A-C	B-C
May/18	1.488 ± 0.054	1.329 ± 0.049	1.081 ± 0.048	0.159 ± 0.007	0.407 ± 0.013	0.248 ± 0.011
Jun/18	1.741 ± 0.059	1.583 ± 0.058	1.288 ± 0.050	0.158 ± 0.004	0.453 ± 0.014	0.295 ± 0.014
Aug/18	2.468 ± 0.073	2.290 ± 0.070	2.016 ± 0.071	0.178 ± 0.007	0.452 ± 0.022	0.273 ± 0.018
Oct/18	2.443 ± 0.132	2.192 ± 0.128	1.874 ± 0.124	0.251 ± 0.006	0.569 ± 0.016	0.318 ± 0.012
Nov/18	2.115 ± 0.086	2.060 ± 0.084	1.754 ± 0.078	0.055 ± 0.005	0.361 ± 0.020	0.306 ± 0.015
Apr/19	1.991 ± 0.056	1.939 ± 0.054	1.666 ± 0.043	0.052 ± 0.003	0.325 ± 0.018	0.272 ± 0.018
May/19	1.846 ± 0.096	1.810 ± 0.092	1.584 ± 0.085	0.036 ± 0.005	0.262 ± 0.013	0.225 ± 0.009
Jun/19	1.765 ± 0.057	1.574 ± 0.059	1.299 ± 0.056	0.190 ± 0.009	0.466 ± 0.017	0.275 ± 0.014

Table A-4 Analysis of variance results for repeated measures linear mixed-effects models testing for the effect of sampling date on the estimated whole-tree NSC pool size, and the effect of sampling date, organ, and their interaction on the estimated organ level NSC pool size and seasonal change of organ NSC pool size of ten mature *Betula papyrifera* trees.

	NSC Pool Size		Seasonal Δ in NSC Pool Size	
	F	*P*	*F*	*P*
Whole-tree				
Sampling Date	51.847	**< 0.001**	NA	NA
Organ level				
Organ	1075.985	**< 0.001**	107.238	**< 0.001**
Sampling Date	34.590	**< 0.001**	20.091	**< 0.001**
Organ * Sampling Date	13.764	**< 0.001**	9.405	**< 0.001**

Table A-5 One-way analysis of variance results for repeated measures linear mixed-effects models testing the effect of sampling date on total non-structural carbohydrate, sugar, and starch concentrations (% dry weight) in root, stem, and crown tissues of ten (N = 10) mature *Betula papyrifera* Marsh. individuals from a monospecific birch stand located at the southern edge of the boreal dry mixedwood forest region in Alberta.

	Total NSC %		Sugar %		Starch %	
	F	*P*	*F*	*P*	*F*	*P*
Fine Roots	30.710	**<0.001**	49.592	**<0.001**	13.299	**<0.001**
Coarse Roots	5.485	**<0.001**	22.279	**<0.001**	11.818	**<0.001**
Inner Bark	10.077	**<0.001**	14.971	**<0.001**	26.479	**<0.001**
Stemwood	19.006	**<0.001**	22.959	**<0.001**	25.165	**<0.001**
Branches	54.992	**<0.001**	49.610	**<0.001**	75.903	**<0.001**
Twigs	24.173	**<0.001**	24.389	**<0.001**	40.451	**<0.001**
Leaves & Buds	64.208	**<0.001**	70.485	**<0.001**	7.589	**<0.001**

Table A-6 Two-tailed paired *t*-test and Wilcoxon Signed-Ranks test results comparing tissue NSC, sugar, and starch concentrations between the first and last sampling dates of the seasonal cycle in mature *Betula papyrifera*. Changes in concentrations between the two dates are presented as the mean difference of % NSC, sugar, and starch, with standard deviation provided in brackets.

	Change in Concentration (Δ %)								
	NSC			Sugar			Starch		
	MD	*t*	*P*	MD	*t*	*P*	MD	*t*	*P*
Fine Roots	-0.554 (0.826)	-2.120	0.063	-0.458 (0.809)	13.5*	0.168	-0.096 (0.628)	-0.483	0.640
Coarse Roots	-0.565 (1.445)	11*	0.105	-1.152 (0.380)	-9.574	**<0.001**	0.587 (1.346)	40*	0.232
Inner Bark	0.605 (0.581)	3.294	**<0.01**	-0.377 (0.433)	-2.751	**<0.05**	0.982 (0.475)	6.533	**<0.001**
Stemwood	0.148 (0.371)	1.263	0.238	-0.128 (0.262)	9*	0.123	0.276 (0.234)	3.733	**<0.01**
Branches	1.726 (1.071)	5.095	**<0.001**	0.134 (0.817)	0.519	0.616	1.592 (0.641)	7.851	**<0.001**
Twigs	1.406 (0.903)	55*	**<0.01**	-0.065 (0.869)	-0.236	0.818	1.471 (0.334)	13.913	**<0.001**
Leaves & Buds	3.382 (3.974)	2.691	**<0.05**	0.872 (2.260)	1.220	0.253	2.510 (2.074)	3.828	**<0.01**

Table A-7 Diameter measurements (cm) and estimated stem volume (cm^3) of the 30 *Betula papyrifera* trees, with averages (± SD) provided for each treatment. Diameter was measured at the bottom (30 cm above the root collar (RC)), breast height (130 cm above the RC), and top (500 cm above the RC) of all stems. Stem volume was estimated by summing the volume of two truncated cones (bottom to breast, and breast to top). One-way analysis of variance results are provided for testing whether diameter and volume differed across treatments.

	Diameter (cm)						Volume (cm^3)	
	Bottom		Breast		Top			
Treatment								
Control	11.30 (1.54)		9.41 (1.08)		7.22 (1.39)		29 169 (8 521)	
Bottom Girdle	14.04 (2.48)		12.00 (1.66)		8.34 (2.01)		44 829 (15 373)	
Top Girdle	11.58 (2.49)		9.79 (2.33)		7.66 (2.36)		32 996 (18 278)	
Double Girdle	13.26 (2.05)		11.07 (1.38)		8.00 (1.13)		38 890 (10 175)	
	F	*P*	*F*	*P*	*F*	*P*	*F*	*P*
	2.763	0.062	3.696	0.024	0.528	0.666	1.861	0.161

Table A-8 One-way analysis of variance results for testing initial differences between control and girdle treatments in total non-structural carbohydrates (NSC), sugar, and starch concentrations (% dry weight) in the roots, stemwood, inner bark, branches, and leaves of 30 mature *Betula papyrifera* trees in June of 2018.

	Total NSC %		Sugar %		Starch %	
	F	*P*	*F*	*P*	*F*	*P*
Roots	0.907	0.451	1.719	0.188	1.914	0.152
Inner bark	1.217	0.323	0.632	0.601	0.863	0.472
Stemwood	1.657	0.201	1.959	0.145	0.907	0.451
Branches	0.221	0.881	1.612	0.211	0.381	0.768
Leaves	3.286	**0.037**	3.634	**0.026**	0.907†	0.451†

Note. † Denotes model corresponding to log-transformed data to meet the assumptions of normality

Table A-9 Repeated measures analysis of variance results testing the effect of sampling date and girdling treatments (controls excluded; bottom girdle n = 7; top girdle n = 8, double girdle n = 7) on total non-structural carbohydrates (NSC), sugar, and starch concentrations (% dry weight) in the roots, stemwood, inner bark, branches, and leaves/buds of 22 mature *Betula papyrifera* trees. For the second sampling date, models excluded the three top girdle and two double girdle trees that exhibited contrasting concentration dynamics, yielding a treatment sample size of n = 5 for both top and double girdle trees, and a total sample size of 25.

	Total NSC %		Sugar %		Starch %	
	F	*P*	*F*	*P*	*F*	*P*
Leaves & buds						
Treatment (T)	0.153	0.860	0.004	0.997	1.535	0.241
Sampling date (S)	78.109	**<0.001**	125.800	**<0.001**	9.695	**<0.001**
T * S	6.917	**<0.001**	9.476	**<0.001**	3.902	**0.001**
Branches						
T	2.411	0.117	1.752	0.200	0.715	0.502
S	100.360	**<0.001**	27.048	**<0.001**	188.832	**<0.001**
T*S	3.112	**0.004**	5.092	**<0.001**	0.992	0.449
Inner bark						
T	50.792	**<0.001**	70.641	**<0.001**	2.501	0.109
S	209.025	**<0.001**	162.945	**<0.001**	32.951	**<0.001**
T*S	28.641	**<0.001**	29.893	**<0.001**	13.513	**<0.001**
Stemwood						
T	26.325	**<0.001**	29.871	**<0.001**	0.346	0.712
S	45.603	**<0.001**	19.338	**<0.001**	39.691	**<0.001**
T*S	34.599	**<0.001**	15.160	**<0.001**	16.100	**<0.001**
Roots						
T	0.874	0.433	1.103	0.352	0.562	0.579
S	17.960	**<0.001**	32.161	**<0.001**	5.436	**<0.001**
T*S	0.803	0.602	0.452	0.885	1.349	0.234

Table A-10 Organ-level sugar concentrations of girdled (BG= bottom girdled, TG = top girdled, DG = double girdled) *Betula papyrifera* trees over time. Diagonal cells shaded dark grey provide the estimated marginal mean and standard error of sugar concentration for each treatment group at each sampling date, and Δ denotes the standard error and significance (Behjamini-Yekutieli, α =0.1) of the paired difference (change) in estimated marginal means between the column date and previous date for each treatment group. Light grey cells denote the difference in estimated marginal means between column group and row group within each sampling date, and each corresponding white cell indicates whether this difference is significant (Fishers LSD, α =0.1). NS= not significant, (*) = $P \leq 0.1$, * = $P \leq 0.05$, ** = $P \leq 0.01$, or *** = $P \leq 0.001$. If an organ section is shaded orange, no 'treatment' by 'sampling date' interaction was detected for the given organ, and the above post-hoc tests were not conducted.

Sugar (% dry weight)

Leaves & buds

	June/18			Aug/18			13 May/19			29 May/19			Jul/19		
	BG	TG	DG	BG	TG	DG	BG	TG	DG	BG	TG	DG	BG	TG	DG
BG	13.37 (0.77)	-1.47 (1.16)	-0.09 (1.12)	16.13 (1.42) Δ:(1.43) NS	0.25 (1.68)	0.98 (1.69)	8.64 (0.53) Δ:(1.32) ***	0.68 (0.75)	0.10 (0.80)	12.24 (0.67) Δ:(0.42) ***	-3.06 (0.84)	-3.84 (0.94)	3.47 (0.94) Δ:(0.89) ***	1.64 (1.24)	1.97 (1.23)
TG	NS	11.90 (0.87)	1.38 (1.19)	NS	16.38 (0.89) Δ:(1.03) ***	0.73 (1.27)	NS	9.32 (0.54) Δ:(0.77) ***	-0.58 (0.81)	**	9.18 (0.49) Δ:(0.21) NS	-0.78 (0.81)	NS	5.11 (0.80) Δ:(0.63) ***	0.33 (1.13)
DG	NS	NS	13.28 (0.82)	NS	NS	17.11 (0.91) Δ:(0.97) ***	NS	NS	8.74 (0.61) Δ:(0.80) ***	***	NS	8.40 (0.65) Δ:(0.48) NS	NS	NS	5.44 (0.79) Δ:(0.70) ***

Sugar NSC (% dry weight)

Branches

	June/18			Aug/18			13 May/19			29 May/19			Jul/19		
	BG	TG	DG	BG	TG	DG	BG	TG	DG	BG	TG	DG	BG	TG	DG
BG	4.97 (0.19)	-0.52 (0.27)	-0.21 (0.22)	4.77 (0.24) Δ:(0.29) NS	0.24 (0.32)	0.13 (0.29)	5.24 (0.21) Δ:(0.31) NS	1.13 (0.57)	1.08 (0.70)	4.64 (0.36) Δ:(0.41) NS	0.98 (0.70)	1.02 (0.80)	1.96 (0.26) Δ:(0.43) ***	2.44 (0.46)	2.11 (0.82)
TG	(*)	4.45 (0.19)	0.31 (0.22)	NS	5.01 (0.21) Δ:(0.27) NS	-0.11 (0.26)	(*)	6.37 (0.53) Δ:(0.56) NS	-0.05 (0.84)	NS	5.62 (0.60) Δ:(0.79) NS	0.04 (0.93)	***	4.40 (0.38) Δ:(0.70) NS	-0.33 (0.87)
DG	NS	NS	4.76 (0.11)	NS	NS	4.90 (0.16) Δ:(0.17) NS	NS	NS	6.32 (0.67) Δ:(0.68) NS	NS	NS	5.66 (0.71) Δ:(0.98) NS	*	NS	4.07 (0.78) Δ:(1.05) NS

Inner bark

	June/18			Aug/18			13 May/19			29 May/19			Jul/19		
	BG	TG	DG	BG	TG	DG	BG	TG	DG	BG	TG	DG	BG	TG	DG
BG	5.45 (0.30)	0.12 (0.49)	0.32 (0.48)	4.82 (0.32) Δ:(0.32) NS	-1.31 (0.43)	-2.54 (0.45)	4.23 (0.32) Δ:(0.33) NS	-3.20 (0.45)	-3.92 (0.43)	4.31 (0.23) Δ: (0.24) NS	-3.22 (0.40)	-4.09 (0.32)	1.10 (0.49) Δ:(0.45) ***	-0.67 (0.54)	-0.98 (0.54)
TG	NS	5.57 (0.38)	0.20 (0.54)	**	3.51 (0.29) Δ:(0.38) ***	-1.23 (0.43)	***	1.03 (0.32) Δ:(0.32) ***	-0.72 (0.43)	***	1.09 (0.32) Δ:(0.35) NS	-0.87 (0.39)	NS	0.43 (0.24) Δ:(0.27) NS	-0.31 (0.33)
DG	NS	NS	5.77 (0.38)	***	**	2.28 (0.32) Δ:(0.38) ***	***	NS	0.31 (0.30) Δ:(0.30) ***	***	*	0.22 (0.22) Δ:(0.20) NS	(*)	NS	0.12 (0.23) Δ:(0.05) NS

Sugar NSC (% dry weight)

Stemwood

	June/18			Aug/18			13 May/19			29 May/19			Jul/19		
	BG	TG	DG	BG	TG	DG	BG	TG	DG	BG	TG	DG	BG	TG	DG
BG	0.69 (0.03)	-0.05 (0.05)	0.02 (0.08)	1.12 (0.06) Δ:(0.06) ***	-0.58 (0.07)	-0.64 (0.08)	1.16 (0.09) Δ:(0.10) NS	-0.66 (0.10)	-0.73 90.09)	1.06 (0.08) Δ:(0.12) NS	-0.64 (0.09)	-0.58 (0.09)	0.56 (0.05) Δ:(0.09) ***	-0.20 (0.06)	-0.10 (0.08)
TG	NS	0.64 (0.04)	0.07 (0.09)	***	0.54 (0.03) Δ:(0.05) NS	-0.06 (0.06)	***	0.50 (0.04) Δ:(0.04) NS	-0.07 (0.05)	***	0.42 (0.04) Δ:(0.04) NS	0.06 (0.05)	**	0.36 (0.03) Δ:(0.08) NS	0.10 (0.07)
DG	NS	NS	0.71 (0.08)	***	NS	0.48 (0.05) Δ:(0.08) (*)	***	NS	0.43 (0.03) Δ:(0.05) NS	***	NS	0.48 (0.05) Δ:(0.05) NS	NS	NS	0.46 (0.07) Δ:(0.08) NS

Roots

	June/18			Aug/18			13 May/19			29 May/19			Jul/19		
	BG	TG	DG	BG	TG	DG	BG	TG	DG	BG	TG	DG	BG	TG	DG
BG	1.94 (0.16)			1.14 (0.11)			1.75 (0.67)			1.09 (0.25)			0.88 (0.22)		
		1.70 (0.12)			0.97 (0.19)			1.11 (0.23)			1.10 (0.20)			1.01 (0.30)	
DG			1.88 (0.07)			1.08 (0.15)			1.74 (0.37)			1.35 (0.28)			1.18 (0.21)

Table A-11 Organ-level starch concentrations of girdled (BG= bottom girdled, TG = top girdled, DG = double girdled) *Betula papyrifera* trees over time. Diagonal cells shaded dark grey provide the estimated marginal mean and standard error of starch concentration for each treatment group at each sampling date, and Δ denotes the standard error and significance (Behjamini-Yekutieli, α =0.1) of the paired difference (change) in estimated marginal means between the column date and previous date for each treatment group. Light grey cells denote the difference in estimated marginal means between column group and row group within each sampling date, and each corresponding white cell indicates whether this difference is significant (Fishers LSD, α =0.1). NS= not significant, (*) = $P \leq 0.1$, * = $P \leq 0.05$, ** = $P \leq 0.01$, or *** = $P \leq 0.001$. If an organ section is shaded orange, no 'treatment' by 'sampling date' interaction was detected for the given organ, and the above post-hoc tests were not conducted.

Starch (% dry weight)

Leaves & buds

	June/18			Aug/18			13 May/19			29 May/19			Jul/19		
	BG	TG	DG	BG	TG	DG	BG	TG	DG	BG	TG	DG	BG	TG	DG
BG	0.82 (0.38)	-0.53 (0.39)	0.14 (0.48)	2.35 (0.92) Δ:(0.10) NS	3.95 (1.94)	3.02 (1.55)	0.70 (0.18) Δ:(0.94) NS	-0.21 (0.21)	-0.45 (0.20)	0.16 (0.03) Δ:(0.18) *	0.29 (0.11)	0.09 (0.06)	0.23 (0.14) Δ:(0.13) NS	0.00 (0.15)	0.13 (015)
TG	NS	0.29 (0.080	0.67 (0.31)	(*)	6.30 (1.25) Δ:(1.71) **	-0.93 (2.12)	NS	0.49 (0.11) Δ:(1.71) **	-0.24 (0.13)	*	0.45 (0.11) Δ:(0.14) NS	-0.20 (0.12)	NS	0.23 (0.05) Δ:(0.11) NS	0.13 (0.07)
DG	NS	*	0.96 (0.30)	(*)	NS	5.37 (1.25) Δ:(1.28) **	*	(*)	0.25 (0.08) Δ:(1.25) **	NS	NS	0.25 (0.05) Δ:(0.08) NS	NS	(*)	0.36 (0.06) Δ:(0.06) NS

Starch NSC (% dry weight)

Branches

	June/18			Aug/18			13 May/19			29 May/19			Jul/19		
	BG	TG	DG	BG	TG	DG	BG	TG	DG	BG	TG	DG	BG	TG	DG
BG	1.18 (0.35)			5.30 (0.21)			2.08 (0.32)			0.73 (0.18)			0.50 (0.06)		
TG		1.63 (0.22)			5.20 (0.59)			1.23 (0.32)			1.08 (0.31)			0.53 (0.09)	
DG			1.58 (0.38)			4.56 (0.68)			1.14 (0.42)			0.90 (0.33)			0.41 (0.06)

Inner bark

	June/18			Aug/18			13 May/19			29 May/19			Jul/19		
	BG	TG	DG	BG	TG	DG	BG	TG	DG	BG	TG	DG	BG	TG	DG
BG	0.36 (0.09)	0.02 (0.12)	0.23 (0.23)	3.87 (0.35) Δ:(0.36) ***	-3.26 (0.38)	-3.48 (0.36)	1.06 (0.21) Δ:(0.40) ***	-0.59 (0.21)	-0.72 (0.22)	1.03 (0.15) Δ:(0.25) NS	-0.24 (0.16)	-0.44 (0.16)	0.32 (0.06) Δ:(0.15) ***	0.00 (0.09)	-0.03 (0.08)
TG	NS	0.38 (0.08)	0.21 (0.22)	***	0.61 (0.13) Δ:(0.15) NS	-0.22 (0.15)	*	0.47 (0.05) Δ:(0.13) NS	-0.13 (0.08)	NS	0.79 (0.05) Δ (0.05) ***	-0.20 (0.09)	NS	0.32 (0.06) Δ:(0.06) ***	-0.03 (0.08)
DG	NS	NS	0.59 (0.21)	***	NS	0.39 (0.07) Δ:(0.21) NS	**	NS	0.34 (0.07) Δ:(0.08) NS	*	*	0.59 (0.07) Δ:(0.08) **	NS	NS	0.29 (0.05) Δ:(0.06) ***

Starch NSC (% dry weight)

Stemwood

	June/18			Aug/18			13 May/19			29 May/19			Jul/19		
	BG	TG	DG	BG	TG	DG	BG	TG	DG	BG	TG	DG	BG	TG	DG
BG	0.16 (0.06)	0.09 (0.09)	0.13 (0.09)	1.44 (0.10) Δ:(0.12) ***	-1.02 (0.14)	-1.28 (0.14)	0.46 (0.05) Δ:(0.11) ***	-0.22 (0.07)	-0.01 (0.07)	0.39 (0.04) Δ:(0.06) NS	0.12 (0.06)	-0.08 (0.06)	0.11 (0.03) Δ: (0.05) ***	0.02 (0.04)	0.09 (0.04)
TG	NS	0.25 (0.06)	0.04 (0.09)	***	0.42 (0.09) Δ:(0.11) NS	-0.26 (0.14)	**	0.24 (0.05) Δ:(0.10) NS	0.21 (0.07)	*	0.51 (0.04) Δ:(0.06) ***	-0.20 (0.06)	NS	0.13 (0.03) Δ:(0.05) ***	0.07 (0.04)
DG	NS	NS	0.29 (0.06)	***	NS	0.16 (0.10) Δ:(0.12) NS	NS	**	0.45 (0.05) Δ:(0.11) (*)	NS	**	0.31 (0.04) Δ:(0.06) NS	(*)	NS	0.20 (0.03) Δ:(0.05) NS

Roots

	June/18			Aug/18			13 May/19			29 May/19			Jul/19		
	BG	TG	DG	BG	TG	DG	BG	TG	DG	BG	TG	DG	BG	TG	DG
BG	0.64 (0.20)			0.26 (0.13)			0.43 (0.08)			0.46 (0.08)			0.33 (0.11)		
		1.08 (0.18)			0.53 (0.19)			0.46 (0.07)			0.28 (0.06)			0.31 (0.13)	
DG			0.72 (0.19)			0.57 (0.11)			0.50 (0.04)			0.34 (0.07)			0.70 (0.28)

Table A-12 Two-tailed paired *t*-test results comparing stemwood and inner bark NSC, sugar, and starch concentrations between the upper and lower stem positions of ungirdled *Betula papyrifera* trees (n = 8) throughout the study period. MD represents the mean difference in tissue concentration between upper and lower stem positions at each date individually, calculated as the upper concentration subtracted from the lower concentration, with standard error provided in brackets

	Difference in concentration (Δ %) between the upper and lower stem positions								
	Total NSC			Sugar			Starch		
	MD	*t*	*P*	MD	*t*	*P*	MD	*t*	*P*
Inner bark									
21 Jun. 18	0.028 (0.287)	0.096	0.926	-0.195 (0.204)	-0.954	0.372	0.222 (0.113)	1.976	**0.089**
31 Aug. 18	-0.600 (0.790)	-0.759	0.473	-0.571 (0.482)	-1.186	0.274	-0.031 (0.357)	-0.087	0.933
29 May. 19	-0.170 (0.514)	-0.331	0.751	0.250 (0.394)	0.634	0.546	-0.415 (0.184)	-2.254	**0.059**
17 Jul. 19	0.675 (0.557)	1.212	0.265	-0.289 (0.354)	-0.817	0.441	0.961 (0.238)	4.037	**0.005**
Stemwood									
21 Jun. 18	0.234 (0.070)	3.324	**0.013**	0.059 (0.067)	0.879	0.409	0.176 (0.036)	4.895	**0.002**
31 Aug. 18	0.469 (0.189)	2.475	**0.042**	-0.225 (0.102)	-2.215	**0.062**	0.692 (0.112)	6.161	**<0.001**
29 May. 19	-0.306 (0.155)	-1.981	**0.088**	-0.374 (0.061)	-6.060	**<0.001**	0.068 (0.145)	0.466	0.655
17 Jul. 19	-0.138 (0.150)	-0.915	0.391	-0.164 (0.051)	-3.203	**0.015**	0.028 (0.120)	0.229	0.826

Table A-13 One-way analysis of variance results testing the effect of girdling treatments on the stem position-specific change in stemwood and inner bark total non-structural carbohydrates (NSC), sugar, and starch concentrations (**Δ** % dry weight) between the initial measurement and August 2018, late May 2019, and July 2019 measurement for 30 mature *Betula papyrifera* trees.

	Total NSC (**Δ** %)		Sugar (**Δ** %)		Starch (**Δ** %)	
	F	*P*	*F*	*P*	*F*	*P*
Aug/18						
Upper stem						
Inner bark	69.855	**<0.001**	19.841	**<0.001**	79.039	**<0.001**
Stemwood	65.909	**<0.001**	15.184	**<0.001**	76.312	**<0.001**
Lower Stem†						
Inner bark	35.459	**<0.001**	15.268	**<0.001**	24.591	**<0.001**
Stemwood	23.303	**<0.001**	7.252	**0.002**	32.914	**<0.001**
Root collar†						
Inner bark	26.925	**<0.001**	6.662	**0.003**	36.720	**<0.001**
Stemwood	15.622	**<0.001**	0.419	0.742	26.322	**<0.001**
29 May/19						
Upper stem						
Inner bark	93.047	**<0.001**	80.338	**<0.001**	6.442	**0.002**
Stemwood	18.229	**<0.001**	14.231	**<0.001**	5.069	**0.007**
Lower Stem						
Inner bark	17.322	**<0.001**	13.629	**<0.001**	3.532	**0.029**
Stemwood	5.990	**0.003**	4.344	**0.013**	13.821	**<0.001**
Root collar						
Inner bark	15.818	**<0.001**	12.569	**<0.001**	2.480	**0.083**
Stemwood	3.861	**0.021**	0.704	0.558	2.950	**0.051**
Jul/19						
Upper stem						
Inner bark	27.625	**<0.001**	18.377	**<0.001**	9.455	**<0.001**
Stemwood	37.099	**<0.001**	8.079	**0.001**	25.033	**<0.001**
Lower Stem						
Inner bark	43.200	**<0.001**	19.401	**<0.001**	33.419	**<0.001**
Stemwood	43.652	**<0.001**	4.044	**0.018**	40.403	**<0.001**

Root collar						
Inner bark	27.719	**<0.001**	11.699	**<0.001**	32.090	**<0.001**
Stemwood	3.861	**<0.001**	2.748	**0.063**	27.892	**<0.001**

Note. † Carbohydrate models excluded the three top girdle and two double girdle trees that exhibited contrasting concentration dynamics, yielding a treatment sample size of n = 5 for both top and double girdle trees, and a total sample size of 25.

Figures

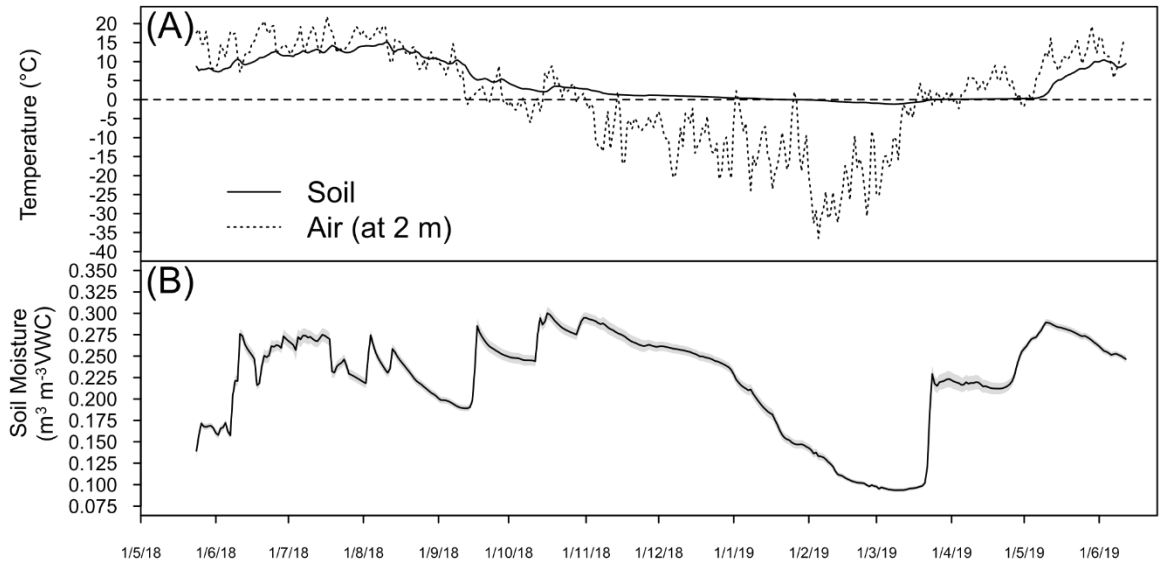

Figure A-1 Average daily (A) soil temperature (at 15 cm depth) and air temperature (at 2 m), and (B) soil moisture (at 15 cm depth). Soil temperature and moisture were measured directly at the study site located in the southern edge of the boreal dry mixedwood forest region in Alberta (54°17'13.59" N, 112°46'27.74" W), but air temperatures were provided by a nearby (within 12 km) weather station in Abee, Alberta. The shaded grey areas denote ± standard error.

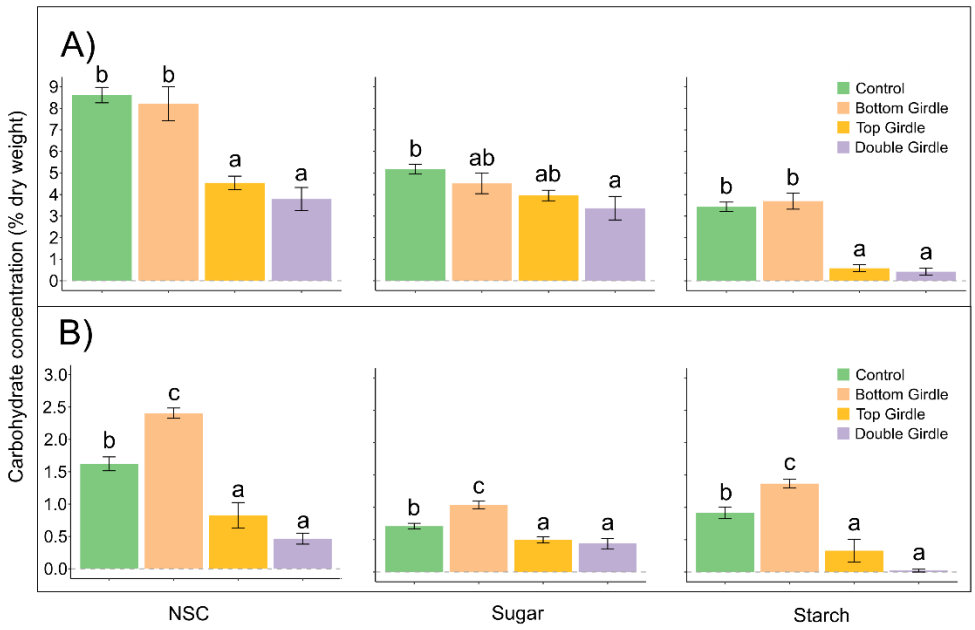

Figure A-2 Average (± standard error) mid-stem (A) inner bark and (B) stemwood carbohydrate concentrations of 30 mature *Betula papyrifera* trees subjected to different stem girdling treatments (control: n = 8, bottom girdle: n = 7, top girdle: n = 8, and double girdle: n = 7). Samples were collected on 31 August 2018. Letters denote significant differences (Tukey's HSD, $\alpha = 0.05$) for each plot.

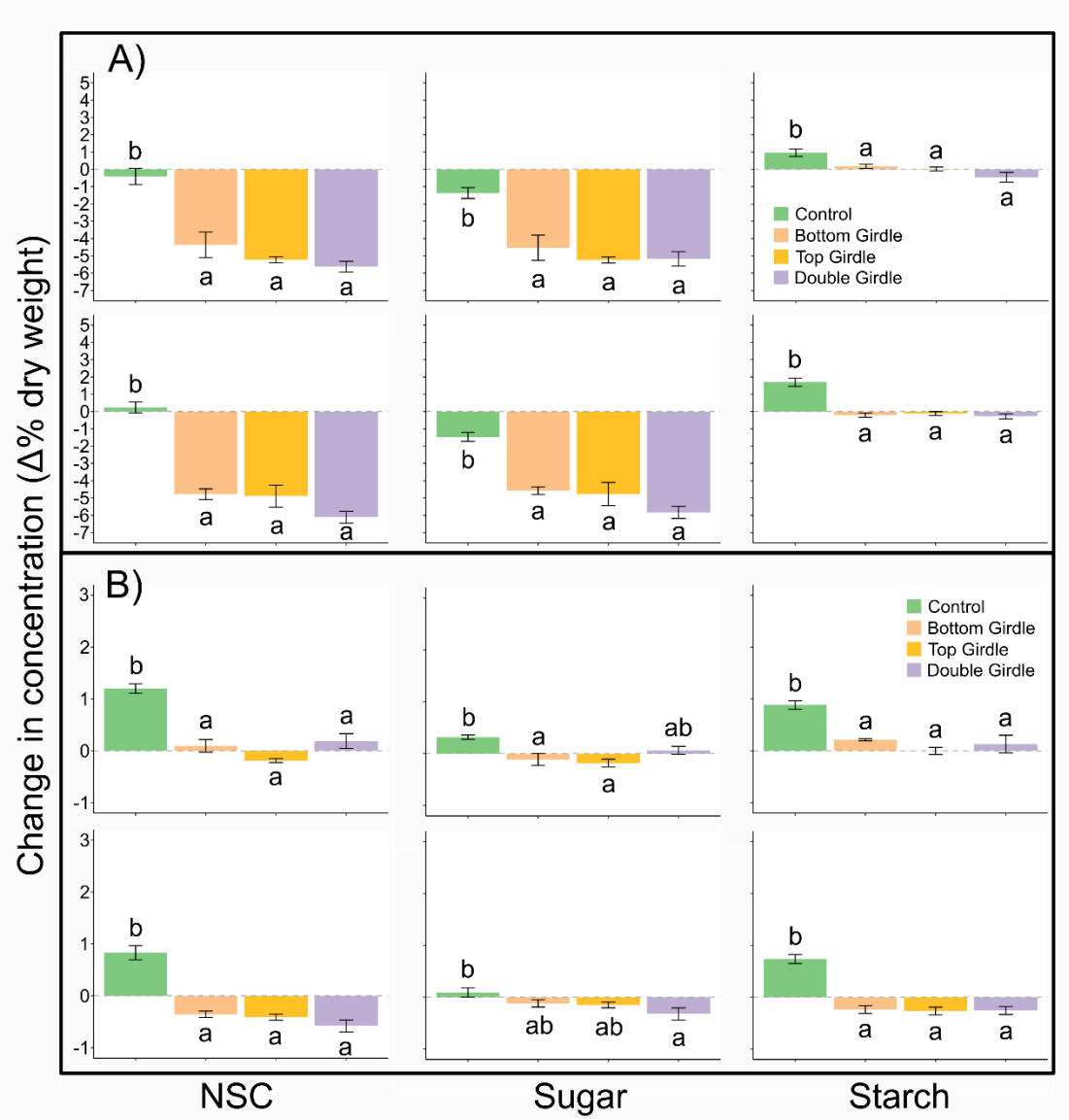

Figure A-3 Average (± standard error) change in upper and lower inner bark (A) and stemwood (B) carbohydrate (NSC, sugar, and starch) concentrations from the initial measurement in 30 mature *Betula papyrifera* trees subjected to different stem girdling treatments (control: n = 8, bottom girdle: n = 7, top girdle: n = 8, and double girdle: n = 7). The change in concentration was calculated as the difference between tissue concentrations at each upper and lower position between 21 June 2018 (initial measurement), and 17 July 2019. Letters denote significant differences (Tukey's HSD, $\alpha = 0.05$) for each plot separately.

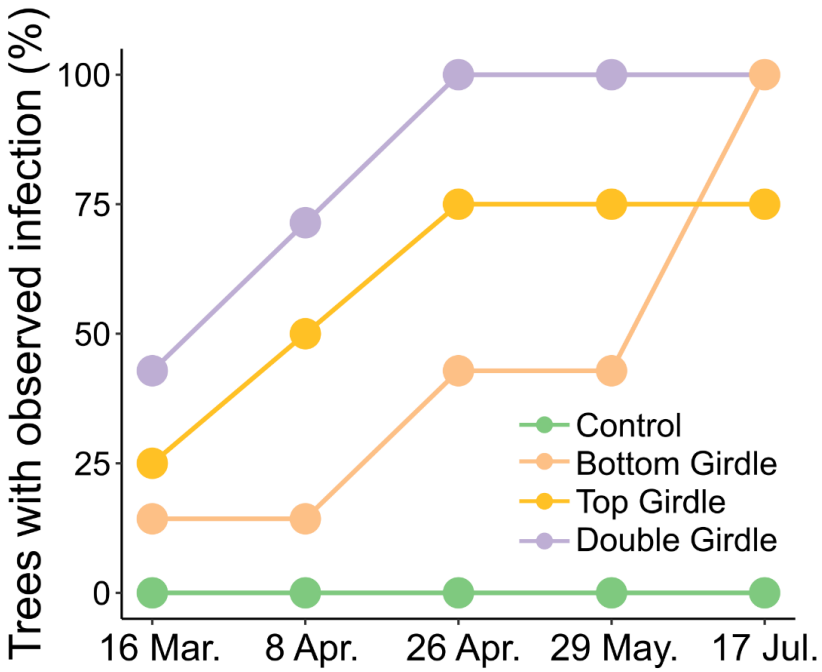

Figure A-4 Percentage of control (n = 8), bottom girdle (n = 7), top girdle (n = 8), and double girdle (n = 7) trees with observed stem tissue fungal infection over the latter half of the study period in 2019.